The study of Tryptophan-Dependent Indole-3-Acetic Acid Biosynthesis pathways in Maize Endosperm

A Dissertation
SUBMITTED TO THE FACULTY OF
UNIVERSITY OF MINNESOTA
BY

Jing Chen

IN PARTIAL FULFILLMENT OF THE REQUIREMENTS
FOR THE DEGREE OF
DOCTOR OF PHILOSOPHY

Advisor: Adrian D. Hegeman

August, 2017

Acknowledgements

First and foremost, I would like to express my appreciation and thanks to my advisor, Professor Adrian Hegeman. His intelligence, patience and immense knowledge guided me through my Ph.D. study. I am grateful that Dr. Hegeman gave me invaluable guidance and helped me along my research progress, such as writing proposals, designing research projects, discussing experiments, and revising this dissertation, just to name a few. I am thankful to have Dr. Hegeman as my advisor, my mentor, and my role model of a scientist. The tremendous support, guidance and genuine sincerity I received from Adrian enriched my graduate school experiences, and the training in his lab will always be a most treasured memory in my life.

I would like to especially thank Professor Jerry Cohen for his advice on my research and career development. His wisdom in academia and in life motived me throughout my graduate study. I am thankful that I received so many helps from Dr. Cohen, starting from recruiting me from China, offering numerous helps in the IAA biosynthesis study, to revising my dissertation and discussing with me about my career path. Thank you, Jerry, for being a most important person that positively changed my life path.

I thank my committee, Dr. William Gray, Dr. Neil Olszewski and Dr. John Ward for the suggestions that you gave me through the discussions in my committee meetings and personal communications. Your advices have proven invaluable in my research progress.

I would like to express my gratitude to all the colleagues in the Hegeman Cohen Gardner research group. It is a pleasure to get to know you and work with you all. I thank Dr. Angela Culler for her previous work in IAA biosynthesis, Dr. Peng Yu and Dr. Nathan Tivendale for their help with GC-MS, Dr. Xing Liu for her help with IAA extraction and methylation, Dr. Kaiting Fan for her help with protein expression and purification. I thank the undergraduate researcher Ms. Cami Bauer for her assistance when I started the IAA biosynthesis project. I thank undergraduate researcher Ms. Cassandra Yee for her assistance in IAA methylation during my pregnancy.

I thank the PBS graduate program and the horticultural science department for hosting and funding my graduate study here.

I thank my parents Jianshe Chen and Qi Huang. They gave me the unconditional love and encouraged me, their only child, to pursue happiness in another country.

Last but not least, I thank my husband Xiaoyi Zhu. I am fortunate to have met you upon my arrival in the United States, to have started a wonderful life with you in a new country, and to have you accompanied all these years. I love you.

Dedication

This dissertation is dedicated to my beloved family: my husband Xiaoyi Zhu, my son Daniel Zhu, and my parents Jianshe Chen and Qi Huang. Thank you for your support and love.

Abstract

Auxin as the most important plant hormone regulates almost all aspects of plant growth and development. Indole-3-acetic acid (IAA), the most abundant form of auxin, plays essential roles in the housekeeping functions. IAA can be *de novo* synthesized via tryptophan-dependent pathways or tryptophan-independent pathways. The findings on the most studied tryptophan-dependent IAA biosynthesis suggested that there may be 4 routes involving 6 key intermediates contribute to the IAA production from tryptophan in maize. Due to the genetic redundancies of the IAA biosynthesis pathways and the low activities of the exogenously expressed enzymes involved in the pathways, the classic genetics and biochemical approaches have proven challenging. The work in chapter 2 demonstrated that maize endosperm *in vitro* system retained a stable and high enzyme activities in the reaction of converting tryptophan to IAA, and converting indole-3-pyruvic acid (IPyA) to IAA enzymatically. Thus, maize endosperm *in vitro* system provides an excellent platform to study tryptophan-dependent IAA biosynthesis. The enzymatic parameters of the IAA biosynthesis reaction using the maize endosperm system were also characterized in chapter 2. The work in chapter 3 is to investigate the contribution of TAA1/YUCCA pathway to the overall tryptophan-dependent IAA biosynthesis in maize endosperm system. This chapter deployed two methodological approaches, the isotopic labeling dilution assay, and the oxygen depletion and $^{18}O_2$ labeling experiments, to address this question. The results from both methods strongly indicated that TAA1/YUCCA is the main tryptophan dependent pathway. Furthermore, the $^{18}O_2$ labeling experiments determined that TAA1/YUCCA pathway contributes at

least 80% of the tryptophan-dependent IAA biosynthesis pathways. In order to get around the obstacles presented by classic genetics methods, the work in chapter 4 aimed to find effective inhibitors that can potentially be used to selectively and temporarily block enzymes in certain IAA biosynthesis routes, at different development stages, under various environmental conditions. Four groups of compounds, including indole derivative inhibitors, tryptophan transaminase inhibitors, kynurenine pathway related inhibitors, and yucasin has been tested. The data suggested that yucasin, very likely targeting at YUCCA, is a very potent inhibitor in the maize endosperm *in vitro* system. AOPP, which is very likely targeting at TAA1, and MPP^+ iodide are also good inhibitors in tryptophan-dependent IAA biosynthesis pathways.

Table of Contents

Section **Page**

List of Tables

List of Figures

Chapter 1

Literature Review

1.1 Overview of auxin

1.1.1 The discovery of auxin

How do plants respond to the outside environment and coordinate their growth and development events throughout their life cycles? This question remained as a mystery for thousands of years. Dating back to the late 1800s, Julius von Sachs attempted to answer this question by hypothesizing the existence of chemical substance that regulate plant organ formation. Around the same time period, Charles Darwin and Francis Darwin, who specialized in botany and briefly researched under Sachs, co-authored the classic book *The Power of Movement in Plants* in 1880. In this book, they expanded on the first experimental data on a mobile signal described in Theophil Ciesielski's work on plant roots' responses to gravity, and reported the result from their pioneering experiments: Light and gravity can be perceived by the shoots and roots of coleoptiles, and cause the bending of downstream tissues (reviewed by Woodward and Bartel, 2005; reviewed by Enders and Strader, 2015). Based on the novel discovery regarding plant phototropism, they elaborated on Ciesielski's hypothesis and proposed that a messenger stimulated by light and gravity can be transmitted to other plant tissues. Around the 1920s, Peter Boysen-Jensen and Frits Went adapted and advanced Darwin's experiments and demonstrated that plant phototropism was caused by the mobility and the uneven distribution of a growth-promoting substance (reviewed by Enders and Strader, 2015). With the compelling evidence about the existence of a plant growth-promoting substance, which we now know it as auxin, the search for compounds with auxin activity became a major research focus during the 1930s. The ground work contributed by many scientists leaded to the discovery of auxin and the successful isolation of heteroauxin in fungi,

which was later determined to be indole-3-acetic acid. The discovery of several auxin compounds through *Avena* assays (reviewed by Went and Thimann, 1937) and the determination of the characteristic chemical structure of auxin molecules (Thimann and Schneider, 1939) marked a new era in the study of auxin.

1.1.2 The classification of Auxin

Auxin can be classified into two categories based on their origin. The naturally occurring active auxins include indole-3-acetic acid (IAA), 4-chloroindole-3-acetic acid (4-Cl-IAA) and phenylacetic acid (PAA). Among them, IAA is the most-studied active form of naturally occurring auxin. It is commonly accepted that IAA is the most abundant auxin in most of the species, nevertheless, 4-Cl-IAA greatly exceeds the IAA level and IAA activity in some *Fabaceae* species, in the reproductive structure especially, such as seeds of *Medicago truncatula*, *Melilotus indicus* and three species of *Trifolium* (Lam et al., 2015). It is also reported that in pea seeds, most of the 4-Cl-Trp can be converted to 4-Cl-IAA via the 4-Cl-IPyA intermediate (Tivendale et al., 2012). As the only non-indolic naturally occurring auxin found in many higher plants species, the role of PAA in plants remains largely unknown (reviewed by Korasick et al., 2013).

Most naturally occurring auxins exist in inactive forms. Some auxin precursors are inactive naturally occurring auxins, such as the intermediates in the IAA biosynthesis pathways, indole-3-acetaldoxime (IAOx), indole-3-acetamide (IAM), indole-3-acetonitrile (IAN), Indole-3-pyruvic acid (IPyA) and indole-3-acetaldehyde (IAAld). There are also some auxins exist in inactive storage form, such as indole-3-butyric acid (IBA), indole-3-propionic acid (IPrA), IAA methyl ester, and other IAA conjugates

(reviewed by Korasick et al., 2013). The auxin intermediates will be further discussed in section 1.2, and the auxin storage forms will be described more in section 1.3.

The synthetic auxins include 2,4-dichlorophenoxyacetic acid (2,4-D), naphthalene acetic acid(NAA), 2,4-dichlorophenoxybutyric acid (2,4-DB), and many compounds with the similar structure. 2,4-D and NAA are the active forms and 2,4-DB is the inactive form. Many compounds in this category are widely used as auxin herbicides for controlling dicot weeds in agriculture. The auxin herbicides can be readily absorbed by plant foliage and root systems and are then translocated to the plant meristems, resulting in many effects, such as the disruption of cell wall formation (Taiz and Zeiger, 2010).

1.2 IAA biosynthesis

The upregulation of IAA levels in plants can be achieved through IAA *de novo* biosynthesis and the release of free IAA from its conjugates (reviewed by Woodward and Bartel, 2005; Korasick et al, 2013; Enders and Strader, 2015). IAA can be *de novo* biosynthesized through a number of proposed routes that can be classified as tryptophan-independent IAA biosynthetic pathways and tryptophan-dependent IAA biosynthetic pathways. The two general routes of IAA *de novo* biosynthesis branch at the compound indole-3-glycerol phosphate, the precursor of indole (Ouyang et al., 2000). The starting point of tryptophan-independent biosynthesis pathways is indole, while in the tryptophan-dependent pathways, the starting point of all downstream pathways is tryptophan, which can be synthesized from the shikimic acid pathway, or can be synthesized from indole by the enzymes encoded by tryptophan synthase beta genes, TSB1 and TSB2 (reviewed by Korasick et al., 2013).

1.2.1 Tryptophan dependent IAA biosynthesis pathways

1.2.1.1 IAOx pathway

As is true for all the tryptophan-dependent IAA biosynthesis pathways, the IAOx pathway was named after the key intermediate in the pathway, indole-3-acetaldoxime (IAOx). The previous research suggested that the IAOx pathway seems to be restricted in the *Brassicaceae* species (Sugawara et al., 2009).

In the metabolism of IAOx, SUR1 and SUR2 are two enzymes that are responsible for the incorporation of IAOx to glucosinolates. SUR1 encodes a C-S lyase (Mikkelsen et al., 2004); and SUR2 encodes a cytochrome p450 monooxygenase CYP83B1 (Barlier et al., 2000). In the *sur1 sur2* double mutant seedlings, IAOx over-accumulated so that plants displayed phenotypes that resembled an IAA overexpression phenotype. This suggests that IAOx is one of the intermediates in a potentially important IAA biosynthesis pathway. An additional piece of evidence supporting this conclusion was from the overexpression of the genes *CYP79B2* and *CYP79B3*. In Arabidopsis, *CYP79B2/3* encode cytochrome P450 monooxygenases CYP79B2/3, which can catalyze the conversion of tryptophan to IAOx (Hull et al., 2000; Zhao et al., 2002). The overexpression of *CYP79B2/3* in the genetic background of *Arabidopsis sur1 sur2* double mutant results in an elevated level of auxin and this result suggesting that IAOx is one of the intermediates in IAA biosynthesis.

The loss-of-function double mutant *cyp79b2 cyp79b3* results in only a minimal effect on IAA abundance, suggesting that the IAOx pathway is not a major tryptophan-dependent pathway in *Arabidopsis*. Moreover, the *cyp79b2 cyp79b3* double mutants showed decreased levels of indole-3-acetonitrile (IAN) and indole-3-acetamide (IAM);

and the synthesis of $^{13}C_6$-IAM and $^{3}C_6$-IAN was confirmed after feeding *cyp79b2 cyp79b3* double mutant with $^{13}C_6$-IAOx. This result suggested that IAOx is the upstream intermediate precursor of IAN and IAM (Zhao et al., 2002; Sugawara et al., 2009; reviewed by Enders and Strader, 2015).

From the previous works discussed above, IAOx is now thought to be the branching point for the synthesis of indole glucosinolates (IGs), IAN and IAM. The majority of IAOx is diverted to IGs production (Bak et al., 2001; Mikkelsen et al., 2004; Nonhebel et al., 2011), whereas only a small portion of IAOx is used for IAA biosynthesis through its downstream intermediates IAM and IAN (reviewed by Tivendale et al., 2014; reviewed by Enders and Strader, 2015). IAN can be then hydrolyzed to IAA by nitrilases in various species, such as *Arabidopsis* (Bartel and Fink, 1994; Normanly et al., 1997), tobacco (Schmidt et al., 1996) and maize (Park et al., 2003), although the mechanisms of IAOx conversion to IAN and IAM are unclear.

1.2.1.2 IAM pathway

IAM widely exists in many plant species (Lehmann et al., 2010; reviewed by Korasick et al., 2013). One interesting observation is that IAM can be detected in species that have no detectable IAOx (reviewed by Korasick et al., 2013), such as rice (Sugawara et al., 2009), squash (Rajagopal et al., 1994), tobacco (Sugawara et al., 2009) and maize (Park et al.,2003; Culler, 2007). This observation suggests that there could be novel mechanisms that contributes to IAM synthesis.

In the IAM pathway, the mechanism of IAM synthesis from tryptophan remains unknown in many species. In *Arabidopsis,* IAM can be synthesized from IAOx by cytochrome P450 monooxygenases CYP79B2/3 (Sugawara et al., 2009). In species

lacking CYP79B2/3 orthologs, however, the synthesis of IAM was hypothesized to be catalyzed by a plant iaaM-type enzyme. The iaaM enzyme is a tryptophan monooxygenase that was discovered in some auxin-synthesizing bacteria and it can catalyze the conversion of tryptophan to IAM. Historically, this pathway was thought to be restricted to such auxin-synthesizing bacteria, such as *Agrobacterium tumifaciens* and *Pseudomonas syringae* and not present in uninfected plants (Patten and Glick, 1996; reviewed by Woodward and Bartel, 2005), but there are reports of the presence of IAM in plants (Pollman et al. 2002).

The formation of IAA through the IAM pathway is completed by the hydrolysis of IAM using the enzyme AMIDASE1 (AMI1). Studies indicated IAM hydrolases from various plant species, including *Arabidopsis*, tobacco, tomato, maize, rice etc., can catalyze the reaction *in vitro* (Pollmann et al., 2003; Pollmann et al., 2006; Nemoto et al., 2009). Overexpression of the tobacco IAM hydrolase gene *NtAMI1* to rescue the transgenic plant phenotypes suggested that IAM can be incorporated into plant cells and converted to IAA *in vivo* (Nemoto et al., 2009). In maize, *ZmAMI1* shares 56% identity and 71% similarity to *AtAMI1* (Lehmann et al., 2010). This suggested that *ZmAMI1* has the potential function of generating IAA by hydrolyzing IAM.

1.2.1.3 TAM pathway

In this pathway, it is not known how tryptophan is converted to TAM, although some grass species have been shown to have tryptophan decarboxylase activity, such as rice and barley (Ueno et al., 2003). TAM used to be considered as an intermediate in the IPyA pathway, and now its involvement in IAA biosynthesis is undecided (Tivendale et al., 2010). Although there is evidence that tryptophan decarboxylase (TDCs) can catalyze

the conversion of tryptophan to TAM and TAM can be converted to IAA in pea roots (Quittenden et al., 2009). Thus, whether TAM is an intermediate in IAA biosynthesis remains currently unclear.

1.2.1.4 IPyA pathway

During the last decade, much progress has been made in the field of IAA biosynthesis, and there is accumulating evidence demonstrated that IPyA pathway is the major pathway in the tryptophan-dependent IAA biosynthesis routes in many species. The IPyA pathway characterizes a IAA biosynthesis pathway that takes a two-step reaction: tryptophan is converted to the intermediate IPyA by the tryptophan aminotransferases encoded by *TRYPTOPHAN AMINOTRANSFERASE OF ARABIDOPSIS 1/TAA RELATED* (*TAA1/TARs*), and then IPyA is converted to IAA in by the flavin-containing monooxygenase encoded by *YUCCAs* (Mashiguchi et al., 2011; Dai X et al., 2013; reviewed by Zhao, 2014; reviewed by Enders and Strader, 2015).

The gene *TAA1* has been found with 3 alleles in *Arabidopsis*, *SHADE AVOIDANCE 3* (*SAV3*), *WEAK ETHYLENE INSENSITIVE 8* (*WEI 8*) and *TRANSPORT INHIBITOR RESPONSE 2* (*TIR2*). The ortholog of *TAA1* in maize is *VANISHING TASSEL 2* (*VT2*). The single mutant of *taa1* in *Arabidopsis* showed altered phenotypes (Tao et al., 2008; Stepanova et al., 2008 and Yamada et al., 2009), on the other hand, the *taa1/tar2* double mutant and *taa1/tar1/tar2* triple mutant showed dramatic phenotypic defects (Stepanova et al., 2008). This suggested the genes in *TAA1/TARs* family have overlapping functions. Although single mutant of *TAA1/TARs* genes in monocot, such as *vt2* in maize, showed obvious defect phenotype. This suggested that the gene redundancy of *TAA1/TARs* is less severe in monocot than in dicot. The overexpression of *TAA1/TARs*

in *Arabidopsis* didn't generate any obvious phenotypes. It is suggested that TAA1/TARs are not the rate-limiting enzymes in the IPyA pathway (Stepanova et al., 2008; Tao et al., 2008). A related aminotransferase, VAS1, was identified as a suppressor of the *taa1* mutant phenotype and it was proposed that VAS1 normally functions as a counterbalance to TAA1-dependent production of IPyA, linking IAA and ethylene biosynthesis (Zheng et al., 2013) and also modulating the balance between the IPyA pathway and tryptophan independent IAA biosynthesis (Pieck et al., 2015).

Compared to TAA1/TARs, the YUCCAs gene family shows more gene redundancy and complexity. YUCCAs has 11 members with essential and overlapping functions, single mutants of YUCCAs showed no obvious phenotypic defects, yet double (*yuc1 yuc4*), triple (*yuc1 yuc2 yuc4; yuc1 yuc4 yuc6*) and quadruple (*yuc1 yuc4 yuc10 yuc11*) mutants showed phenotypes that were vaguely connected with the defect in IAA biosynthesis (reviewed by Zhao, 2014). Recently it is reported that a quintuple mutant *yucQ* (*yuc3 yuc5 yuc7 yuc8 yuc9*) showed a root development defect phenotype, which can be rescued by the application of low levels of IAA supplemented in the growth media (Chen et al., 2014). The different phenotypes displayed by combinations of *yucca* mutants suggested that YUCCAs may function spatially in different developmental stages and tissue types (reviewed by Zhao, 2014).

In a study of selecting for light signaling using activation tagging, the discovery of *yuc1* mutants with IAA overproduction and downstream auxin response upregulation phenotype lead to the discovery of the connection between *YUCCA* and auxin (reviewed by Zhao, 2014). Moreover, considering that the overexpression of TAA1/TARs showed no obvious phenotype, this result suggested YUCCAs are the rate-limiting enzyme in the

IPyA pathway. YUCCAs are the monooxygenases that contain FAD and can catalyze the oxidative decarboxylation of IPyA to IAA using NADPH as an electron donor. The reaction starts with 2 electrons transferred from NADPH to FAD to form $NADP^+$ and $FADH_2$, $FADH_2$ then oxidized by O_2 to form a C4a-hydroperoxyflavin (or maybe C4a-peroxyflavin) intermediate. Lastly, the YUCCA reaction completed with IPyA oxidatively decarboxylated by the C4a-(hydro)peroxyflavin intermediate (Dai et al., 2013).

1.2.1.5 IAAld pathway

Based on several lines of evidence that show: 1) IAAld exists in some plant species; 2) the application of IAAld resulted in an upregulation of free IAA levels; 3) the ARABIDOPSIS ALDEHYDE OXIDASE1 (AAO1) can catalyze the conversion of IAAld to IAA (Seo et al., 1998), IAAld was once thought to be a promising intermediate involved in the IPyA pathway (reviewed by Woodward and Bartel, 2005). Although now the involvement of IAAld in IAA biosynthesis is questionable because the *Arabidopsis aba3* mutant, which lacks a cofactor required for the AAO1 activity, showed no IAAld accumulation and IAA related defects (Mashiguchi et al., 2011; reviewed by Korasick et al., 2013).

1.2.2 Tryptophan-independent IAA biosynthesis pathways

Using stable isotopic labeling tryptophan to study auxotrophic mutants of maize and Arabidopsis, both *in vivo* and *in vitro* evidence has shown the possibility of a tryptophan independent pathway (reviewed in Tivendale et al., 2014).

Further studies on the transgenic line with antisense indole-3-glycerol phosphate synthase (IGS) RNA suggested that the branching point for tryptophan-dependent pathway and tryptophan-independent pathway is the compound indole-3-glycerol phosphate (IGP) (Ouyang et al., 2000). A relevant recent study indicated that a cytosol-localized tryptophan synthase α subunit, indole synthase, participates in tryptophan-independent pathway and has important role in the apical-basal pattern formation in early embryogenesis of Arabidopsis (Wang et al., 2015). A genetic mutant study suggested that tryptophan-independent pathway can be elevated due to the functional loss of tryptophan catabolism (Pierck et al., 2015).

1.3 The IAA reservoir

In Arabidopsis, it was reported that only 1% of IAA are in the form of free IAA, most of the IAA exist as inactive forms in the IAA reservoir (Tam et al., 2000). Plant IAA levels can be down-regulated by storing the *de novo* synthesized IAA in many inactive forms, such as IAA conjugates, IBA and IBA conjugates. In the IAA storage pool, some of the inactive auxin can be reversibly activated to free IAA, some of them are also potentially destined for degradation. The vast IAA reservoir in homeostasis was proposed to be essential for coordinating IAA *de novo* biosynthesis, storage, degradation, and transport in the plant growth and development (Cohen and Bandurski, 1982).

1.3.1 IAA conjugates and methyl IAA

IAA conjugates can be categorized into two groups, the amide-linked IAA and the ester-linked IAA. Sugar can be ester-linked to IAA and inactivate it, the reaction can be reversed by hydrolysis. It is proposed that amino acid, peptides, proteins can be amide-

linked to IAA by GH3-like enzymes (Staswick et al., 2005). One group of IAA amino acids conjugates, such as IAA-Leu and IAA-Ala, can be amino-hydrolysed and release free IAA (Rampey et al., 2004). The other group of IAA amino acids conjugates, such as IAA-Asp and IAA-Glu appear to be less likely to be hydrolysed to release its free IAA (Ludwig-Müller, 2011). They are thought to play a role in the IAA degradation process discussed in section 1.4. IAA can also be stored as methyl IAA by IAA CARBOXYMETHYLTRANSFERASE1 (IAMT1) in *Arabidopsis* (Qin et al., 2005), although the function of methyl-IAA is unclear and the endogenous levels of methyl IAA are extremely low.

The composition of IAA conjugates varied among species. In Arabidopsis, it was found that 90% of IAA conjugates are amide-linked IAA, 10% are ester-linked IAA and about 1% are free IAA (Cohen and Bandurski, 1982; Tam et al., 2000; reviewed by Woodward and Bartel, 2005). In contrast to the amino acid conjugates more often found, the major IAA conjugate forms found in bean (*Phaseolus vulgaris*) are an IAA peptide and an IAA protein (Bialek and Cohen, 1986; Walz et al., 2002).

1.3.2 IBA and IBA conjugates

IBA as an inactive form of naturally occurring auxin can be converted to IAA in a chain of reactions featuring the β-oxidation step, resembling the fatty acid catabolic pathway (Epstein and Ludwig-Müller, 1993, reviewed by Woodward and Bartel, 2005). Similar to IAA conjugates, IBA conjugates can also be found in ester-linked forms and amide-linked forms. Although in Arabidopsis, different from IAA conjugates, most IBA conjugates are ester-linked (Ludwig-Müller et al., 1992).

1.4 IAA degradation

While IAA conjugation may be considered a reversible IAA inactivation process, IAA degradation is an irreversible form of IAA by inactivation. It was hypothesized that IAA degradation may have an important role in auxin detoxification (Cohen and Bandurski, 1982). The direct ring oxidation pathway for IAA catabolism has been the subject of a number of studies in several plant species over the last 25 years, including *Arabidopsis*, rice, corn, and broad bean (Ljung et al., 2002). The first report of IAA oxidation to oxindole-3-acetic acid (OxIAA) was in the basidiomycete *Hygrophorus conicus* (reviewed in Bandurski et al., 1995). OxIAA and DiOxIAA were later found to be synthesized by *Zea mays* and *Vicia faba*, respectively, following feeding of 1-[^{14}C]-IAA. It has now been reported in many species, including algae (Jacobs, 1993), bryophytes (Záveská Drábková et al., 2015), Scotch pine (Ernstsen et al., 1987), tomato (Riov and Bangerth, 1992), and orange (Chamarro et al., 2001). Isotope dilution experiments showed that OxIAA was a naturally occurring compound in *Zea mays* endosperm and shoot tissues, occurring in amounts about the level of free IAA in these tissues (Normanly et al., 2005). OxIAA is further metabolized in maize by hydroxylation at the 7 position, and by glucose addition to form 7-OH-OxIAA-glucoside (Nonhebel et al., 1985). 7-OH-OxIAA has also been identified as a catabolite of IAA in germinating kernels of *Zea mays* (Lewer and Bandurski 1987). In Arabidopsis, the inactive form of IAA that is destined for degradation are mainly 2-oxoindole-3-acetic acid (oxIAA) and oxIAA-glucose (oxIAA-Glu) (Östin et al., 1998; Ljung et al., 2002; Kai et al., 2007). Past the initial first steps, the details of IAA catabolism mechanisms and pathways in Arabidopsis are mostly unknown. It was proposed that further modification of oxIAA to

oxIAA-hexose, oxIAA-sugar, oxIAA-Asp/Glu, di-oxIAA, di-oxIAA-Asp, (di-)xoIAA-Asp/Glu-sugar are in the IAA catabolic pathway and low levels of N-(6-hydroxyindol-3-ylacetyl)-phenylalanine, and N-(6-hydroxyindol- 3-ylacetyl)-valine were detected in seedlings (Kai et al., 2007). Additionally, IAA degradation may not always start with the compound oxIAA. For instance, IAA-Asp can be oxidized to oxIAA-Asp or di-oxIAA-Asp in many species (reviewed by Normanly, 2010; reviewed by Ljung, 2002; reviewed by Korasick et al., 2013). The genes encoding the enzymes catalyzing the first step in the oxIAA metabolic pathway were characterized in rice (Zhao et al., 2013) and Arabidopsis (Porco et al., 2016; Zhang et al., 2016; Mellor et al., 2016). In Arabidopsis, DIOXYGENASE OF AUXIN OXIDATION (DAO) comprises a small subfamily of the 2-oxoglutarate and Fe(II) [2-OG Fe(II)] dependent dioxygenase superfamily. Biochemical and genetic studies have revealed critical physiological functions of DAO during plant growth and development (Zhao et al., 2013; Zhang et al., 2016; Porco et al., 2016).

1.5 IAA transport

The IAA transport is characterized as a dynamic process of influxing and effluxing. In terms of cytoplasm IAA transport, AUXIN RESISTANT1/LIKE AUX1 (AUX1/LAX) is the enzyme family that regulate IAA influx, long PIN-FORMED (PIN) enzyme family and ATP-BINDING CASSETTE SUBFAMILY B (ABCB) are the enzyme families that control IAA efflux. Genetic studies on *aux1/lax* mutants suggested that different members from AUX1/LAX family may play various roles in auxin polar transport (Jones et al., 2008; Vandenbussche et al., 2010; Bainbridge et al., 2008; Péret et al., 2012). The variances of plasma membrane localization and expression pattern shown

in long PINs (PIN1, PIN2, PIN4 AND PIN7) also demonstrated that PINs are important to differentially regulate auxin transport (reviewed by Zažímalová et al., 2010). Besides the localization and auxin specificity (what type of auxins the transporter can transport) differences, ABCB family has a unique group of enzymes, ABCB4 and ABCB21, can function reversely as efflux/influx transporters depending on the cytoplasmic auxin concentration (Kamimoto et al., 2012). It is widely understood that the diverse characteristics of IAA transports are essential to meet the requirements of the dynamic process in plant growth and development.

There are also ER associated IAA transporters from the short PIN enzyme family and PIN-LIKES (PILS) enzyme family. They are thought to be important for auxin compartmentation and auxin metabolism (Barbez et al., 2012; reviewed by Enders and Strader, 2015).

The postulated existence of some sort of auxin transport mechanism was initiated as early as the late 1800s by Charles Darwin. We now believe that polar IAA transport is involved in almost all aspects of plant growth and development, such as the formation of the polar plant axis as well as later formation of the root and shoot apex. In the root apex, both local auxin biosynthesis and auxin transport has been observed with the regulation of auxin gradient, planar polarity, lateral root initiation and development (Ljung et al., 2005; Peterson et al., 2009; Ikeda et al., 2009; reviewed by Overvoorde et al., 2010). Although it is commonly known that auxin has an important role in root structure establishment, many aspects about its mechanism functioning on auxin regulation remains unclear (reviewed by Ljung, 2013).

1.6 Maize endosperm enzyme system

Maize endosperm as a model for study tryptophan-dependent IAA biosynthesis has many advantages. The maize endosperm contains all the precursors, cofactors and enzymes that are necessary to produce IAA, and IAA can be accumulated at the rate of 190 ng per gram fresh weight per hour (Jensen and Bandurski, 1994).

The subcellular localization of IAA biosynthesis pathways allows us to be able to focus on the tryptophan-dependent pathway in the maize endosperm enzyme system. It is found that tryptophan-independent IAA biosynthesis route occurs in the caryopses, and tryptophan-dependent IAA biosynthesis route occurs in the etioplasts (Rekoslavskaya, 1995). Our purification procedure on maize endosperm retained the tryptophan-dependent IAA biosynthesis route with a stable and high IAA generating velocity. The determination of *Km* and *Vmax* for tryptophan to IAA conversion is described in Chapter 2. Furthermore, there is no IAOx formation being detected in the in vitro maize endosperm preparations (Culler, 2007). Therefore, maize endosperm provides an ideal enzyme system to study the tryptophan-dependent IAA biosynthesis.

1.7 Literature Cited

Bainbridge K, Guyomarc S, Bayer E, Swarup R, Bennett M, Mandel T and Kuhlemeier C (2008) Auxin influx carriers stabilize phyllotactic patterning. Genes & Development 22: 810-823

Bak S and Feyereisen R (2001) The involvement of two P450 enzymes, CYP83B1 and CYP83A1, in auxin homeostasis and glucosinolate biosynthesis. Plant Physiology **127**: 108-118

Bandurski R, Cohen J, Slovin J, and Reinecke D (1995) Auxin biosynthesis and metabolism, in Plant Hormones: Physiology, Biochemistry and Molecular Biology, P Davies, Editor, Kluwer Academic Publishers: Dordrecht, Boston, London. ISBN 0-7923-2984-8. p. 39-65

Barbez E, Kubeš M, Rolčík J, Béziat C, Pěnčík A, Wang B, Rosquete MR, Zhu J, Dobrev P, Lee Y, Zažímalovà E, Petrášek J, Geisler M, Friml J and Kleine-Vehn J (2012) A novel putative auxin carrier family regulates intracellular auxin homeostasis in plants. Nature **485**: 119-122

Barlier I, Kowalczyk M, Marchant A, Ljung K, Bhalerao R, Bennett M, Sandberg G and Bellini C (2000) The SUR2 gene of Arabidopsis thaliana encodes the cytochrome P450 CYP83B1, a modulator of auxin homeostasis. Proceedings of the National Academy of Sciences of the United States of America **97**: 14819-14824

Bartel B and Fink GR (1994) Differential regulation of an auxin-producing nitrilase gene family in Arabidopsis thaliana. Plant Biology **91**: 6649-6653

Bialek K and Cohen JD (1986) Isolation and partial characterization of the major amide-linked conjugate of indole-3-acetic acid from *Phaseolus vulgaris L*. Plant Physiology **80**: 99-104

Chamarro J, Östin A and Sandberg G (2001) Metabolism of indole-3-acetic acid by orange
(*Citrus sinensis*) flavedo tissue during fruit development. Phytochemistry 57, 179–187.

Chen Q, Dai X, De-Paoli H, Cheng Y, Takebayashi Y, Kasahara H, Kamiya Y and Zhao Y (2014) Auxin overproduction in shoots cannot rescue auxin deficiencies in Arabidopsis roots. Plant Cell Biology **55**: 1072-1079

Cohen JD and Bandurski RS (1982) Chemistry and physiology of the bound auxins. Annual Review of Plant Physiology **33**: 403-430

Culler AH (2007) Tryptophan-dependent indole-3-acetic-acid biosynthesis pathway in *Zea mays.* Ph.D. dissertation, University of Minnesota, 84 pp.

Dai X, Mashiguchi K, Chen Q, Kasahara H, Kamiya Y, Ojha S, Dubois J, Ballou D and Zhao Y (2013) The biochemical mechanism of auxin biosynthesis by an Arabidopsis

YUCCA flavin-containing monooxygenase. Journal of Biological Chemistry **288**: 1448-1457

Enders TA and Strader LC (2015) Auxin activity: Past, present, and future. American Journal of Botany **102**: 180-196

Epstein E and Ludwig-Müller J (1993) Indole-3-butyric acid in plants: occurrence, synthesis, metabolism and transport. Physiologia Plantarum **88**: 382-389

Ernstsen A, Sandberg G and Lundström K (1987) Identification of oxindole-3-acetic acid, and metabolic conversion of indole-3-acetic acid to oxindole-3-acetic acid in Pinus sylvestris seeds.
Planta 172: 47–52

Hull AK, Vij R and Celenza JL (2000) *Arabidopsis* cytochrome P450s that catalyze the first step of tryptophan-dependent indole-3-acetic acid biosynthesis. Proceedings of the National Academy of Sciences of the United States of America **97**: 2379-2384

Ikeda Y, Men S, Fischer U, Stepanova AN, Alonso JM, Ljung K and Grebe M (2009) Local auxin biosynthesis modulates gradient directed planar polarity in Arabidopsis. Nature Cell Biology **11**: 731-738

Jacobs WP (1993) A search for some angiosperm hormones and their metabolites in *Caulerpa paspaloides* (Chlorophyta). Journal of Phycology **29**: 595–600

Jensen PJ and Bandurski RS (1994) Metabolism and synthesis of indole-3-acetic acid (IAA) in *Zea mays*. Plant Physiology **106**: 343-351

Jones AR, Kramer EM, Knox K, Swarup R, Bennett MJ, Lazarus CM, Leyser HMO and Grierson CS (2008) Auxin transport through non-hair cell sustains root-hair development. Nature Cell Biology **11**: 78-84

Kai K, Horita J, Wakasa K and Miyagawa H (2007) Three oxidative metabolites of indole-3-acetic acid from *Arabidopsis thaliana*. Phytochemistry **68**: 1651-1663

Kaminoto Y, Terasaka K, Hamamoto M, Takanashi K, Fukuda S, Shitan N, Sugiyama A, Suzuki H, Shibata D, Wang B, Pollmann S, Geisler M and Yazaki K (2012) Arabidopsis ABCB21 is a facultative auxin importer/exporter regulated by cytoplasmic auxin concentration. Plant Cell Physiology **53**: 2090-2100.

Korasick DA, Enders TA and Strader LC (2013) Auxin biosynthesis and storage forms. Journal of Experimental Botany **64**: 2541-2555

Lam HK, McAdam SAM, McAdam EL and Ross JJ (2015) Evidence that chlorinated auxin is restricted to the *Fabaceae* but not to the *Fabeae*. Plant Physiology **168**: 798-803

Last RL, Bissinger PH, Mahoney DJ, Radwanski ER and Fink GR (1991) Tryptophan mutants in Arabidopsis: the consequences of duplicated tryptophan synthase beta genes. The Plant Cell **3**: 345-358

Lehmann T, Hoffmann M, Hentrich M and Pollmann S (2010) Indole-3-acetamide-dependent auxin biosynthesis: A widely distributed way of indole-3-acetic acid production? European Journal of Cell Biology **89**: 895-905

Lewer P and Bandurski RS (1987) Occurrence and metabolism of 7-hydroxy-2-indolinone-3-acetic acid in Zea mays. Phytochemistry 26:1247-1250

Ljung K (2013) Auxin metabolism and homeostasis during plant development. Development **140**: 943-950

Ljung K, Hull AK, Celenza J, Yamada M, Estelle M, Normanly J and Sandberg (2005) Sites and regulation of auxin biosynthesis in Arabidopsis roots. The Plant Cell **17**: 1090-1104

Ljung K, Hull AK, Kowalczyk M, Marchant A, Celenza J, Cohen JD and Sandberg G (2002) Biosynthesis, conjugation, catabolism and homeostasis of indole-3-acetic acid in Arabidopsis thaliana. Plant Molecular Biology **50**: 309-332

Ludwig-Müller (2011) Auxin conjugates: their role for plant development and in the evoluation of land plants. Journal of Experimental Botany **62**: 1757-1773

Mashiguchi K, Tanaka K, Sakai T, Sugawara S, Kawaide H, Natsume M, Hanada A, Yaeno T, Shirasu K, Yao H, McSteen P, Zhao Y, Hayashi K, Kamiya Y and Kasahara H (2011) The main auxin biosynthesis pathway in *Arabidopsis.* Proceedings of the National Academy of Sciences of the United States of America **108**: 18512-18517

Mellor N, Band LR, Pěnčík A, **Novák O, Rashed A, Holman T, Wilson MH, Voß U, Bishopp A, King JR, Ljung K, Bennett MJ and Owen MR** (2016) Dynamic regulation of auxin oxidase and conjugating enzymes AtDAO1 and GH3 modulates auxin homeostasis. Proceedings of the National Academy of Sciences of the United States of America **113**:11022-11027

Mikkelsen MD, Naur P and Halkier BA (2004) *Arabidopsis* mutants in the C-S lyase of glucosinolate biosynthesis establish a critical role for indole-3-acetaldoxime in auxin homeostasis. The Plant Journal **37**: 770-777

Nemoto K, Hara M, Suzuki M, Seki H, Muranaka T and Mano Y (2009) The NtAMI1 gene functions in cell division of tobacco BY-2 cells in the presence of indole-3-acetamide. FEBS Letters **583**: 487-492

Nonhebel HM, Kruse LI and Bandurski RS (1985) Indole-3-acetic acid catabolism in *Zea mays* seedlings. Metabolic conversion of oxindole-3-acetic acid to 7-hydroxy-2-oxindole-3-acetic acid 7'-O-beta-D-glucopyranoside. J Biol Chem. 260:12685-12689

Nonhebel H, Yuan Y, Al-Amier H, Pierck M, Akor E, Ahamed A, Cohen JD, Celenza JL and Normanly J (2010) Redirection of tryptophan metabolism in tobacco by ectopic expression of an Arabidopsis indolic glucosinolate biosynthetic gene. Phytochemistry **72**: 37-48

Normanly J (2010) Approaching cellular and molecular resolution of auxin biosynthesis and metabolism. Cold Spring Harbor Perspecives in Biology 2: a001594

Normanly J, Grisafi P, Fink GR and Bartel B (1997) Arabidopsis mutants resistant to the auxin effects of indole-3-acetonitrile are defective in the nitrilase encoded by the NIT1 gene. The Plant Cell **9**: 1781-1790

Normanly J, Slovin JP and Cohen JD (2010) Auxin biosynthesis and metabolism. In: Plant Hormones: Biosynthess, Signal Transduction, Action! (3rd edition). P.J. Davies, ed. Kluwer Academic Publ., Dordrecht, pp. 36-62

Östin A, Kowalyczk M, Bhalerao RP and Sandberg G (1998) Metabolism of indole-3-acetic acid in Arabidopsis. Plant Physiology **118**: 285-296

Ouyang J, Shao X and Li J (2000) Indole-3-glycerol phosphate, a branchpoint of indole-3-acetic acid biosynthesis from the tryptophan biosynthetic pathway in *Arabidopsis thaliana*. The Plant Journal **24**: 327-333

Overvoorde P, Fukaki H and Beeckman T (2010) Auxin control of root development. Cold Spring Harbor Perspectives in Biology 2: a001537

Park WJ, Kriechbaumer VK, Müller A, Piotrowski M, Meeley RB, Gierl A and Glawischnig E (2003) The nitrilase ZmNIT2 converts indole-3-acetonitrile to indole-3-acetic acid. Plant Physiology **133**: 794-802

Patten CL and Glick BR (1996) Bacterial biosynthesis of indole-3-acetic acid. Canadian Journal of Microbiology **42**: 207-220

Péret B, Swarup K, Ferguson A, Seth M, Yang Y, Dhondt S, James N, Casimiro I, Perry P, Syed A, Yang H, Reemmer J, Venison E, Howells C, Perez-Amador MA, Yun J, Alonso J, Beemster GTS, Laplaze L, Murphy A, Bennett MJ, Nielsen E and Swarup R (2012) AUX/LAX genes encoded a family of auxin influx transporters that perform distinct functions during Arabidopsis development. The Plant Cell **24**: 2874-2885

Peterson SV, Johansson AI, Kowalczyk M, Makoveychuk A, Wang JY, Moritz T, Grebe M, Benfey PN, Sandberg G and Ljung K (2009) An auxin gradient and

maximum in the Arabidopsis root apex shown by high-resolution cell-specific analysis of IAA distribution and synthesis. The Plant Cell **21**: 1659-1668

Pieck M, Yuan Y, Godfrey J, Fisher C, Zolj S, Vaughan D, Thomas N, Wu C, Ramos J, Lee N, Normanly J and Celenza JL (2015) Auxin and tryptophan homeostasis are facilitated by the ISS1/VAS1 aromatic aminotransferase in *Arabidopsis*. Genetics 201:185-199

Pollmann S, Müller A, Piotrowski M and Weiler EW (2002) Occurrence and formation of indole-3-acetamide in *Arabidopsis thaliana*. Planta 216, 155-161

Pollmann S, Neu D, Lehmann T, Berkowitz O, Schäfer T and Weiler EW (2006) Subcellular localization and tissue specific expression of amidase 1 from Arabidopsis thaliana. Planta **224**: 1241-1253

Pollmann S, Neu D and Weiler EW (2003) Molecular cloning and characterization of an amidase from Arabidopsis thaliana capable of converting indole-3-acetamide into the plant growth hormone, indole-3-acetic acid. Phytochemistry **62**: 293-300

Porco S, Pencik A, Rashed A, Voß U, Casanova-Sáez R, Bishopp A, Golebiowska A, Bhosale R, Swarup R, Swarup K, Peňáková P, Novák O, Staswick P, Hedden P, Phillips AL, Vissenberg K, Bennett MJ and Ljung K (2016) Dioxygenase-encoding

AtDAO1 gene controls IAA oxidation and homeostasis in Arabidopsis. Proceedings of the National Academy of Sciences of the United States of America **113**:11016-1102

Qin G, Gu H, Zhao Y, Ma Z, Shi G, Yang Y, Pichersky E, Chen H, Liu M, Chen Z and Qu LJ (2005) An indole-3-acetic acid carboxylmethyltransferase regulates Arabidopsis leaf development. The Plant Cell **17**: 2693-2704

Quittenden LJ, Davies NW, Smith JA, Molesworth PP, Tivendale ND and Ross JJ (2009) Auxin biosynthesis in pea: Characterization of the tryptamine pathway. Plant Physiology **151**: 1130-1138

Radwanski ER, Barczak AJ and Last RL (1996) Characterization of tryptophan synthase alpha subunit mutants of Arabidopsis thaliana. Molecular and General Genetics **253**: 353-361

Rajagopal R, Tsurusaki K, Kannangara G, Kuraishi S and Sakurai N (1994) Natural Occurrence of indoleacetamide and amidohydrolase activity in etiolated aseptically-grown squash seedlings. Plant & Cell Physiology **35**: 329-339

Rampey RA, LeClere S, Kowalczyk M, Ljung K, Sandberg G and Bartel B (2004) A family of auxin-conjugated hydrolases that contributes to free indole-3-acetic acid levels during Arabidopsis germination. Plant Physiology **135**: 978-988

Rekoslavskaya NI (1995) Pathways of indoleacetic acid and tryptophan synthesis in developing maize endosperm: studies *in vitro*. Russian Journal of Plant Physiology **42**:143–151.

Riov J and Bangerth F (1992) Metabolism of auxin in tomato fruit tissue: Formation of high molecular weight conjugates of oxindole-3-acetic acid via the oxidation of indole-3-acetylaspartic acid. Plant Physiology 100, 1396-1402

Schmidt RC, Muller A, Hain R, Bartling D and Weiler EW (1996) Transgenic tobacco plants expressing the Arabidopsis thaliana nitrilase II enzyme. The Plant Journal **9**: 683-691

Seo M, Akaba S, Oritani T, Delarue M, Bellini C, Caboche M and Koshiba T (1998) Higher activity of an aldehyde oxidase in the auxin-overproducing *superroot1* mutant of *Arabidopsis thaliana*. Plant Physiology **116**: 687-693

Staswick PE, Serban B, Rowe M, Tiryaki I, Maldonado MT, Maldonado MC and Suza W (2005) Characterization of an Arabidopsis enzyme family that conjugates amino acids to indole-3-acetic acid. The Plant Cell **17**: 616-627

Stepanova AN and Alonso JM (2016) Auxin catabolism unplugged: Role of IAA oxidation in auxin homeostasis. Proceedings of the National Academy of Sciences of the United States of America **113**:10742-10744

Stepanova AN, Robertson-Hoyt J, Yun J, Benavente LM, Xie DY, Doležal K, Schlereth A, Jürgens G and Alonso JM (2008) TAA1-mediated auxin biosynthesis essential for hormone crosstalk and plant development. Cell **133**: 177-191

Sugawara S, Hishiyama S, Jikumaru Y, Hanada A, Nishimura T, Koshiba T, Zhao Y, Kamiya Y and Kasahara H (2009) Biochemical analyses of indole-3-acetaldoxime-dependent auxin biosynthesis in *Arabidopsis*. Proceedings of the National Academy of Sciences of the United States of America **106**: 5430-5435

Taiz L and Zeiger E (2010) Plant Physiology. Sinauer Associates Inc., Publishers, Sunderland, Massachusetts U.S.A

Tam YY, Epstein E and Normanly J (2000) Characterization of auxin conjugates in *Arabidopsis*. Low steady-state levels of indole-3-acetyl-aspartate, indole-3-acetyl-glutamate, and indole-3-acetyl-glucose. Plant Physiology **123**: 589-596

Tao Y, Ferrer JL, Ljung K, Pojer F, Hong F, Long JA, Li L, Moreno JE, Bowman ME, Ivans LJ, Cheng Y and Lim J (2008) Rapid synthesis of auxin via a new tryptophan-dependent pathway is required for shade avoidance in plants. Cell **133**: 164-176

Thimann KV and Schneider CL (1939) The relative activity of different auxins. American Journal of Botany **26**: 328-333

Tivendale ND, Davidson SE, Davies NW, Smith JA, Dalmais M, Bendahmane AI, Quittenden LJ, Sutton L, Bala RK, Signor CL, Thompson R, Horne J, Reid JB and Ross JJ (2012) Biosynthesis of the halogenated auxin, 4-chloroindole-3-acetic acid. Plant Physiology **159**: 1055-1063

Tivendale ND, Davies NW, Molesworth PP, Davidson SE, Smith JA, Lowe EK, Reid JB and Ross JJ (2010) Reassessing the role of N-Hydroxytryptamine in auxin biosynthesis. Plant Physiology **154**: 1957-1965

Tivendale ND, Ross JJ and Cohen JD (2014) The shifting paradigms of auxin biosynthesis. Trend in Plant Science **19**: 44-51

Ueno M, Shibata H, Kihara J, Honda Y and Arase S (2003) Increased tryptophan decarboxylase and monoamine oxidase activities include Sekiguchi lesion formation in rice infected with *Magnaporthe grisea*. The Plant Journal **36**: 215-228

Vandenbussche F, Petrášek J, Žádníková P, Hoyerová K, Pešek B, Raz V, Swarup R, Bennett M, Zažímalová E, Benková E and Van Der Straeten D (2010) The auxin influx carriers AUX1 and LAX3 are involved in auxin-ethylene interactions during apical hook development in Arabidopsis thaliana seedlings. Development **137**: 597-606

Walz A, Park S, Slovin JP, Ludwig-Müller J, Momonoki YS and Cohen JD (2002) A gene encoding a protein modified by the phytohormone in indoleacetic acid. Proceedings of the National Academy of Sciences of the United States of America **99**: 1718-1723

Wang B, Chu J, Yu T, Xu Q, Sun X, Yuan J, Xiong G, Wang G, Wang Y and Li J (2015) Tryptophan-independent auxin biosynthesis contributes to early embryogenesis in *Arabidopsis*. Proceedings of the National Academy of Sciences of the United States of America **112**: 4821–4826

Went FW and Thimann KV (1937) Phytohormones. Macmillan, New York, New York, USA

Woodward AW and Bartel B (2005) Auxin: Regulation, action and interaction. Annals of Botany **95**: 707-735

Yamada M, Greenham K, Prigge MJ, Jensen PJ and Estelle M (2009) The TRANSPORT INHIBITOR RESPONSE2 gene is required for auxin synthesis and diverse aspects of plant development. Plant Physiology **151**: 168-179

Záveská Drábková L, Dobrev PI and Motyka V (2015) Phytohormone profiling across the bryophytes. PLoS One **10**, e0125411

Zhang J, Lin JE, Harris C, Pereira FCM, Wu F, Blakeslee JJ and Peer WA (2016) DAO1 catalyzes temporal and tissue-specific oxidative inactivation of auxin in *Arabidopsis thaliana*. Proceedings of the National Academy of Sciences of the United States of America **113**:11010–11015

Zhao Y (2014) Auxin biosynthesis. The Arabidopsis Book. doi: 10.1199/tab.0173

Zhao Y, Hull AK, Gupta NR, Goss KA, Alonso J, Ecker JR, Normanly J, Chory J and Celenza JL (2002) Trp-dependent auxin biosynthesis in Arabidopsis: involvement of cytochrome P450s CYP79B2 and CYP79B3. Genes & Development **16**: 3100-3112

Zhao Z, Zhang Y, Liu X, Zhang X, Liu S, Yu X, Ren Y, Zheng X, Zhou K, Jiang L, Guo X, Gai Y, Wu C, Zhai H, Wang H and Wan J (2013) A role for a dioxygenase in auxin metabolism and reproductive development in rice. Developmental Cell **27**:113–112

Zheng Z, Guo Y, Novak O, Dai X, Zhao Y, Ljung K, Noel JP and Chory J (2013) Coordination of auxin and ethylene biosynthesis by the aminotransferase VAS1. Nature Chemical Biology **9**: 244–246

Zažímalová E, Murphy AS, Yang H, Hoyerová K, and Hošek P (2010) Auxin transporters - Why so many? Cold Spring Harbor Perspectives in Biology 2: a001552

Chapter 2

Characterization of the Maize Endosperm Enzyme System

Overview

Auxin is the most essential plant hormone and the study in auxin biosynthesis has always been a great focus in the field of plant biology. Despite much progress toward understanding the IAA biosynthesis pathways in recent years the auxin biosynthesis pathways still remain mysterious in many aspects. This is especially true for the YUCCA pathway due to the genetic redundancy and the great obstacles associated with obtaining enzymes with high activity for study via classic biochemical approaches. This study takes an alternative approach to obtain high enzyme activity by successfully generating a maize endosperm *in vitro* reaction system, which has a stable and high enzyme activity in the conversion of isotopically labeled tryptophan to IAA, and for converting isotopically labeled IPyA to IAA. The enzymatic parameters of IAA biosynthesis reaction using the maize endosperm system were also characterized in this chapter. The work in this chapter proved that the maize endosperm *in vitro* system can provide an excellent platform to study IAA biosynthesis, and thus has been successfully used for additional experimentation described in chapter 3 and chapter 4.

2.1 Introduction

Auxin, as one of the essential plant hormones, regulates and coordinates almost all aspects of plant growth and development. Based on over 100 years of studies on auxin, it is revealed that auxin plays an essential role in an extensive spectrum of plant growth activities throughout its life cycle, ranging from embryogenesis (Cohen et al., 1992 and Liu et al., 1993), cell elongation, division and differentiation (reviewed by Fukuda, 2004 and Friml et al., 2010 and Ohashi-Ito et al., 2013), tropisms (Friml et al., 2002 and reviewed by Larson, 2016), establishment of the apical-basal axis and subsequent apical

dominance, root initiation (Blakesley et al., 1991 and Ljung et al., 2005), flowering (Cheng et al., 2006), abscission (Abeles et al., 1964 and Ellis et al., 2005), to wound and stress responses (Shani et al., 2017). There are four forms of natural occurring auxin discovered in plants, including indole-3-acetic acid (IAA), indole-3-butyric acid (IBA), phenylactic acid (PAA), and 4-chloroindole-3-acetic acid (4-Cl-IAA) (Normanly et al., 2010). Among different forms of endogenous auxin, the most abundant and essential form is IAA, while other forms, such as 4-Cl-IAA have specialized roles (Simon and Petrášek, 2011 and Ozga et al., 2017).

Although IAA has an inclusive range of functions in plants, our understanding in IAA biosynthesis pathways is elusive. One of the major research obstacles is due to the IAA biosynthesis pathway redundancy (Cohen et al., 2003), which results from the complex housekeeping roles that IAA plays. There are tryptophan-dependent (reviewed by Zhao, 2010) and tryptophan-independent auxin biosynthesis pathways (Normanly et al., 1993 and reviewed by Mano et al., 2012) coexisting in plants. Within the most studied tryptophan-dependent pathways, there are 4 distinct pathways involving 6 key intermediates leading to the IAA production (reviewed by Tivendale et al., 2014). From a classical genetic perspective, these redundant pathways with spatially and temporarily overlapping functions of genes make obtaining viable mutants with apparent phenotypes very difficult.

Another classic research approach to tryptophan-dependent IAA biosynthesis is to illuminate the functions of enzymes that are involved in IAA production. Tremendous work via biochemical approaches *in vitro* have been attempted, although expressing gene

products in their native forms exogenously and obtaining significantly high enzyme activities *in vitro* has proven challenging (Dai et al., 2013).

The goals of this chapter include: obtain maize endosperm sample with high enzyme activity; depict the enzymatic characteristics of tryptophan dependent IAA biosynthesis pathways in the maize endosperm *in vitro* system; determine whether IPyA can be converted to IAA enzymatically in the maize endosperm system.

My work, building on the early work of Culler (2007) in our lab, has adopted and optimized the purification of the maize endosperm membrane fraction as an *in vitro* system for studying IAA biosynthesis. In this study, I have established a maize endosperm *in vitro* system that can convert tryptophan or key intermediates to IAA with a stable and high efficiency, and I have determined the enzymatic characteristics of the integral tryptophan-dependent IAA biosynthesis pathway in maize endosperm system, thus, laying the groundwork for further studies of auxin biosynthesis.

2.2 Materials and Methods

2.2.1 Maize endosperm purification and sample preparation

Bicolor sweet corn (*Zea mays L.*) was purchased from local grocery stores. Corn, deionized water, 50 mM piperazine-1,4-bis(2-hydroxypropanesulfonic acid) (POPSO) buffer pH 8.5, containing 4 mM ethylenediaminetetraacetic acid (EDTA), glassware (three 1000 mL beakers and two 40 mL glass homogenizers) and two centrifuge rotors (JA-14 rotor for Beckman high speed centrifuge, Type 45 Ti rotor for Beckman ultracentrifuge) were pre-chilled in a 4°C cold room overnight before proceeding with the purification protocol.

Beakers and glass homogenizers were kept on ice. The corn was shucked, rinsed with pre-chilled deionized water, and wiped dry using paper towels. The rows of kernels were sliced with a razor blade, and then the kernel content was expressed by scraping against the rim of a beaker and collected. Approximately 50 to 70 mL of liquid endosperm was collected from one regular-sized corn ear. Due to the capacity of the 45 Ti rotor, six to eight ears were prepared for each purification experiment. The corn sample and parts of glassware that were in direct contact with the corn sample were not touched by experimenter's hands, to avoid for contamination and heat transfer from hands. The liquid endosperm was pressed through two layers of cheesecloth with a pre-chilled lemon squeezer. This yielded the crude purified liquid endosperm, which was further processed in a pre-chilled 40 mL glass homogenizer. After all the crude liquid endosperm was thoroughly homogenized, it was transferred into two pre-chilled centrifuge bottles, and subjected to centrifugation at 1,000 × g for 10 minutes at 4°C using the JA-14 rotor.

After processing in the centrifuge, the floating white fatty layer was removed with a metal spatula, and the yellow supernatant was targeted for collection. At this stage, the sample can be used for enzymatic assays, in which case an equal amount of 50 mM POPSO buffer was added to the supernatant and then homogenized. The homogenate at this stage was referred to as a purification 'stage 1' sample.

If further purification was required, the supernatant was divided into six Beckman centrifuge tubes, and subjected to ultracentrifugation in 45Ti at 100,000 × g for 2 hours at 4°C. After centrifugation, three layers were present in the tube. The top layer was clear cytosol, the middle layer was a thin bright yellow layer, and the bottom layer was a white

firm starchy pellet. The target layer was the middle layer, and its texture varied from viscous liquid to jelly, most often a mixture of the two textures, depending on different batches of corn. Note that these three layers were not compact, thus caution was taken not to disturb them when collecting the middle layer. A 10 mL pipette was used to remove the top layer, then a 1 mL Eppendorf pipette and a metal spatula were used to collect the middle layer. The bottom layer was discarded. All of the middle layer samples were collected and homogenized. This homogenized product was referred to as purification 'stage 2'.

For purification stage 3, the synthetic Zwitterionic 3-12 detergent, N-dodecyl-N,N-dimethyl-3-amino-1-propanesulfonate, was added to the purification stage 2 sample to achieve a final concentration of 2 mM. The sample was incubated in a shaker at 300 rpm for 2 hours at 25°C. It was then centrifuged at 100,000 × g for 1 hour at 4°C. The supernatant was collected, and this supernatant was the purification stage 3 sample (purification stage 3).

For most of my work, unless otherwise noted, the purification stage 2 sample was used. To achieve high and consistent enzyme activity, large quantities of corn were prepared, and all the yellow middle layers were collected, homogenized, aliquoted into 1 mL per 1.5 mL Eppendorf tubes, snap frozen in liquid nitrogen and then stored in a -80°C freezer for long-term usage. Each time, before running an enzymatic reaction, the purification stage 2 sample was thawed on ice, and then homogenized with POPSO buffer (volume ratio of stage 2 sample to POPSO buffer is 1:5).

2.2.2 Biosynthesis of IAA from tryptophan in maize endosperm

2.2.2.1 Enzymatic reaction procedure

Maize endosperm purification stage 2 sample was the enzyme sample I used in most of my experiments for its high enzyme activity (Culler, 2007). 1 tube (1 mL/tube) of maize endosperm purification stage 2 aliquot was thawed on ice, 5 mL of 50 mM POPSO buffer pH 8.5, containing 4 mM EDTA was added. The mixture was homogenized, then the homogenate was transferred into a 15 ml falcon tube. 1M ascorbate was freshly prepared and added into the homogenate to achieve a final concentration of 1 mM. A 15 mL polypropylene conical centrifuge tube (Falcon brand, Corning, New York) containing the prepared enzyme sample was placed in a 25°C water bath about 10 minutes before starting the reaction.

L-[$^{13}C_{11}$,$^{15}N_2$]tryptophan (Item # CNLM-2475-H-PK, Cambridge Isotope Laboratories, Tewksbury, MA) was used as the substrate in the enzymatic reaction. 840 ng of isotopically labeled tryptophan was added per 1 mL corn sample (the tryptophan substrate concentration was 3.84 µm) to start the reaction. During the course of reaction, the Falcon tubes were kept in a 25°C water bath, and the sample was gently rocked every minute. A 0.25 mL aliquot of reaction sample was taken out at specific time intervals as designed in an experiment.

[$^{13}C_6$]indole-3-acetic-acid (Item # CLM-1896, Cambridge Isotope Laboratories, Tewksbury, MA) used as the internal standard for quantification (Cohen et al., 1986), generally 62.5 ng of [$^{13}C_6$]IAA was added to each 0.25 mL reaction aliquot.

To stop the reaction, the reaction aliquots were first boiled in water for 5 minutes, and then centrifuged at 10,000 × g for 5 minutes. Then the supernatant was transferred

(obtaining 0.2 mL from 0.25 mL reaction aliquot) to a new tube pre-loaded with 0.2 mL of 50:50 1 M phosphoric acid to sodium phosphate buffer pH 2.5 to a final volume of 0.4 mL.

2.2.2.2 IAA Extraction and Methylation

IAA was extracted from the quenched reaction mixture by adding 0.4 mL ethyl acetate to each of the 0.4 mL reaction aliquots. The samples were vortexed, and allowed to settle on the bench until discrete aqueous and ethyl acetate layers formed. Alternatively, I would subject the samples to centrifugation to speed up the process. The vortex and centrifugation steps were repeated once. About 0.35 mL of the ethyl acetate phase was transferred to a clean glass vial. Caution was taken not to transfer any water. Anhydrous methanol (9 µL) was added to each glass vial to a 2.5% final concentration. A volume of ethereal diazomethane (Cohen, 1984), usually 0.25 mL, was added into each glass vial. The samples were kept in the fume hood while the methylation reaction ran for 10 minutes. The samples were evaporated to dryness under nitrogen with gentle heating (sand bath). Samples were removed as soon as possible upon drying. Plasticizer-free tips and pestles (Microman pipettes, Gilson, Middleton, WI) were used to add 20 µL ethyl acetate into the glass vials containing the dried sample, in order to resuspend the samples. Samples were transferred into crimp top vials with PTFE/red rubber septa (Part # 27239, Sigma-Aldrich, St Louis, MO) were selected for the instrument. Then the glass vials for GC-MS analysis were capped and loaded on the GC-MS autosampler tray.

2.2.2.3 Detecting IAA biosynthesis rate using GC-MS

Methylated samples were analyzed by GC-MS. All samples discussed in this chapter were analyzed by Agilent 6890A GC/5973 MS (Agilent Technologies, Palo Alto, California) equipped with an G2614A autosampler (Agilent Technologies, Palo Alto, California). The 7683 series injection tower (Agilent Technologies, Palo Alto, California) was modified with a merlin microseal high-pressure septum (Catalog # 22812, Restek, Bellefonte, PA). The capillary GC column used was Zebron ZB-5MS with 10 m × 0.18 mm ID, 0.18 um film thickness. (Part # 7CD-G010-08, Phenomenex, Torrance, CA). Helium carrier gas was supplied at the rate of 0.5 mL/min. The splitless inlet was set at the temperature of 290 °C and pressure of 13.2 kPa. The sample data was acquired in the Selective Ion Monitoring (SIM) mode. The MS source temperature was set at 230 °C, the MS Quad temperature was set at 150 °C, and the oven temperature was programmed from 70 °C to 240 °C at 45 °C/min. The methyl-IAA ion from endogenous IAA occurs at *m/z* 189 and its quinolinium ion occurs at *m/z* 130. The methylated [$^{13}C_{10}$,$^{15}N_1$]IAA synthesized from [$^{13}C_{11}$,$^{15}N_2$]tryptophan occurs at *m/z* 200 and its quinolinium ion occurs at *m/z* 140. The [$^{13}C_6$]IAA internal standard generates ions at *m/z* 195 and 136. The IAA biosynthesis rate was detected by monitoring the ratio of [$^{13}C_{10}$,$^{15}N_1$]IAA ions at *m/z* 140, to [$^{13}C_6$]IAA internal standard ions at *m/z* 136. The IAA biosynthesis rate was then determined by calculate IAA produced over certain periods of time.

2.2.3 Enzyme kinetics determination of IAA biosynthesis in maize endosperm sample

Three tubes of maize endosperm (stage 2; 1 mL per tube) were thawed on ice and pooled. 15 mL POPSO buffer was added into the thawed 3 mL maize endosperm sample,

and then homogenized. Freshly made aqueous 1 mM acetic acid was added to the homogenate up to a 1 mM final acetic acid concentration just prior to starting the reaction. The 18 mL of diluted endosperm was divided into eight 15 mL Falcon tubes each containing 2.25 mL and each serving as a vessel for a separate reaction. In this experiment, stable isotope labeled tryptophan, [$^{13}C_{11}$,$^{15}N_2$]tryptophan, was used as substrate and reaction rates were determined by following the appearance of [$^{13}C_{10}$,$^{15}N_1$]IAA following derivatization and GC-MS. A methanolic [$^{13}C_{11}$,$^{15}N_2$]tryptophan substrate solution was freshly made prior the reaction, and the concentration was confirmed spectrophotometrically using the tryptophan molar extinction coefficient 6,060 M^{-1} cm^{-1} at 282 nm (Bandurski et al., 1974). The reactions were started by addition of substrate solution to the maize endosperm samples to achieve a series of final concentrations for the labeled substrate. Eight different substrate concentrations were tested at a time for the purpose of measuring the steady state kinetics for this conversion reaction. The eight substrate concentrations, 0.483, 0.965, 1.93, 3.96, 7.72, 15.44, 30.88, and 61.76 μM, were selected to bracket the initial estimates of K_M for this reaction. Aliquots (0.25 mL) of each reaction were removed into 1.5 mL microcentrifuge tubes and quenched at the following times: 0, 1, 2, 4, 8, 16, and 32 minutes, from the start of the reaction. To quench the reaction, the reaction aliquots were first boiled in water for 5 minutes, and then centrifuged at 10,000 × g for 5 minutes. The supernatant was transferred to a new tube pre-loaded with equal volume of 50:50 1 M phosphoric acid to sodium phosphate buffer pH 2.5. All eight enzymatic reactions with different substrate concentrations were incubated in the 25°C water bath, and the sample

was gently rocked every minute. IAA extraction and methylation and data analysis is the same as described in sections 2.2.2.2 and 2.2.2.3.

2.2.4 Biosynthesis of IAA from IPyA in maize endosperm system

2.2.4.1 Synthesis of [$^{13}C_{11}$,$^{15}N_1$] IPyA

A 50 mM pH 8.0 sodium phosphate buffer was prepared by adding 94.7% Na_2HPO_4 and 5.3% NaH_2PO_4. A broad range bacterial transaminase, which is a recombinant enzyme expressed in *Escherichia coli*, (SKU # T7684, Sigma Aldrich, St Louis, MO) was prepared by dissolution in 50 mM sodium phosphate buffer to a final concentration of 0.2 mg/mL. The transaminase solution was pipetted into 100 µL aliquots, flash frozen in liquid nitrogen and stored at –80°C until needed. IPyA was synthesized by combining: 1 mg [$^{13}C_{11}$,$^{15}N_2$]tryptophan; 1 mg α-ketoglutarate (CAS # 328-50-7, Sigma Aldrich, St Louis, MO); 20 µL 5 mM pyridoxal 5'-phosphate (CAS # 41468-25-1, Sigma Aldrich, St Louis, MO); and 20 µg transaminase in up to 1 mL of 50 mM sodium phosphate buffer in a 1.5 mL microcentrifuge tube. The solution was gently mixed avoiding the formation of bubbles. The reaction tube was covered with aluminum foil to avoid light exposure, and the reaction was allowed to proceed at 37°C for 3 hours. The reaction was stopped by adding 1 mL 10 mM ascorbic acid and 50 µL 25% phosphoric acid to the reaction mixture, to bring the pH to 2.5. [$^{13}C_{11}$,$^{15}N_1$]IPyA was extracted from the reaction by adding 0.6 mL of ethyl acetate, mixing by vortex and removing the ethyl acetate phase to a 2 mL amber glass vial. The extraction was performed twice yielding a final volume of ethyl acetate [$^{13}C_{11}$,$^{15}N_1$]IPyA solution of 1.2 mL. The [$^{13}C_{11}$,$^{15}N_1$]IPyA solution was then dried under a stream of nitrogen gas to

dryness, taking caution not to over-dry the samples. The residue of [$^{13}C_{11}$,$^{15}N_1$]IPyA was next re-suspend in 1 mL 50% isopropanol. The synthesized [$^{13}C_{11}$,$^{15}N_1$]IPyA was capped in an amber glass vial and stored in the –80°C freezer. The yield of [$^{13}C_{11}$,$^{15}N_1$]IPyA synthesized was approximately 0.1 mg. This sample was used within two days (Liu, 2012).

2.2.4.2 IPyA to IAA reaction assay

For this assay, [$^{13}C_{11}$,$^{15}N_1$]IPyA was made fresh from [$^{13}C_{11}$,$^{15}N_2$]tryptophan (following the protocol described above) was used as the substrate in the reaction. The concentration of [$^{13}C_{11}$,$^{15}N_1$]IPyA was determined each time before use. To determine the concentration of [$^{13}C_{11}$,$^{15}N_1$]IPyA, 0.1 mg of unlabeled IPyA was added to the labeled IPyA as an internal standard. Because IPyA is unstable and degrades during the GC-MS analysis, NaB^2H_4 was added to reduce IPyA to stable indole-3-lactic acid (ILA) prior to quantitative analysis (Liu, 2012).

The reaction was started by adding [$^{13}C_{11}$,$^{15}N_1$]IPyA to the maize endosperm enzyme reaction system. In this assay, 840 ng of [$^{13}C_{11}$,$^{15}N_1$]IPyA was added to 1 mL of maize endosperm stage 2 enzyme sample to initiate the reaction. Aliquots (0.25 mL) of the reaction were sampled at various time points. The aliquots were quenched by boiling for 5 minutes, subjected to centrifugation for 5 minutes at 10,000 × g, and the supernatants were transferred to an acidic reaction stop reagent (50:50 1 M phosphoric acid to sodium phosphate buffer pH 2.5) to fully stop the reaction. Extraction and quantification of [$^{13}C_{10}$,$^{15}N_1$]IAA were accomplished using the same protocol described in sections 2.2.2.2 and 2.2.2.3.

2.3 Results

2.3.1 Variation in enzyme activity from different maize endosperm purification batches

After each purification stage, the liquid maize endosperm was assayed to determine the level of enzyme activity for the conversion of tryptophan to IAA. The maize endosperm at stage 2 purification demonstrated almost 100% conversion after 30 minutes (See **Figure 2-2**), while maize endosperm at stage 1 purification exhibits only 40% conversion in 30 minutes (See **Figure 2-1**). Maize endosperm purification stage 2 was used for all subsequent experiments described in this chapter.

The IAA biosynthetic enzyme activity also varies among different batches of corn and between preparations, although the same scientific conclusions can be drawn from varied enzyme activities resulting from different corn sample preparations (such as maize endosperm stage 2 enzyme sample used in **Figure 2-2** were varied in IAA biosynthesis activity as stage 2 samples used in **Figure 3-8**; other varied enzyme activities from different preparation batches of corn are not shown). Experiments in each section discussed in this chapter used the same batch and sample preparation of maize endosperm for the purpose of experimental consistency and to enable cross-comparison.

2.3.2 Maize endosperm enzymes retain activity over a 5-hour reaction time

The enzymatic reaction system was setup as described above and incubated at 25°C water bath. Tryptophan substrate was re-fed at 256 minutes after the tryptophan conversion has reached the plateau at around 30 minutes. Maize endosperm enzyme showed high conversion activity with comparable initial rate as the initial substrate

feeding (This re-feeding experiment used D5-tryptophan as substrate, data not shown). This result suggested that maize endosperm enzyme activity can be retained for at least 5 hours.

2.3.3 Solvent effects on enzyme activity

When running the enzymatic reactions, substrate and inhibitors are frequently dissolved in isopropanol and methanol. Solvent composition in the assay reaction derived from these solvents may be as high as 5% of a reaction mixture volume. Both isopropanol and methanol have been tested in maize endosperm reaction system, and neither exhibited any positive or negative effect on reaction rate at this concentration.

2.3.4 Steady state kinetics of tryptophan to IAA conversion by maize endosperm preparation

In this experiment, the velocity of [$^{13}C_{10}$,$^{15}N_1$]IAA biosynthesis at various concentrations of excess substrate followed the linear regression within the first 16 minutes. Thus, the initial rates were determined using IAA produced within the time frame of 16 minutes. The initial velocities of [$^{13}C_{10}$,$^{15}N_1$]IAA synthesis from various concentrations of [$^{13}C_{11}$,$^{15}N_2$]tryptophan are shown in **Table 2-1**. The Michaelis-Menten kinetics (**Figure 2-3**) determined that in the maize endosperm IAA biosynthesis reaction, the K_M is 5.78 μM, and the v_{max} is 18.22 ng/minute.

2.3.5 Conversion of IPyA to IAA by maize endosperm preparation

In this conversion assay, 13,750 unit of catalase was added to each 5 mL reaction remove hydrogen peroxide to prevent its reaction with IPyA to form IAA non-enzymatically. Over the time span of 128 minutes, nearly 100% of the substrate

[$^{13}C_{11}$,$^{15}N_1$]IPyA was enzymatically converted to [$^{13}C_{10}$,$^{15}N_1$]IAA using the maize endosperm stage 2 purification reaction system (See **Figure 2-4**). In comparison, the negative control with no maize endosperm enzyme was added yielded no [$^{13}C_{10}$,$^{15}N_1$]IAA production.

2.4 Discussion

One of the goals of this study was to determine whether IPyA can be converted to IAA enzymatically in the maize endosperm *in vitro* reaction system. I have successfully shown that isotope labeled IPyA can be enzymatically converted to IAA using the maize endosperm system described herein. Maize endosperm is an excellent *in vitro* system for studying the conversion of tryptophan to IAA.

Another goal of this study was to understand the enzymatic characteristics of the tryptophan dependent IAA biosynthesis pathway in this maize endosperm *in vitro* system. This study generated important enzymatic parameters that will facilitate further investigations that differentiate IAA biosynthesis pathways, described in Chapter 3 and inhibitor studies described in Chapter 4, using this maize endosperm *in vitro* system.

This study shows the high enzyme activities of the tryptophan-dependent IAA biosynthesis reaction using purification stage 1 and stage 2 (**Figure 2-1** and **Figure 2-2**). This study also tested that both the purification stage 1 and stage 2 from the maize endosperm *in vitro* system kept at room temperature can maintain a high enzyme reaction activity in a time period about 5 hours (data from the re-feeding experiment using D5-tryptophan as the substrate are not shown). The extended time window of active enzyme enables maize endosperm to be a stable *in vitro* platform for enzyme reaction experiments and inhibition assays. Plus, this reaction system can tolerate organic solvents

to at least 5% of its reaction volume without interfering its enzyme activity. The solvent tolerance also ensured a stable enzyme system in inhibitor assays studied in Chapter 4 (data from the solvent tolerance experiment using D5-tryptophan are not shown).

2.5 Tables

Initial [$^{13}C_{11}$,$^{15}N_2$]tryptophan concentration	Reaction initial rate
0.48 μM	1.44 ng/minute
0.97 μM	2.59 ng/minute
1.93 μM	4.56 ng/minute
3.96 μM	7.17 ng/minute
7.72 μM	10.22 ng/minute
15.44 μM	13.56 ng/minute
30.88 μM	15.69 ng/minute
61.76 μM	16.42 ng/minute

Table 2-1. The initial velocities of [$^{13}C_{10}$,$^{15}N_1$]IAA biosynthesis reaction using various [$^{13}C_{11}$,$^{15}N_2$]tryptophan substrate concentrations.

2.6 Figures

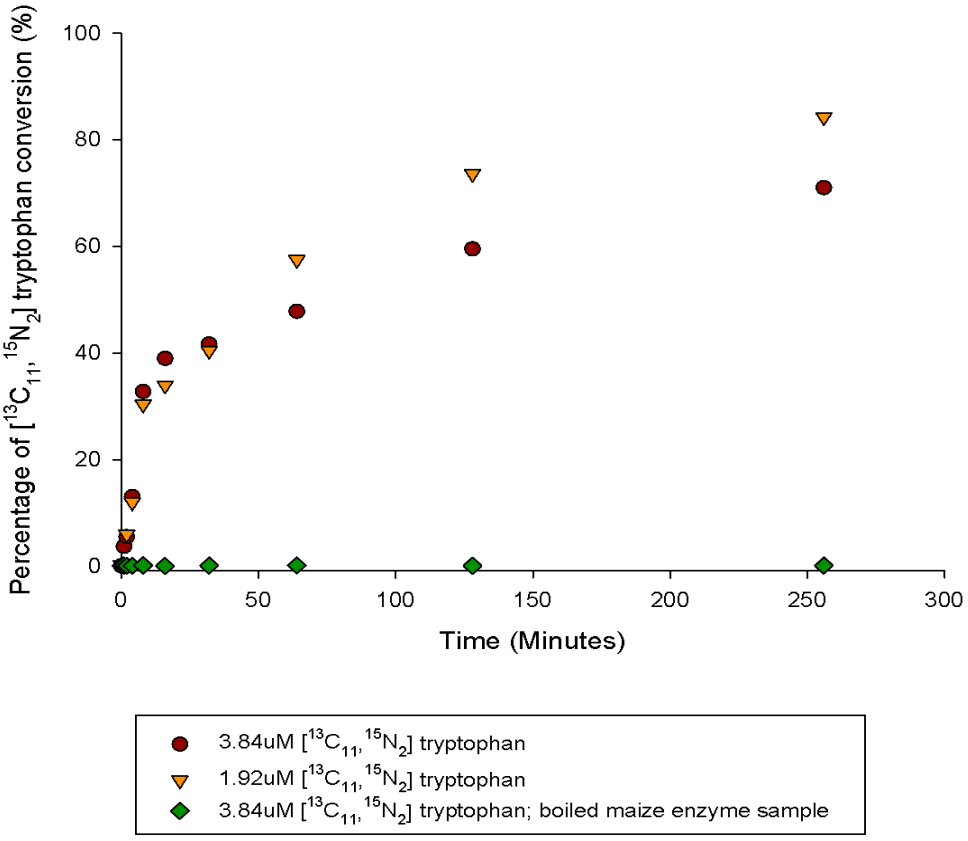

Figure 2-1. The percentage of [$^{13}C_{10}$,$^{15}N_1$]IAA production from tryptophan conversion using maize endosperm stage 1 purification within the time period of 256 minutes.

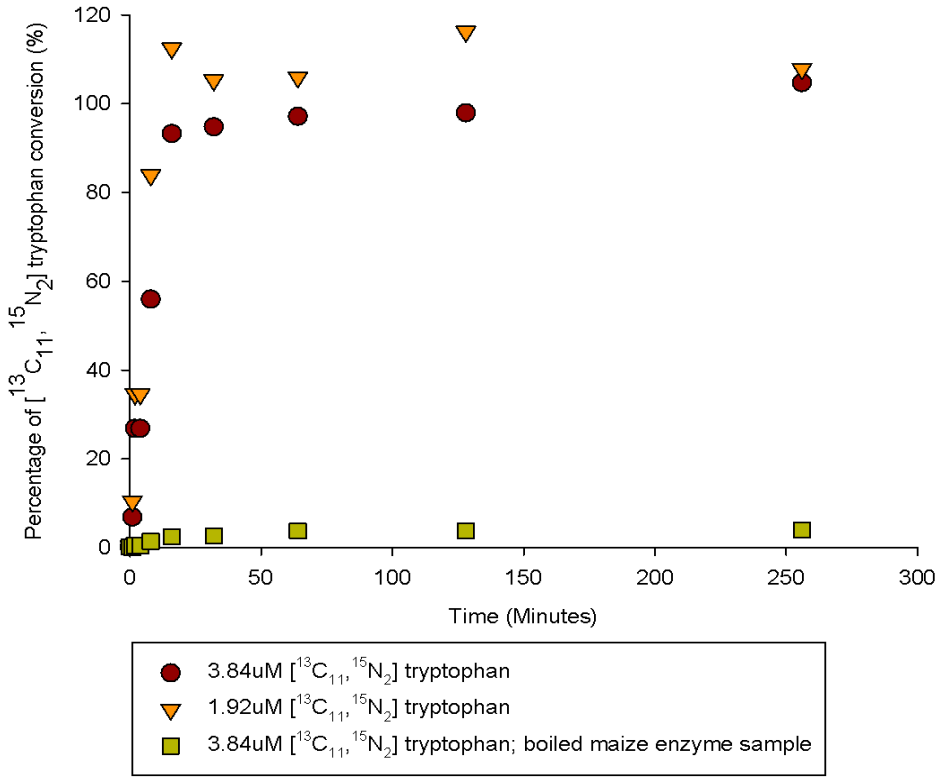

Figure 2-2. The percentage of [$^{13}C_{10}$,$^{15}N_1$]IAA production from tryptophan conversion using maize endosperm stage 2 purification within the time period of 256 minutes

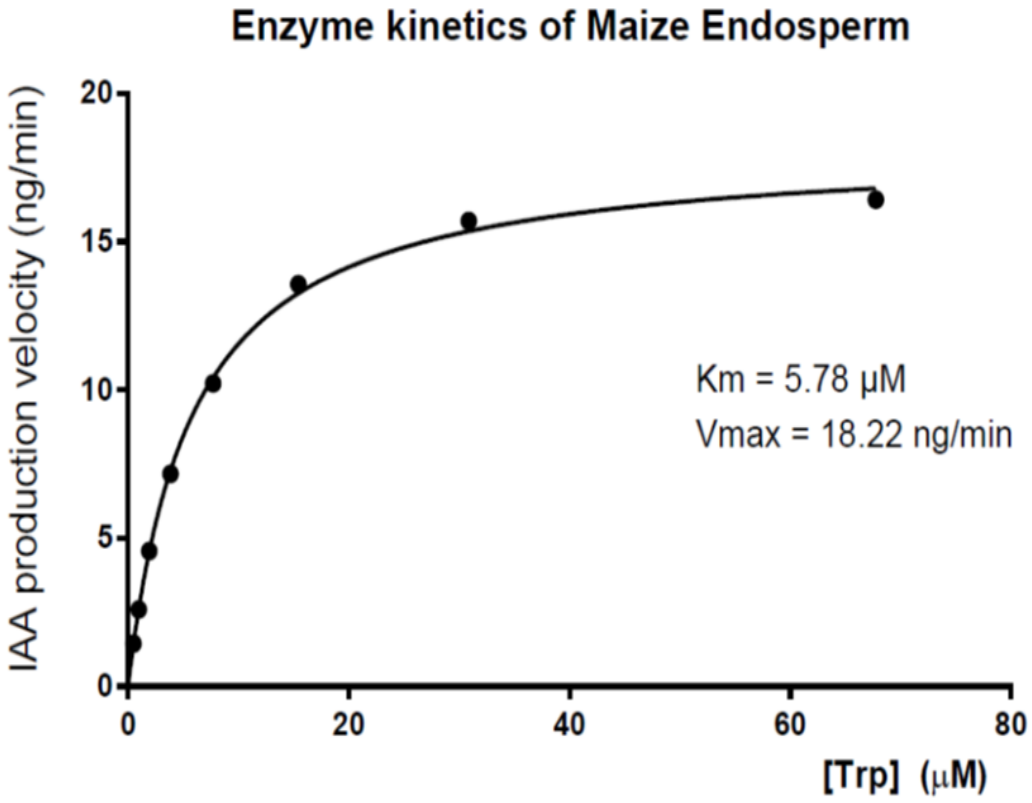

Figure 2-3. Determine the IAA biosynthesis enzyme kinetics parameters K_M and v_{max} in the Michaelis-Menten enzyme kinetics study.

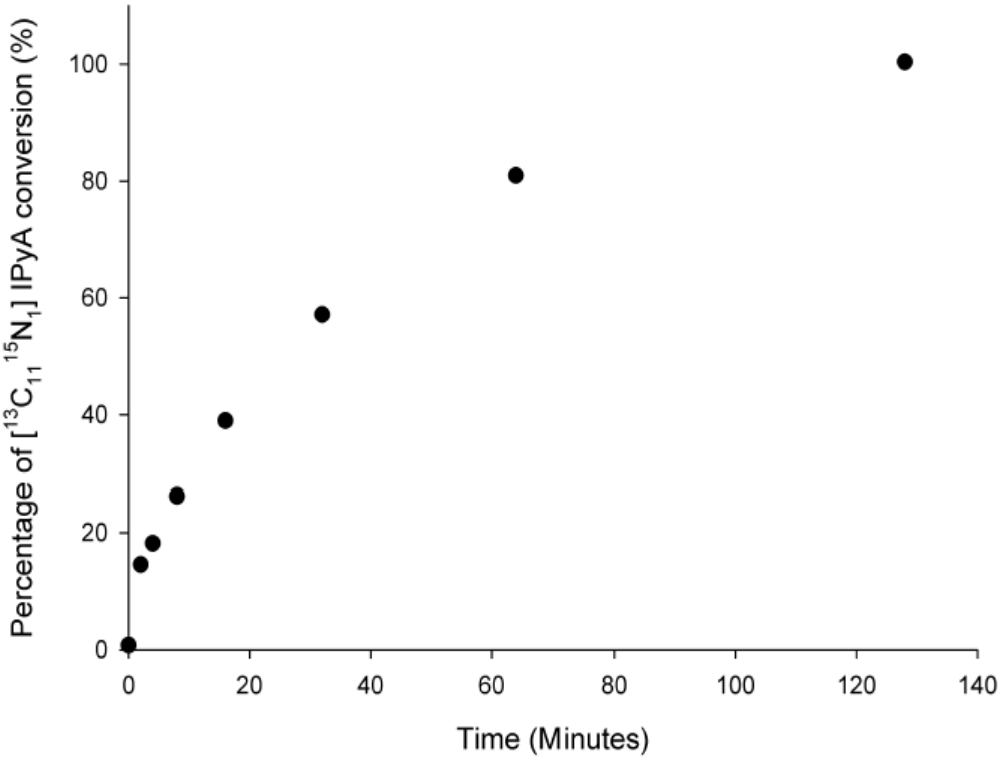

Figure 2-4. [$^{13}C_{11}$,$^{15}N_1$]IPyA conversion to [$^{13}C_{10}$,$^{15}N_1$]IAA in the reaction of 128 minutes.

2.7 Literature Cited

Abeles FB and Rubinstein B (1964) Regulation of ethylene evolution and leaf abscission by auxin. Plant Physiology **39**: 963-969

Blakesley D, Weston GD and Hall JF (1991) The role of endogenous auxin in root initiation. Plant Growth Regulation **10**: 341-353

Cheng Y, Dai X and Zhao Y (2006) Auxin biosynthesis by the YUCCA flavin monooxygenase controls the formation of floral organs and vascular tissues in Arabidopsis. Genes & Development **20**: 1790-1799

Cohen JD (1984) Convenient apparatus for the generation of small amounts of diazomethane. Journal of Chromatography A **303**: 193-196

Cohen JD, Baldi BG and Slovin JP (1986) 13C6-[Benzene Ring]-indole-3-acetic acid a new internal standard for quantitative mass spectral analysis of indole-3-acetic acid in plants. Plant Physiology **80**: 14-19

Cohen JD, Slovin JP and Hendrickson AM (2003) Two genetically discrete pathways convert tryptophan to auxin: more redundancy in auxin biosynthesis. Trends in plant sciences **8**:197-199

Culler AH (2007) Tryptophan-dependent indole-3-acetic-acid biosynthesis pathway in *Zea mays.* Ph.D. dissertation, University of Minnesota, 105 pp.

Dai X, Mashiguchi K, Chen Q, Kasahara H, Kamiya Y, Ojha S, Dubois J, Ballou D and Zhao Y (2013) The biochemical mechanism of auxin biosynthesis by an Arabidopsis YUCCA flavin-containing monooxygenase. Journal of Biological Chemistry **288**: 1448-1457

Ellis CM, Nagpal P, Young JC, Hagen G, Guilfoyle TJ and Reed JW (2005) *AUXIN RESPONSE FACTOR1* and *AUXIN RESPONSE FACTOR2* regulate senescence and floral organ abscission in Arabidopsis thaliana. Development **132**: 4563-4574

Friml J and Ding Z (2010) Auxin regulates distal stem cell differentiation in Arabidopsis roots. Proceedings of the National Academy of Science **107**: 12046-12051

Friml J, Wiśniewska J, Benková E, Mendgen K and Paime K. (2002) Lateral relocation of auxin efflux regulator PIN3 mediates tropism in *Arabidopsis*. Nature **415**: 806-809

Fukuda H (2004) Signals that control plant vascular cell differentiation. Nature Reviews Molecular Cell Biology **5**: 379-391

Larson ER (2016) A fresh look at the role of auxin in PIN trafficking. Plant Physiology **172**: 821-822

Ljung K, Hull AK, Celenza J, Yamada M, Estelle M, Normanly J and Sandberg G (2005) Sites and regulation of auxin biosynthesis in Arabidopsis roots. Plant Cell **17**: 1090-1104

Liu CM, Xu ZH and Chua NH (1993) Auxin polar transport is essential for the establishment of bilateral symmetry during early plant embryogenesis. Plant Cell **5**: 621-630

Liu X (2012) Roles of multiple mechanisms in regulating auxin levels during plant growth and development. Ph.D. dissertation, University of Minnesota, 35-37 pp.

Mano Y and Nemoto K (2012) The pathway of auxin biosynthesis in plants. Journal of Experimental Botany **63**: 2853-2872

Michalczuk L, Cooke TJ and Cohen JD (1992) Auxin levels at different stages of carrot somatic embryogenesis. Phytochemistry **31**:1097-1103

Normanly J, Cohen JD and Fink GR (1993) Arabidopsis thaliana auxotrophs reveals a tryptophan-independent biosynthesis pathway for indole-3-acetic acid. Proceedings of the National Academy of Science **90**: 10355-10359

Normanly J, Slovin JP and Cohen JD (2010) Auxin biosynthesis and metabolism. In: Plant Hormones: Biosynthess, Signal Transduction, Action! (3rd edition). P.J. Davies, ed. Springer Netherlands. Pages 36-62

Ohashi-Ito K, Oguchi M, Kojima M, Sakakibara H and Fukuda H (2013) Auxin-associated initiation of vascular cell differentiation by LONESOME HIGHWAY. Development **140**: 765-769

Ozga JA, Kaur H, Savada RP and Reinecke (2017) DM Hormonal regulation of reproductive growth under normal and heat-stress conditions in legume and other model crop species. J Exp Bot [doi: 10.1093/jxb/erw464]

Shani E, Salehin M, Zhang Y, Sanchez SE, Doherty C, Wang R, Mangado CC, Song L, Tal I, Pisanty O, Ecker JR, Kay SA, Pruneda-Paz J and Estelle M (2017) Plant Stress tolerance requires auxin-sensitive Aux/IAA transcriptional repressors. Current Biology **27**: 437-444

Simon S and Petrášek J (2011) Why plants need more than one type of auxin. Plant Sci. **180**:454–460.

Tivendale ND, Ross JJ and Cohen JD (2014) The shifting paradigms of auxin biosynthesis. Trends in Plant Science **19**: 44-51

Zhao Y (2010) Auxin biosynthesis and its role in plant development. Annual Review of Plant Biology **61**: 49-64.

Chapter 3

VT2/SPI1 Pathway is the Main Tryptophan-dependent IAA Biosynthesis Pathway in Maize Endosperm

Overview

Based on our current understanding about tryptophan-dependent IAA biosynthesis, it is proposed that there may be four routes leading tryptophan to IAA production in maize. With other tryptophan-dependent IAA biosynthesis pathways largely unclear, the TAA1/YUCCA pathway is the most well studied. Although our knowledge about the TAA1/YUCCA pathway has expanded greatly in recent years, the contribution of TAA1/YUCCA pathway to the overall tryptophan-dependent IAA biosynthesis is still unknown. This chapter discussed two methodological approaches, the isotopic labeling dilution assay, and the oxygen depletion and $^{18}O_2$ labeling experiments, to answer this question and determined that the TAA1/YUCCA pathway contributes 80% of the IAA *de novo* synthesis through the tryptophan-dependent routes.

3.1 Introduction

As the most essential form of auxin, indole-3-acetic acid (IAA) can be synthesized *de novo* using tryptophan as a starting material. Pathways using tryptophan as the substrate to anabolize IAA are designated as tryptophan-dependent biosynthetic pathways. Based on our current knowledge, there are four proposed tryptophan-dependent IAA biosynthetic routes possibly in maize. Indole-3-acetamide (IAM), Indole-3-pyruvate (IPyA), tryptamine (TAM), indole-3-acetaldoxime (IAOx) and indole-3-acetonitrile (IAN) and indole-3-acetaldehyde (IAAld) are the six key intermediates that have been suggested as involved in the four tryptophan-dependent biosynthesis pathways. The proposed tryptophan-dependent biosynthetic pathways in maize are shown in **Figure 3-1**.

3.1.1 IAOx pathway

IAOx, is an important indolic metabolic intermediate in Arabidopsis, and is situated at an important branch point between the synthesis of indole glucosinolates (IGs), IAN and IAM, and possibly IAAld. Both IAN and IAM can then be converted to the downstream product IAA. IAN is also the precursor in Arabidopsis for camalexin biosynthesis (Nonhebel et al., 2011). However, the IAOx pathway seems to be restricted in *Brassicaceae* species. In maize, no co-orthologs of *Arabidopsis* CYP79B2/3 have been identified, no detectable IAOx has been observed, although genes encoding nitrilases have been identified leaving open the question of whether this route exists in the maize system (Park et al., 2003 and Kriechbaumer et al., 2007). IAAld is converted into IAA via the action of IAAld oxidases (Seo et al., 1998), although the conversion rate is very low in maize endosperm (Culler, 2007).

3.1.2 TAM pathway

For this pathway, no genes have been identified in maize for the conversion of tryptophan to TAM, although other grass species, such as rice and barley, have been shown to have tryptophan decarboxylase activity (Ueno et al., 2003). A pathway was previously proposed that would convert tryptamine to N-hydroxyl-tryptamine (NHT) by YUCCA, however, this possibility was subsequently shown to be incorrect, as YUCCA is now known to be responsible for the conversion of IPyA to IAA, and the previous reported product NHT was shown to be not authentic NHT (Tivendale et al., 2010). It may be premature to eliminate the contribution of some version of this pathway entirely because there is evidence of TAM being converted to IAA in pea roots (Quittenden et al., 2009).

3.1.3 IAM pathway

Some auxin-synthesizing bacteria use the iaaM protein, which is thought to be a tryptophan monooxygenase enzyme to generate the intermediate IAM (Comai and Kosuge, 1982). Historically, this pathway was thought to be restricted to such phytopathogenic bacteria. There is evidence suggesting that plants have also inherited some aspects of this route. For example, IAM has been found across many plant species (Lehmann et al., 2010). In *Arabidopsis* IAM is generated by IAOx, whereas in species lacking CYP79B2/3 orthologs, such as maize, this first step may be catalyzed by an iaaM-type enzyme. The second step of the pathway is the convertion of IAM to IAA. Studies indicate that IAM hydrolases present in various plant species, including *Arabidopsis*, tobacco, tomato, maize, rice etc., can catalyze the reaction *in vitro* (Pollmann et al., 2003; Nemoto et al., 2009). Overexpression of the tobacco IAM hydrolase gene *NtAMI1* to rescue transgenic plant phenotypes suggests that IAM can be incorporated into plant cells and converted to IAA *in vivo* (Nemoto et al., 2009). In maize, *ZmAMI1* shares 56% identity and 71% similarity to *AtAMI1* (Lehmann et al., 2010). No genetic mutant data have been reported in this pathway, however.

3.1.4 IPyA pathway

The IPyA pathway is also known as the TAA1/YUCCA pathway. This pathway involves two reaction steps (Mashiguchi et al., 2011). In the first reaction step, tryptophan is converted to the intermediate IPyA by a tryptophan aminotransferase, TAA1. In Arabidopsis, the TAA/TARs family, TAA1 and TAR 1-4 have been identified. TAA1 converts tryptophan to IPyA, and TAR2 has an overlapping role in ethylene response as shown in a genetic study where the *taa1 tar2* double mutant had a more

severe phenotype than either single mutant (Stepanova et al., 2008). *Sav3*, the mutant allele of TAA1, is associated with shade avoidance response (Tao et al., 2008); and another mutant allele of TAA1, *wei8*, is involved in the ethylene response (Stepanova et al., 2008). Mutant *tar2* is involved in naphthylphthalamic acid-induced root shortening (Yamada et al., 2009). In maize, vt2 is a co-ortholog of TAA1/TAR1/TAR2 (Phillips et al., 2011).

The second reaction step of this pathway is the oxidative decarboxylation reaction of IPyA to IAA catalyzed by YUCCA. YUCCAs in plants are part of a larger flavin-containing monooxygenase gene family, which shares sequence similarity to FMOs in mammals. YUCCA genes have been identified in all plants with sequenced genomes. Overexpression of yucca genes result in elevated free IAA level indicating that YUCCA catalyzes a rate-limiting step in IAA biosynthesis (Zhao et al., 2001; Yamamoto et al., 2007).

Biochemical studies have shown that Arabidopsis YUCCA can catalyze the reaction of IPyA to IAA (PPA to PAA) by using FAD as a cofactor, and NADPH as hydride donor (Dai et al., 2013).

In Arabidopsis, out of 29 putative flavin monooxygenases, there are 11 members that belong to the YUCCA family. Genetic studies have shown that: 1) single YUCCA gene knock-outs do not generate obvious phenotypes because of the overlapping functions among genes in the YUCCA family; 2) attempts to knock out all YUCCA genes result in lethality; and 3) studies on yucca double, triple and quadruple mutants show that YUCCAs participate in fundamental functions throughout plant growth and development, spatially and with some degree of overlap. To sum up, in the case of

YUCCA, genetic approaches are limited in their capacity to provide in-depth information to answer the question of YUCCA functions and its role played in IAA biosynthesis pathways in Arabidopsis due to redundancy.

In maize, genetic evidence suggests that spi1 (sparse inflorescence1) is associated with IAA biosynthesis (Gallavotti et al., 2008), ZmYuc1 is transiently expressed during seed development and is specific to endosperm (LeClere et al., 2010) and the defective endosperm18 maize mutant, characterized as having loss of expression of ZmYuc1, is very low in free IAA content (Bernardi et al., 2012). This genetic evidence implies that TAA1-YUCCA may be the major pathway, although there are other possible scenarios that could result in the same genetic observation, moreover, free IAA only constitutes a small portion of total IAA present in the cell (due to conjugation), thus biochemical studies of YUCCA function are needed to fully characterize this pathway in maize.

In this chapter, two research methods have been implemented to study the VT2/SPI1 pathway in maize, which is known as the counterpart of the TAA1/YUCCA pathway in Arabidopsis. The central question in this chapter concerns the extent of the contribution of the VT2/SPI1 pathway to tryptophan-dependent IAA biosynthesis in maize endosperm. To answer this question, this chapter approached the topic using two different methodological approaches: the isotopic labeling dilution assays discussed in Section 3.2.1, and the oxygen depletion and $^{18}O_2$ labeling experiments discussed in Section 3.2.2 and 3.2.3.

In the isotopic labeling dilution assay, my hypothesis is that the isotopic enrichment of labeled IAA from labeled tryptophan will be greatly diminished with the addition of excessive amount of unlabeled IPyA, the intermediate in YUCCA pathway;

whereas there are much less diminishing effects on isotopic enrichment of labeled IAA with the addition of other unlabeled intermediates thought to involve in tryptophan-dependent IAA biosynthesis pathways. The rationale is that the presence of an unlabeled intermediate will reducing the isotopic enrichment of the labeled IAA by dilution of labeled intermediate pools. Thus, if the addition of a specific unlabeled intermediate greatly reduces the isotopic enrichment of labeled IAA one may conclude that the pathway that uses that intermediate plays a major role in IAA biosynthesis.

Based on our current knowledge of tryptophan-dependent pathways (discussed in Chapter 1, Section 1.2) and the mechanism of the YUCCA reaction (Dai et al., 2013), it is suggested that the sole entry of O_2 among all known IAA biosynthetic pathways in maize is in the step of converting IPyA to IAA by YUCCA enzyme. The hypothesis of the oxygen depletion and $^{18}O_2$ labeling experiments is that YUCCA pathway is the main pathway among all tryptophan-dependent IAA biosynthesis pathways in maize endosperm. YUCCA pathway can be turned off by removing oxygen from the reaction system, and can be switched on by restoring the oxygen supply; moreover, if restore the oxygen using $^{18}O_2$, the portion of IAA produced via the YUCCA pathway can be distinguished from other tryptophan-dependent pathways.

3.2 Material and Methods

3.2.1 Isotopic label dilution assay

In the isotopic label dilution experiment, five unlabeled IAA biosynthesis intermediates, IAAld (CAS # 20095-27-6, Sigma Aldrich, St Louis, MO), IAN (CAS # 771-51-7, Sigma Aldrich, St Louis, MO), IAM (CAS # 879-37-8, Sigma Aldrich, St

Louis, MO), TAM (CAS # 61-54-1, Sigma Aldrich, St Louis, MO) and IPyA (CAS # 392-12-1, Sigma Aldrich, St Louis, MO), were tested individually in three replicated assays. The same batch of maize endosperm was used for all fifteen isotopic labeling dilution assays. In each assay, the unlabeled intermediate was mixed with the isotopically labeled substrate [$^{13}C_{11}$,$^{15}N_2$]tryptophan in a concentration ratio of 5:1. Nine data points were collected over a time span of 256 minutes to measure both initial velocity and total conversion percentage of [$^{13}C_{10}$,$^{15}N_1$]IAA bioproduction in the presence of excess putative unlabeled intermediates.

For each of the assays, 0.5 mL of maize endosperm (purification stage 2) was thawed on ice and diluted with 2.5 mL of POPSO buffer. The mixture was homogenized well by a glass homogenizer. The homogenate was then transferred into a 15 mL Falcon tube, and 3 µL of 1 M ascorbic acid was added into the 3 mL of enzyme homogenate to reach a final concentration of 1 mM.

In a 1.5 mL Eppendorf tube, 2.52 µg isotopically labeled tryptophan (840 ng [$^{13}C_{11,}$$^{15}N_2$]tryptophan per mL of maize endosperm) was mixed with 12.6 µg of unlabeled intermediate (4200 ng testing intermediate per mL of maize endosperm).

To start the reaction, the mixture of isotopically labeled tryptophan and unlabeled testing intermediate was transferred into the 15 mL Falcon tube containing maize endosperm. The start time of this reaction was recorded and 0.25 mL aliquots were removed and quenched at reaction time intervals of: 0 minute; 2 minutes; 4 minutes; 8 minutes; 16 minutes; 32 minutes; 64 minutes; 128 minutes; and 256 minutes. After the aliquots were obtained, 25 ng [$^{13}C_6$]IAA was added into each aliquot tube for quantification purposes. The aliquots were then quenched by boiling for 5 minutes and

subjected to centrifugation at 10,000 g for 5 minutes. The supernatant was then removed to a new tube and buffered with an equal volume of 50:50 1M phosphoric acid: sodium phosphate, pH 2.5.

Labeled and unlabeled IAA were extracted, methylated and quantified following the same protocol discussed in Section 2.2.2.2. The initial velocity and production percentage of the [$^{13}C_{10}$,$^{15}N_1$]IAA biosynthesis reaction were determined by calculating the ratio of [$^{13}C_{10}$,$^{15}N_1$]IAA ions at *m/z* 140, to the internal standard [$^{13}C_6$] IAA ions at *m/z* 136.

3.2.2 Oxygen depletion experiment

One 3 mL conical bottomed glass reaction vial (Item # W986297NG, Wheaton, Millville, NJ) was used for preparing the isotopically labeled substrate solution. As discussed below, one 5 mL conical bottomed glass reaction vial (Item # W986299NG, Wheaton, Millville, NJ) was used for preparing the maize endosperm enzyme sample and housing the enzyme reaction and another 5 mL conical bottomed glass reaction vial contained argon gas that was used to flush the syringes. The experimental instrument setup is shown in Figure 3-8, Panels A, B and C.

The substrate [$^{13}C_{11}$,$^{15}N_2$]tryptophan solution was prepared, and the concentration of the solution was determined by a spectrophotometer. The molar extinction coefficient of IAA in methanol is 6060 at 282 nm in the UV absorption spectrum (Bandurski et al., 1974). The concentration of [$^{13}C_{11}$,$^{15}N_2$]tryptophan was 5.78 µM. This substrate solution was sealed using a polypropylene hole cap with a Teflon PTFE/silicone septum in a 3 mL glass reaction vial. The vial was purged with argon gas and maintained at a slightly positive pressure using a bubbler connected to the reaction vial via Tygon gas lines and

needles (**Figure 3-8, panel A**). The tip of the argon gas supply needle was submerged in the substrate solution to help remove dissolved oxygen from solution. The vial was flushed with argon gas for 5 minutes to ensure complete removal of air trapped in the vial and dissolved in the solution. The argon source and bubbler were removed after the completion of argon flushing.

A total of 1 mL of maize endosperm (purification stage 2) was thawed on ice and mixed with 5 mL of prechilled 50mM POPSO buffer pH 8.5, containing 4mM EDTA. The mixture was homogenized in a glass homogenizer (only needed about 10 passes up and down because the maize endosperm stage 2 aliquots were homogenized well before they stored in -80 °C freezer). The volume of the enzyme homogenate used in the reaction was determined based on the concentration of [$^{13}C_{11}$,$^{15}N_2$]tryptophan solution. For this experiment, the maize endosperm enzyme sample, the [$^{13}C_{11}$,$^{15}N_2$]tryptophan substrate solution, and 5 µl of 1 M ascorbic acid were combined to make a 5 mL reaction system. 840 ng [$^{13}C_{11}$,$^{15}N_2$]tryptophan per mL of reaction volume was used in this oxygen depletion experiment. The volume of [$^{13}C_{11}$,$^{15}N_2$]tryptophan solution was calculated, and then the volume of maize endosperm sample was calculated accordingly to reach a final reaction volume of 5 mL.

After volume calculations, the determined amount of maize endosperm enzyme sample was transferred into the 5 mL conical bottomed glass reaction vial. 5 µL of 1 M ascorbic acid was added into the enzyme sample to reach a final concentration of 1 mM. A V-shape stirring bar was placed in the glass vial. This 5 mL reaction vial containing maize endosperm enzyme sample was sealed by a polypropylene hole cap with a Teflon PTFE/silicone septum. The reaction vial was placed on ice. The magnetic stirrer was

turned on and the argon source needle and a bubbler needle was inserted. The apparatus setup is shown in **Figure 3-8, panel B**. In order to avoid enzyme denaturation that may result from bubbling through the protein solution, both needle tips were positioned above the maize endosperm solution. The reaction vial was flushed with argon gas for about 20 minutes to sufficiently remove air from the reaction system. The argon flush was continuously supplied in this enzyme reaction vial during the entire oxygen depleted stage in order to promptly remove the minimal amount of air that may be introduced by syringe injections during the enzyme reaction and to maintain the reaction atmosphere at slightly above atmospheric pressure during the experiment.

A clean and empty 5 mL glass vial was sealed by a polypropylene hole cap with a Teflon PTFE/silicone septum. The argon source and bubbler needles were inserted through the septa. The empty glass vial was flushed with argon gas for 1 minute. This argon vial was used for flush the dead space in the syringes prior to use.

Before starting the reaction, ice used to cool the maize endosperm enzyme sample was removed. The temperature of the reaction system was allowed to equilibrate to 25 °C. The dead space of the syringe was flushed with argon using the argon gas vial. To start the reaction, the syringe needle was rapidly taken out from the argon gas vial and inserted in the substrate vial. The substrate solution was drawn from the 3 mL glass vial that containing the [$^{13}C_{11}$,$^{15}N_2$]tryptophan solution. The substrate was injected immediately into the 5 mL reaction glass vial that containing the maize endosperm enzyme sample (See **Figure 3-8, panel C**). The reaction start time was recorded.

Aliquots of 0.25 mL volume were removed from the 5 mL reaction using an argon-flushed syringe at six time points (0 minutes, 2 minutes, 4 minutes, 8 minutes, 16

minutes and 32 minutes) during the oxygen depleted stage. The syringe used to take aliquots was argon flushed using the argon vial, each time before drawing the samples. Once the reaction aliquot was taken from the oxygen depleted enzyme reaction vial, it was quenched immediately and IAA was extracted by mixing vigorously in the stop reagent mixture. The stop reagent mixture was composed of 0.25 mL 50:50 1 M phosphoric acid: sodium phosphate, pH 2.5 and 0.4 mL ethyl acetate. A quantity of 25 ng [$^{13}C_6$]IAA was used as an internal standard in each aliquot for quantification.

Oxygen was introduced into the enzyme reaction system after 32 minutes, by removing the argon source needle, the bubbler needle, and the vial cap. Aliquots of 0.25 mL volume were taken from the reaction vial at eight times points (33 minutes, 34 minutes, 36 minutes, 40 minutes, 48 minutes, 64 minutes, 96 minutes and 160 minutes), transferred to the stop reagent mixtures, and processed as described above.

IAA was methylated and quantified following the protocol described in Section 2.2.2.2. The conversion percentages of [$^{13}C_{11}$,$^{15}N_2$]tryptophan to [$^{13}C_{10}$, $^{15}N_1$]IAA were determined by calculating the ratio of [$^{13}C_{10}$,$^{15}N_1$]IAA ions at *m/z* 140 and 200, to the internal standard [$^{13}C_6$]IAA ions at *m/z* 136 and 195.

3.2.3 $^{18}O_2$ labeling experiment

3.2.3.1 Oxygen depleted reaction stage

A mixture of 1 mL of maize endosperm (purification stage 2) and 5 mL prechilled 50mM POPSO buffer pH 8.5, containing 4mM EDTA was homogenized by a glass homogenizer. 1 M ascorbic acid was added to the enzyme sample to reach a final concentration of 1 mM. The volume of the enzyme reaction system was 5 mL. The

enzyme component of this reaction was sealed in a 5 mL conical bottomed glass reaction vial using a polypropylene hole cap with a Teflon PTFE/silicone septum. The [$^{13}C_{11}$,$^{15}N_2$]tryptophan solution was prepared and sealed in a separate 3 mL glass vial with a similar cap assembly. Air was completely removed from both the enzyme reaction vial and the substrate solution vial by flushing with argon.

The apparatus and experimental procedure of the oxygen depleted stage of $^{18}O_2$ labeling experiment were essentially the same as described above in section 3.2.2. (See **Figure 3-8, panel A, B and C**). 840 ng [$^{13}C_{11}$,$^{15}N_2$]tryptophan per mL of reaction volume was used in the $^{18}O_2$ labeling experiment. The substrate was injected into the 5 mL reaction glass vial to start the reaction. Reaction aliquots were taken out of the reaction by syringes. Once being drawn out from the oxygen depleted reaction vial, all aliquots were quenched immediately and IAA extracted simultaneously in the stop reagent mixture described in section 3.2.2. Five 0.25mL sample aliquots were taken from the reaction sequentially during the oxygen depleted stage at 1 minutes, 2 minutes, 4 minutes, 8 minutes and 16 minutes.

3.2.3.2 $^{18}O_2$ labeling reaction stage

The $^{18}O_2$ labeling reaction stage of this experiment is shown in **Figure 3-8, panel D**. The reaction vial was supplied with the gas mix of 99 atom% $^{18}O_2$ and argon gas in a 1:4 ratio (item# 578673, Sigma Aldrich, St Louis, MO) after 16 minutes. The $^{18}O_2$ labeling reaction stage was sampled by taking aliquots at 18 minutes, 20 minutes, 24 minutes, 32 minutes, 48 minutes, 80 minutes and 144 minutes. Aliquots were taken out of the reaction vials, quenched and extracted in the same way as in the oxygen depleted stage described in section 3.2.2.

3.2.3.3 Data analysis

IAA was methylated following the same protocol discussed in section 2.2.2.2. The samples were analyzed using the Thermos Fisher triple quadruple tandem mass spectrometer in the Selected Reaction Monitoring (SRM) method. The production percentage of [$^{13}C_{10}$,$^{15}N_1$]IAA synthesized from [$^{13}C_{11}$,$^{15}N_2$]tryptophan was determined by calculating the ratio of [$^{13}C_{10}$,$^{15}N_1$]IAA ions to the internal standard [$^{13}C_6$]IAA ions. The production percentage of [$^{13}C_{10}$,$^{15}N_1$,$^{18}O_1$]IAA was determined by calculating the ratio of [$^{13}C_{10}$,$^{15}N_1$,$^{18}O_1$]IAA ions to the internal standard [$^{13}C_6$]IAA ions. The [$^{13}C_{10}$,$^{15}N_1$]IAA production were measured by monitoring the *m/z* transition of precursor ion to quinolinium ion from 200 to 140, the [$^{13}C_{10}$,$^{15}N_1$,$^{18}O_1$]IAA ions were measured by monitoring the *m/z* transition from 202 to 140, and the internal standard [$^{13}C_6$]IAA ions were measured by *m/z* transition from 195 to 136.

3.3 Results

3.3.1 Isotopic label dilution assays

In the isotopic label dilution assays, the reaction of [$^{13}C_{11}$,$^{15}N_2$]tryptophan to [$^{13}C_{10}$,$^{15}N_1$]IAA with the addition of five unlabeled IAA intermediates have been measured. The percentage of [$^{13}C_{10}$,$^{15}N_1$]IAA synthesized over a time span of 256 minutes are shown with the inclusion of either the IAAld potential intermediate in **Figure 3-2**, IAM potential intermediate in **Figure 3-3**, IAN potential intermediate in **Figure 3-4**, TAM potential intermediate in **Figure 3-5,** or IPyA potential intermediate in **Figure 3-6**.

The initial rate of [$^{13}C_{11}$,$^{15}N_2$]tryptophan (840 ng per mL of maize endosperm stage 2) to [$^{13}C_{10}$,$^{15}N_1$]IAA is 10.99 ng min^{-1} mL^{-1} (S.D. +/- 0.18) without unlabeled

intermediate. With the addition of 5 times excess amount of IPyA (4.2 µg per mL), the initial rate of [$^{13}C_{11}$,$^{15}N_2$]tryptophan conversion to [$^{13}C_{10}$,$^{15}N_1$]IAA drops to 3.67 ng min^{-1} mL^{-1} (S.D. +/- 0.14). Whereas with the addition of 5 times excess amount (4.2 µg per mL) of IAAld, IAN, IAM or TAM, the initial rates of [$^{13}C_{11}$,$^{15}N_2$]tryptophan conversion to [$^{13}C_{10}$,$^{15}N_1$]IAA were 8.40 ng min^{-1} mL^{-1} (S.D. +/- 0.30), 9.62 ng min^{-1} mL^{-1} (S.D. +/- 0.18), 10.27 ng min^{-1} mL^{-1} (S.D. +/- 0.26) and 10.96 ng min^{-1} mL^{-1} (S.D. +/- 0.09) respectively. These results are listed in **Table 3-1** and shown graphically in **Figure 3-7**. Within the time range of 256 minutes, the final extent of conversion of [$^{13}C_{11}$,$^{15}N_2$]tryptophan to [$^{13}C_{10}$,$^{15}N_1$]IAA with no unlabeled intermediate addition was 57.40% (S.D. +/- 3.15%), and the final conversion percentage dropped to 25.17% (S.D. +/- 0.72) with the addition of 5 times excessive amount of unlabeled IPyA. Whereas the final conversion percentage of [$^{13}C_{11}$,$^{15}N_2$]tryptophan to [$^{13}C_{10}$,$^{15}N_1$]IAA with the addition of IAAld, IAN, IAM and TAM were 62.43% (S.D. +/- 1.10%), 64.25% (S.D. +/- 0.55%), 69.13% (S.D. +/- 2.74%) and 69.31% (S.D. +/- 2.17%). These final conversion percentage data are provided in **Table 3-2** and shown graphically in **Figure 3-8**.

3.3.2 Oxygen depletion Assay

As shown in **Figure 3-10**, during the oxygen depleted stage, the biosynthesis conversion percentage of [$^{13}C_{11}$,$^{15}N_2$]tryptophan to [$^{13}C_{10}$,$^{15}N_1$]IAA increased slightly from 3% to 7% during the 32 minutes following enzyme addition. After removing the cap of the reaction vial, the reaction system was exposed to the air. During this oxygen restored stage, the biosynthesis conversion percentage of [$^{13}C_{11}$,$^{15}N_2$]tryptophan to [$^{13}C_{10}$,$^{15}N_1$]IAA increased over time from an initial value of ~6-7% to 25% at 160 minutes.

3.3.3 $^{18}O_2$ labeling experiment

The data are shown in **Figure 3-11**. The conversion of [$^{13}C_{11}$,$^{15}N_2$]tryptophan to [$^{13}C_{10}$,$^{15}N_1$]IAA during the oxygen depleted stage again increased only slightly from ~0.6% to 1.6% over 16 minutes. The reaction was then supplied with a gas mix of 99 atom% $^{18}O_2$ and argon gas in a 1:4 ratio. During this $^{18}O_2$ restored stage, the percent conversion of [$^{13}C_{11}$,$^{15}N_2$]tryptophan to [$^{13}C_{10}$,$^{15}N_1$]IAA increased steadily from ~1.6% to ~3.5% over 144 minutes.

The production of [$^{13}C_{10}$,$^{15}N_1$,$^{18}O_1$]IAA from [$^{13}C_{11}$,$^{15}N_2$]tryptophan and natural abundance $^{18}O_2$ was negligible. With the supply of ^{18}O labeled 20% oxygen in argon gas, the production of [$^{13}C_{10}$,$^{15}N_1$,$^{18}O_1$]IAA increased steadily to 12.13% at 144 minutes.

3.4 Discussion

The results from isotopic label dilution experiment, oxygen depletion and $^{18}O_2$ labeling experiment support the same conclusion that the VT2/SPI1 pathway is the predominant pathway amongst the tryptophan-dependent biosynthesis routes in in maize endosperm. The work in this chapter also developed important experimental protocols that will facilitate future $^{18}O_2$ labeling experiments in IAA biosynthesis studies *in vitro* and *in vivo.*

3.4.1 Isotopic label dilution experiments

In the isotopic label dilution assay, unlabeled biosynthetic pathway intermediates (IAAld, IAN, IAM, TAM and IPyA) were tested individually to see if their addition in excess would reduce the fold enrichment of labeled IAA generated from labeled tryptophan in the maize endosperm system.

The data demonstrates that an addition of unlabeled IPyA in 5-fold excess over labeled tryptophan decreased the initial rate of isotopic labeled IAA biosynthesis by about 3-fold, and dropped the total conversion percentage to half that of control lacking cold IPyA. These data suggest that IPyA is a major intermediate in tryptophan-dependent IAA biosynthesis in the maize endosperm *in vitro* system. However, the initial rate of IPyA addition sample is not as expected as 1/6 of the control initial rate. The much higher initial rate been detected may be due to the fact that IPyA is very labile in aqueous environment. One possible explanation is that, during the preparation and the introduction of the IPyA solution into the reaction system, a unneglectable amount of IPyA was likely diverged to the non-enzymatic conversions, instead of being fed in the IAA biosynthesis pathways. The additions of unlabeled intermediates, IAAld, IAN, IAM and TAM, did not dramatically interfere with the reaction initial rates. While some reduction in observed initial rate may be due to competitive inhibition, rather than intermediate pool dilution, the absence of a significant difference in percent conversion vs. control supports the conclusion that pathways involving intermediates IAAld, IAN, IAM and TAM were not significantly utilized for IAA production. These isotope dilution experiments strongly suggest that IAAld, IAN, IAM and TAM are not the major intermediates in the tryptophan-dependent IAA biosynthesis pathways.

3.4.2 Oxygen depletion Assay

The oxygen depletion experiment demonstrated the maize endosperm pathway is oxygen dependent. The production of [$^{13}C_{10}$,$^{15}N_1$]IAA is greatly inhibited when oxygen was removed from the maize endosperm reaction system within the time range of 0 to 32

minutes; the enzymatic activity was immediately restored, when resupplying oxygen at the 32-minutes time point.

Small amounts of oxygen are sufficient to support the YUCCA reaction. In the oxygen depletion experiment, therefore, it is critical to follow the protocol that includes removing all oxygen dissolved in solutions, flushing the maize endosperm reaction vial continuously with argon gas, and flushing the dead space of syringes each time before taking samples. Note that there is a slight increase in the initial 16 minutes (See **Figure 3-10**), that is likely to be due to residual oxygen in the system, or possibly due to oxygen introduced during the initial substrate injection. It is important to note, however, that a new plateau is reached fairly quickly as would be consistent with consumption of small amounts of residual oxygen, but that the reaction does not proceed until additional oxygen is introduced into the reaction vessel. These experiments demonstrate that after the minimal amount of residual oxygen was consumed, the enzymatic synthesis of new IAA production stops and that production resumes once oxygen is restored to the reaction.

3.4.3 $^{18}O_2$ labeling experiment

Note that for these experiments, the protocol for quenching and extracting IAA product from reaction aliquots was modified to avoid acid, which catalyzes oxygen/solvent exchange from carboxylic acids, and to remove the IAA as quickly as possible into a distinct ethyl acetate phase so that even uncatalyzed oxygen/solvent exchange is minimized. In experiments other than oxygen depletion and $^{18}O_2$ labeling experiment, the sample aliquots were boiled for 5 minutes and centrifuged at 10,000 × g for 5 minutes. Then the supernatant was transferred to an acidic reaction stop reagent

(50:50 1 M phosphoric acid to sodium phosphate buffer pH 2.5). IAA was then extracted from the quenched reaction mixture by adding ethyl acetate. In the modified protocol used for the $^{18}O_2$ labeling experiments, however, reaction aliquots were quenched by transfer into a two-phase mixture of acidic reaction stop reagent and ethyl acetate immediately followed by vigorous mixing. Under these conditions the reaction was quenched and IAA was extracted into the ethyl acetate immediately minimizing oxygen exchange chemistry. This modification maintains rapid enzymatic quenching while minimizing ^{18}O to ^{16}O back exchange.

The sole entry point of molecular oxygen (O_2) among all tryptophan-dependent IAA biosynthetic pathways is via the VT2/SPI1 (or TAA1/YUCCA) pathway. Thus, one can selectively label the IAA produced by the VT2/SPI1 pathway using the [^{18}O]-labeled oxygen gas. The IAA product synthesized from [$^{13}C_{11}$,$^{15}N_2$]tryptophan via the VT2/SPI1 pathway will be incorporate ^{18}O from molecular oxygen resulting in the [^{18}O]-labeled [$^{13}C_{10}$,$^{15}N_1$,$^{18}O_1$]IAA product. The reaction mechanism is shown in **Figure 3-13**. The IAA product synthesized from [$^{13}C_{11}$,$^{15}N_2$]tryptophan via other pathways do not use oxygen in the reactions. Thus, the IAA generated from other proposed tryptophan-dependent pathways will be in the form of [$^{13}C_{10}$,$^{15}N_1$]IAA. The unique oxygen incorporation characteristics of VT2/SPI1 pathway enables us to measure the relative utilization of the VT2/SPI1 pathway vs. other tryptophan-dependent IAA biosynthesis pathways. As shown in the results, the IAA biosynthesis from the VT2/SPI1 pathway is the major pathway. Assuming there was no $^{16}O/^{18}O$ back exchange during the experiment, IPyA pathway in maize constituted 80% of the IAA production via the tryptophan-dependent pathways. Considering there were still likely a minimal amount of

$^{16}O/^{18}O$ back exchange events occurred during the experiment process, it can be assumed that the IPyA pathway constituted more than the measured 81% of the IAA production through tryptophan-dependent pathways in the maize endosperm *in vitro* system.

One future research direction of this work will be to apply the [^{18}O]-labeling technique to the study of IAA biosynthesis pathway *in vivo*. By using ^{18}O to selectively incorporate label into IAA via the IPyA pathway, one can potentially measure the relative involvement of the IPyA pathway in various auxin-mediated phenomena in plants. These include, but are not limited to: photomorphogenic responses, such as shade avoidance responses, high temperature responses, tropism responses, and wounding responses.

We can consider the shade avoidance response as an example because a study by Tao and coworkers (Tao et al., 2008) demonstrated that IPyA pathway plays an important role in the shade avoidance response. The low red to far-red (R:FR) ratio perceived by phytochromes triggered TAA1 overexpression and increased the free IAA level, and then upregulated the downstream shade avoidance syndrome (SAS) in plants (Tao et al., 2008). To answer the question regarding to what extent the IPyA pathway was involved in the shade avoidance responses, we can label the IPyA pathway by eliminating $^{16}O_2$ gas during the growing conditions, keeping etiolated seedlings in dark phase to block photosynthesis, and flushing the growth chamber with $^{18}O_2$ gas. By control of light quality in a photomorphogenic level to induce shade avoidance response in plants, we can quantify [^{18}O]-IAA production and measure IAA biosynthesis via the IPyA pathway. This labeling strategy has significant potential for providing novel insight into the function and regulation of overlapping auxin biosynthetic pathways and auxin mediated environmental/developmental signaling.

3.4.4 Conclusions

With these experiments, I have shown that the YUCCA pathway is the major tryptophan-dependent IAA biosynthesis pathway in the maize endosperm *in vitro* system. This conclusion is supported by both isotopic label dilution experiments where IPyA, the major intermediate in the YUCCA pathway, causes the largest fold dilution of label of all of the pathway intermediates tested. The conclusion is also supported by: 1) the low level of IAA synthesis observed under conditions of oxygen depletion; and 2) the incorporation of ^{18}O into IAA observed in the [$^{18}O_2$]-labeling experiments.

3.5 Tables

Intermediate addition	Initial rate (ng min^{-1} ml^{-1})
None	10.99 ± 0.18
IPyA addition	3.67 ± 0.14
IAAld addition	8.40 ± 0.30
IAN addition	9.62 ± 0.18
IAM addition	10.27 ± 0.26
TAM addition	10.96 ± 0.09

Table 3-1. Initial rate of [$^{13}C_{11}$,$^{15}N_2$]tryptophan to [$^{13}C_{10}$,$^{15}N_1$]IAA conversion in the presence and absence of a five-fold excess each of five intermediates, IPyA, IAAld, IAN, IAM and TAM.

Intermediate addition	Trp to IAA conversion (%)
None	57.40 ± 3.15
IPyA addition	25.17 ± 0.72
IAAld addition	62.43 ± 1.10
IAN addition	64.25 ± 0.55
IAM addition	69.13 ± 2.74
TAM addition	69.31 ± 2.17

Table 3-2. Conversion percentage of [$^{13}C_{11}$,$^{15}N_2$]tryptophan to [$^{13}C_{10}$,$^{15}N_1$]IAA over a time period of 256 minutes in the presence and absence of five-fold excess each of five intermediates, IPyA, IAAld, IAN, IAM and TAM.

3.6 Figures

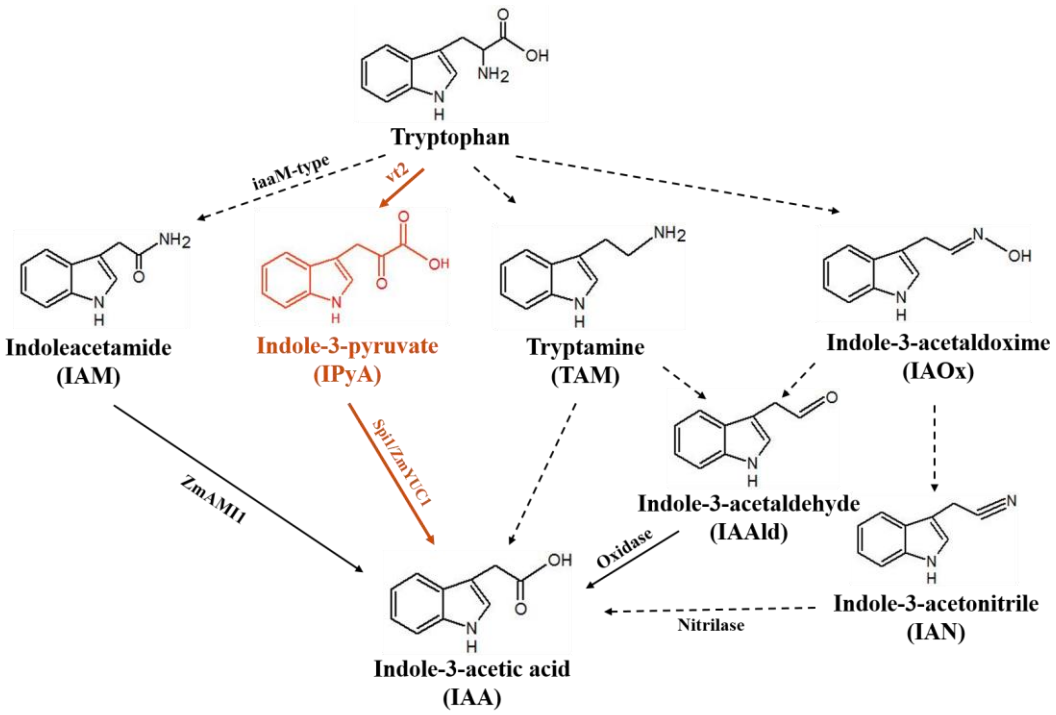

Figure 3-1. Potential tryptophan-dependent IAA biosynthesis pathways in Z. mays. The solid lines represent the pathways/reactions have been reported. The dotted lines represent the pathway/reactions have not been confirmed in maize.

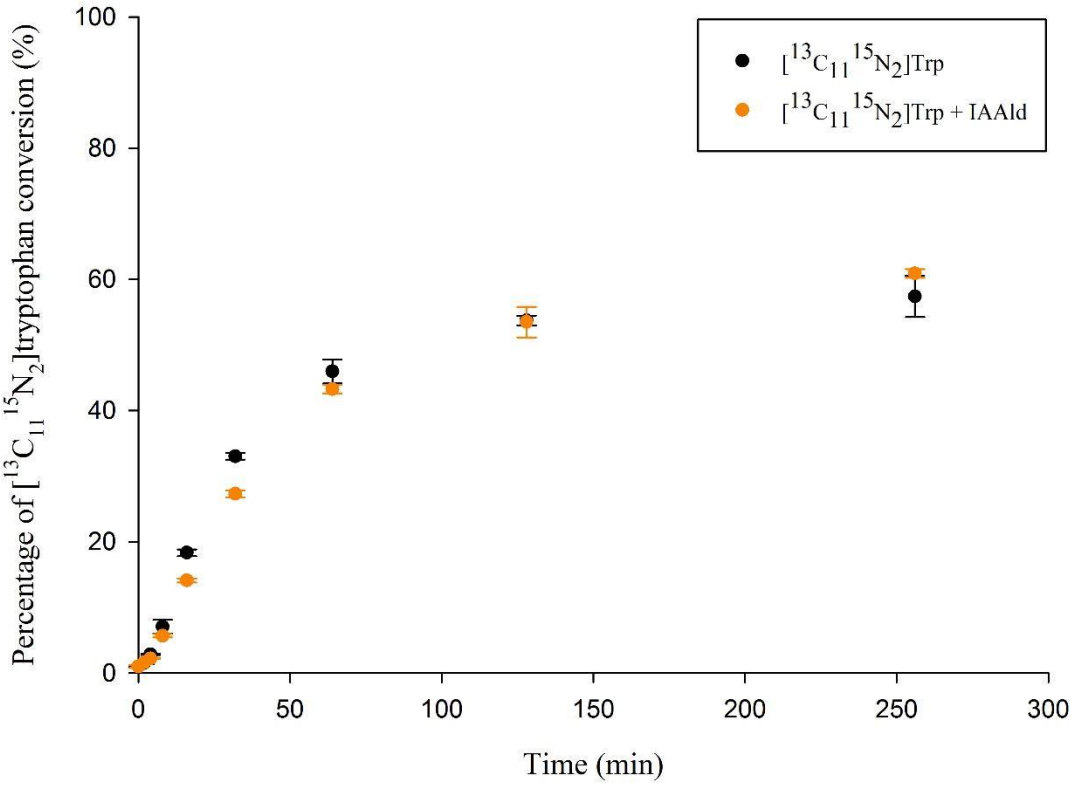

Figure 3-2. Conversion of [$^{13}C_{11}$,$^{15}N_2$]tryptophan to [$^{13}C_{10}$,$^{15}N_1$]IAA in 256 minutes in the presence and absence of large amounts of IAAld (4.2ug IAAld per ml of stage 2 purified maize endosperm enzymes). Error bars represent standard deviation from the mean of three replicates for each treatment.

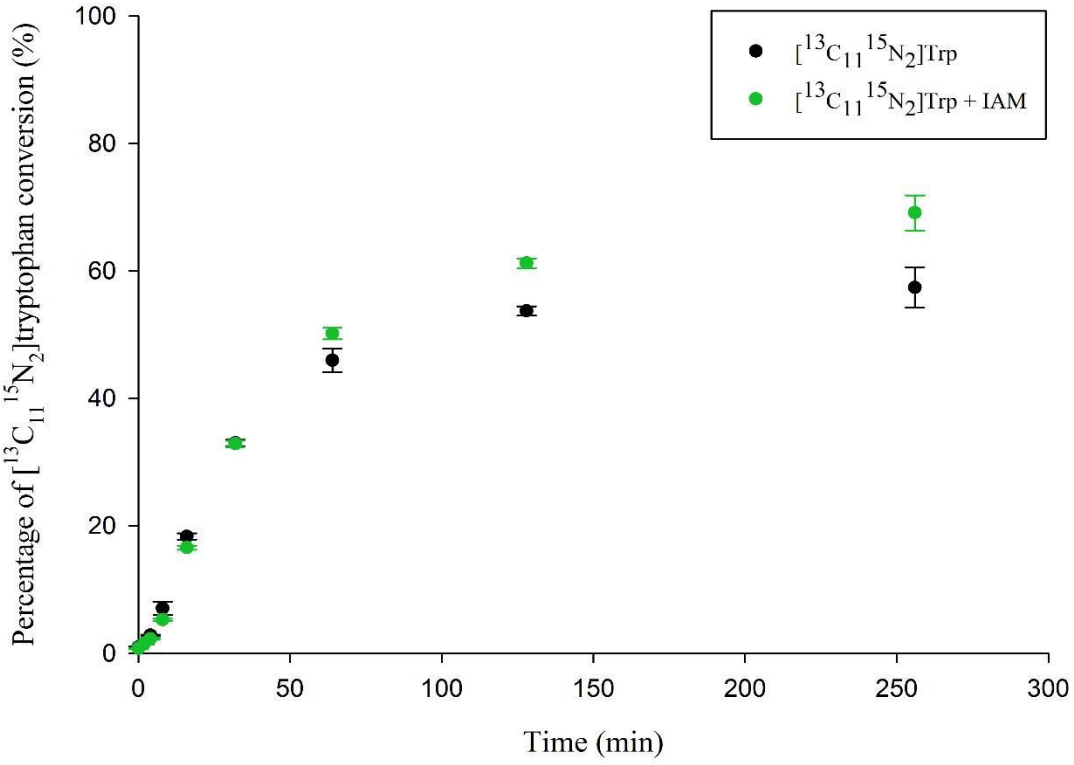

Figure 3-3. Conversion of [$^{13}C_{11}$,$^{15}N_2$]tryptophan to [$^{13}C_{10}$,$^{15}N_1$]IAA in 256 minutes in the presence and absence of large amounts of IAM (4.2ug IAM per ml of stage 2 purified maize endosperm enzymes). Error bars represent standard deviation from the mean of three replicates for each treatment.

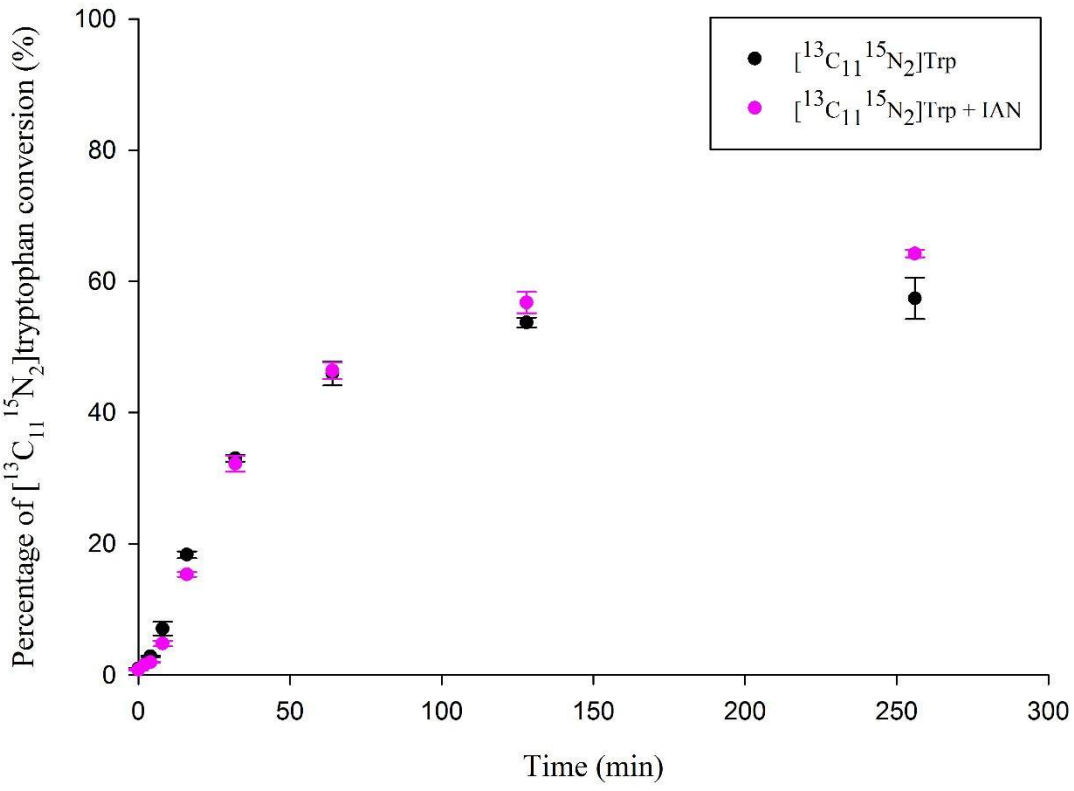

Figure 3-4. Conversion of [$^{13}C_{11}$,$^{15}N_2$]tryptophan to [$^{13}C_{10}$,$^{15}N_1$]IAA in 256 minutes in the presence and absence of large amounts of IAN (4.2ug IAN per ml of stage 2 purified maize endosperm enzymes). Error bars represent standard deviation from the mean of three replicates for each treatment.

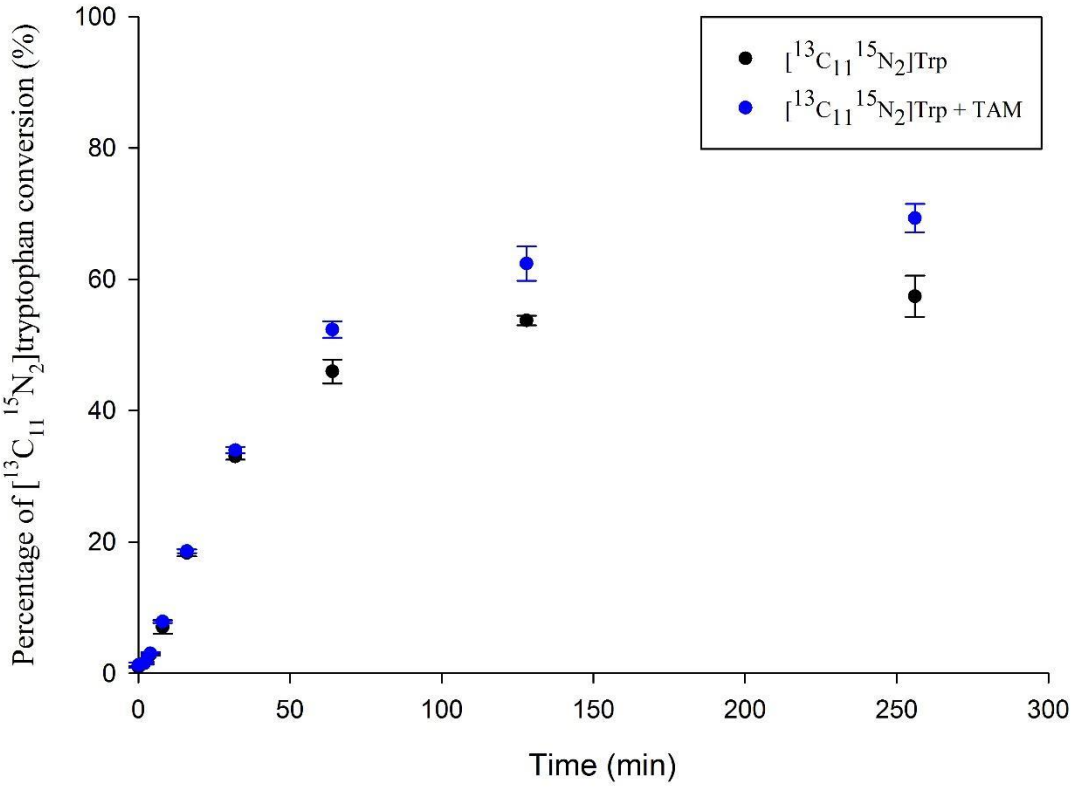

Figure 3-5. Conversion of [$^{13}C_{11}$,$^{15}N_2$]tryptophan to [$^{13}C_{10}$,$^{15}N_1$]IAA in 256 minutes in the presence and absence of large amounts of TAM (4.2ug TAM per ml of stage 2 purified maize endosperm enzymes). Error bars represent standard deviation from the mean of three replicates for each treatment.

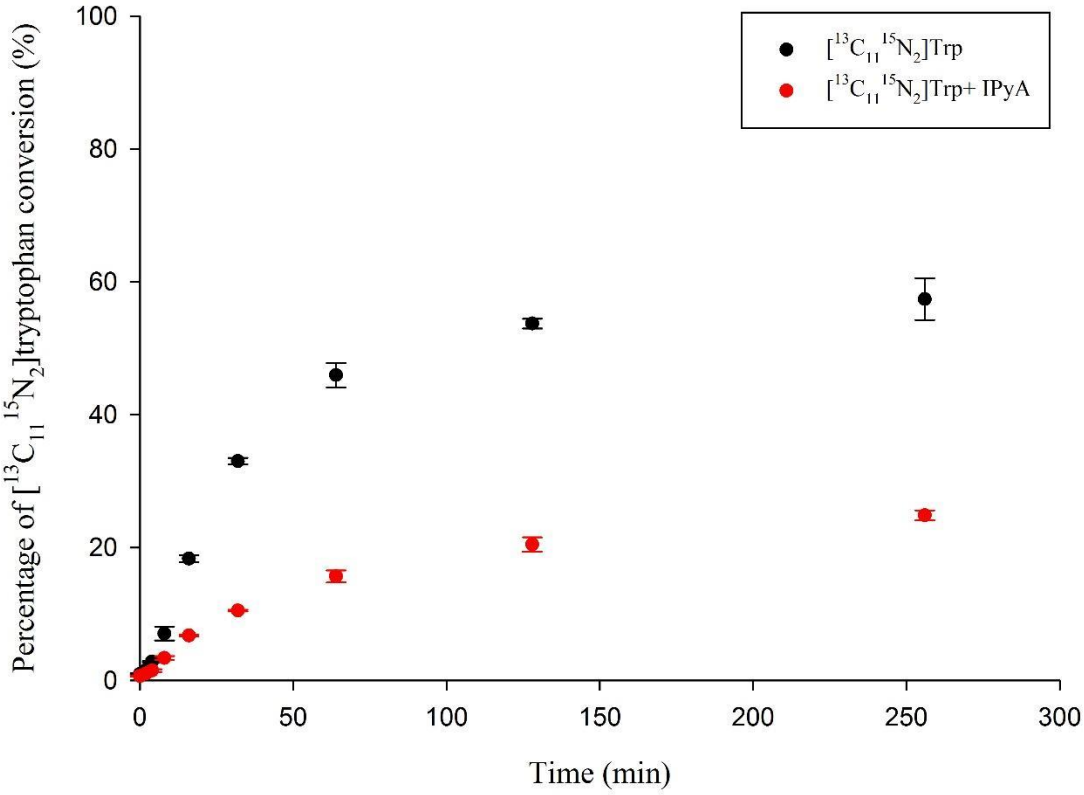

Figure 3-6. Conversion of [$^{13}C_{11}$,$^{15}N_2$]tryptophan to [$^{13}C_{10}$,$^{15}N_1$]IAA in 256 minutes in the presence and absence of large amounts of IPyA (4.2ug IPyA per ml of stage 2 purified maize endosperm enzymes). Error bars represent standard deviation from the mean of three replicates for each treatment.

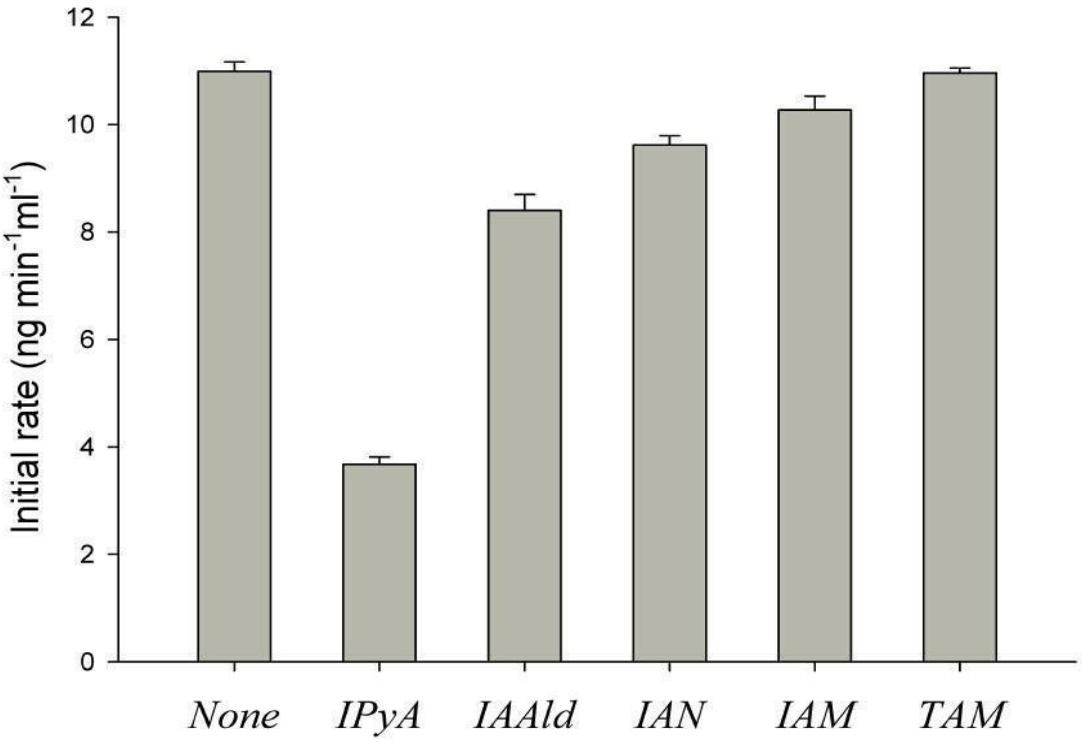

Figure 3-7. The initial rates of [$^{13}C_{11}$,$^{15}N_2$]tryptophan conversion to [$^{13}C_{10}$,$^{15}N_1$]IAA, with no intermediate addition (Column 1), and with 5 times excess addition of intermediates, IPyA, IAAld, IAN, IAM and TAM respectively (Column 2-5).

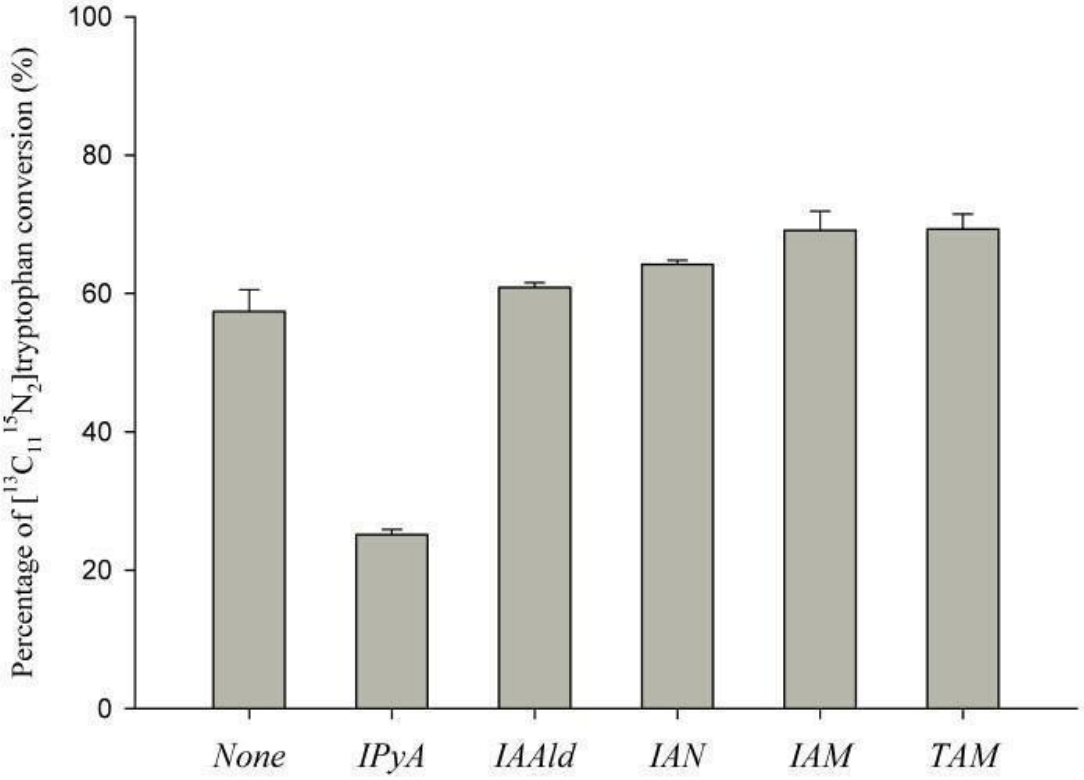

Figure 3-8. Percentage of [$^{13}C_{11}$,$^{15}N_2$]tryptophan conversion in 256 minutes with no intermediate addition (Column 1), and with 5 times excess addition of intermediates, IPyA, IAAld, IAN, IAM and TAM respectively (Column 2-5).

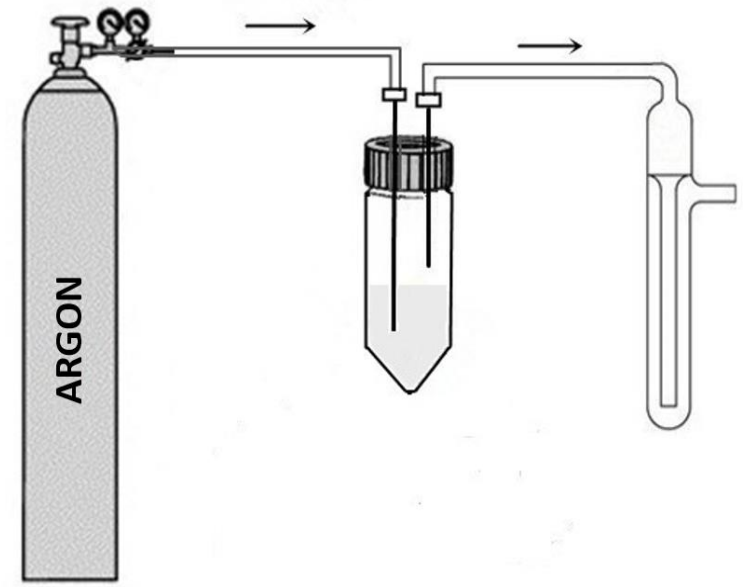

(A)

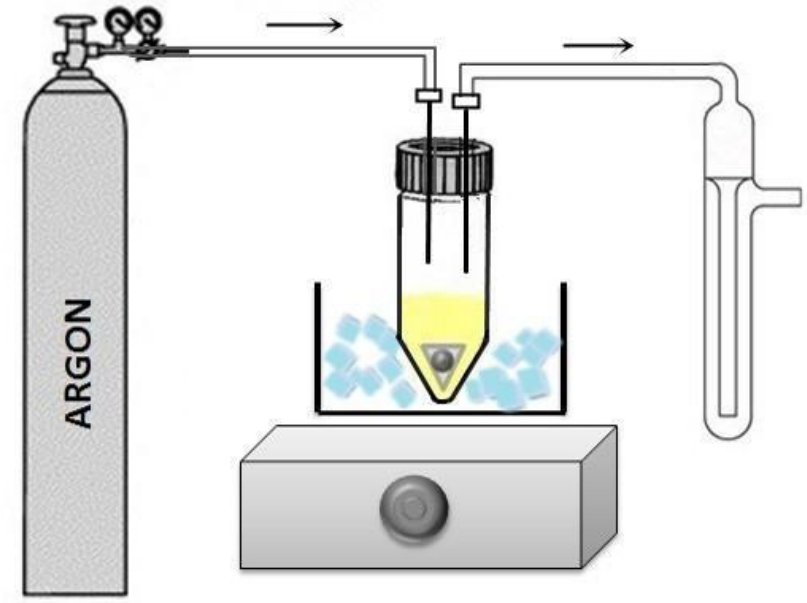

(B)

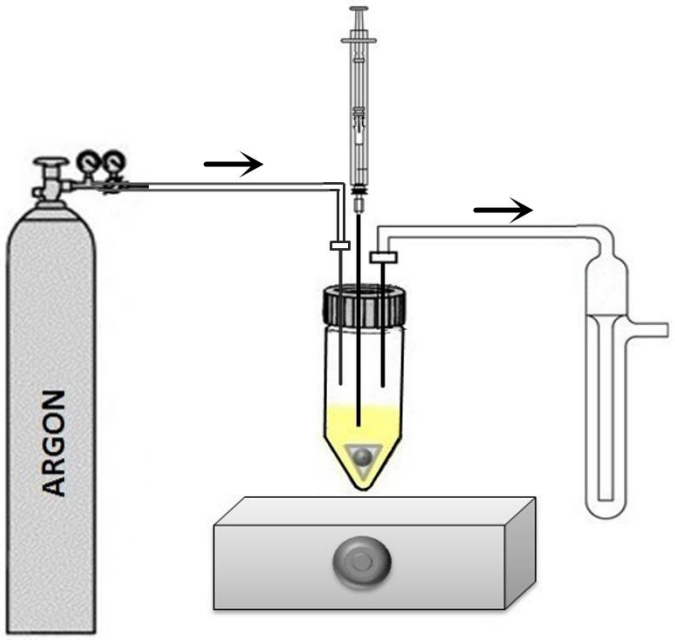

(C)

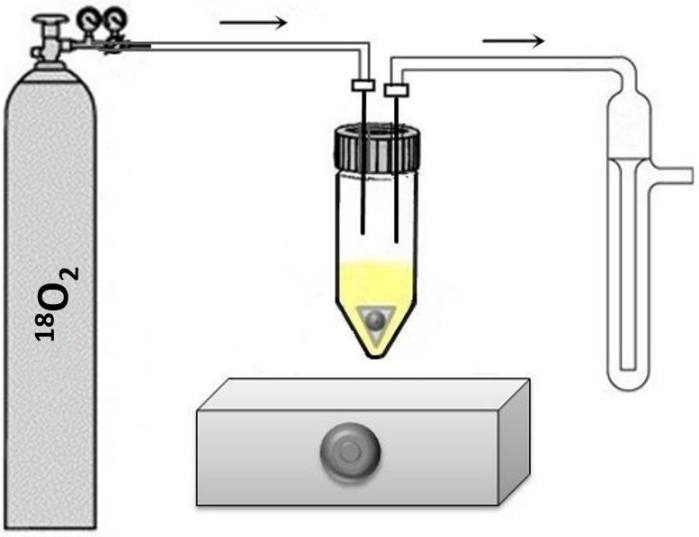

(D)

Figure 3-9. The instrument setup for oxygen depletion experiment (Panel A, B and C; discussed in section 3.2.2), and $^{18}O_2$ labeling experiment (Panel A, B, C and D; discussed in section 3.2.3).

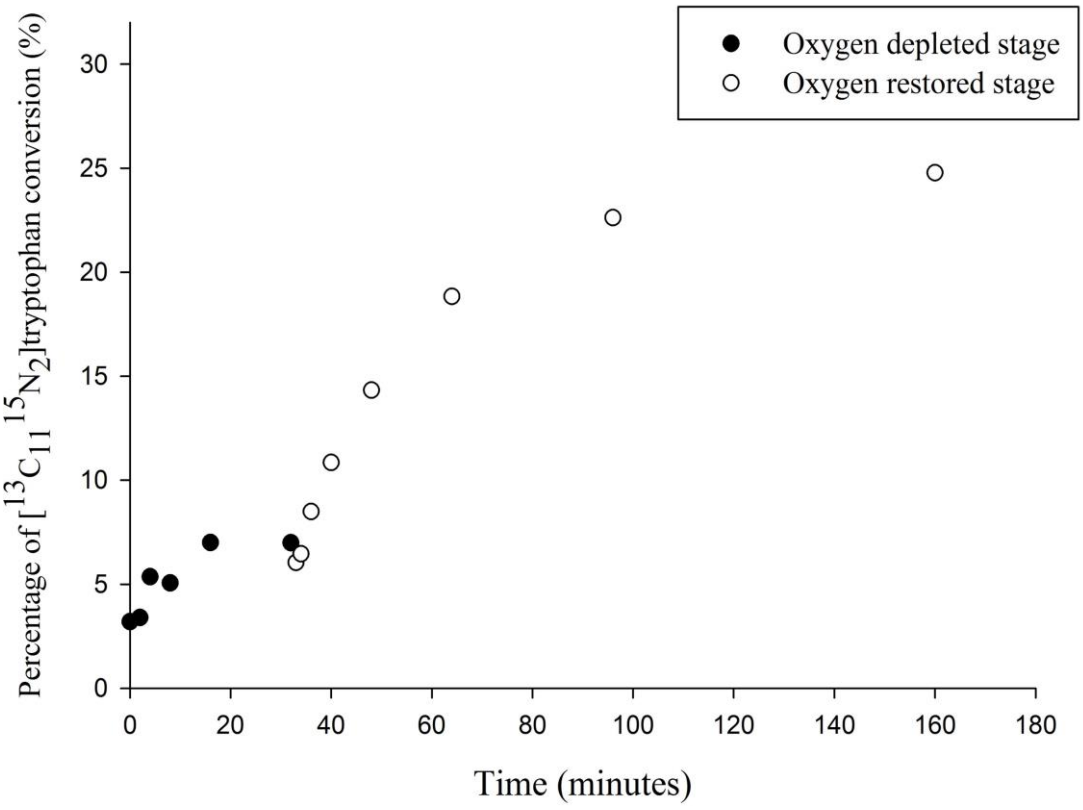

Figure 3-10. Oxygen depletion experiment. The reaction was started by adding [$^{13}C_{11}$,$^{15}N_2$]tryptophan in to an oxygen-depleted reaction system. The reaction was exposed to air at time point 32 minutes. Each dot represents the sampling time in a continuous reaction.

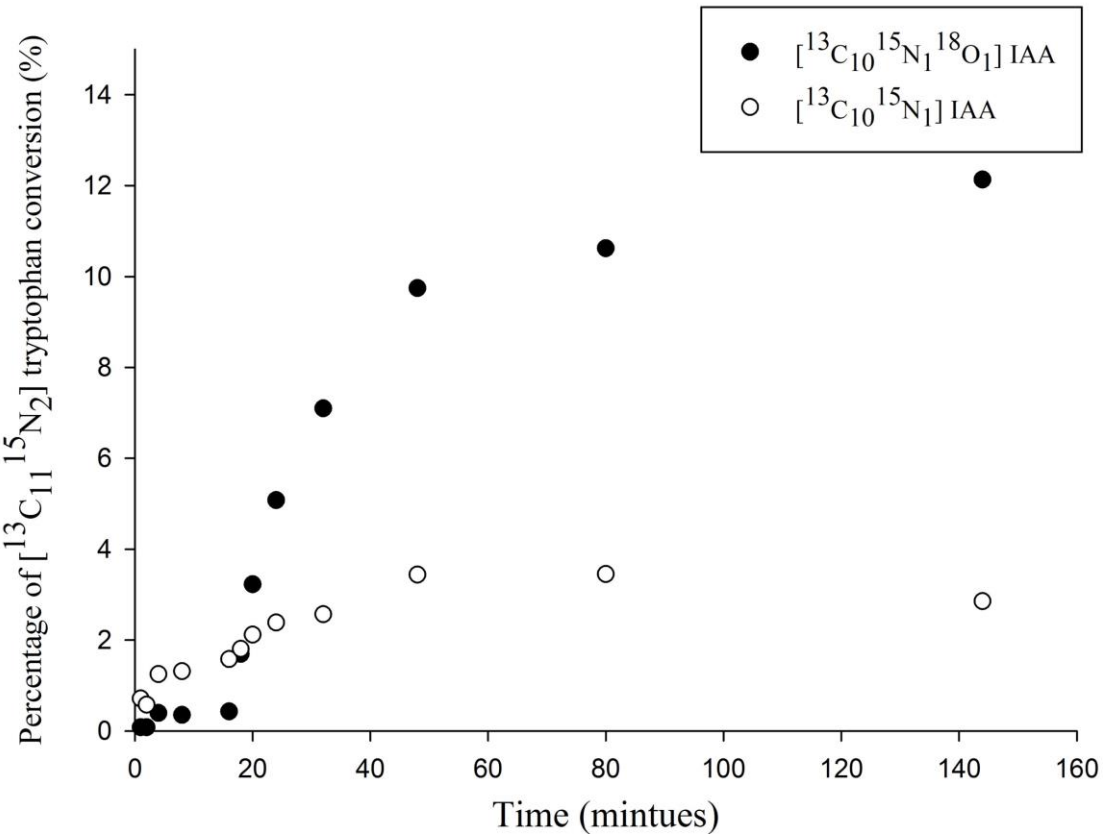

Figure 3-11. $^{18}O_2$ labeling experiment. The reaction was started by adding [$^{13}C_{11}$,$^{15}N_2$]tryptophan in to an oxygen-depleted reaction system. The reaction was supplied with $^{18}O_2$ at time point 18 minutes. Each dot represents the sampling time in a continuous reaction.

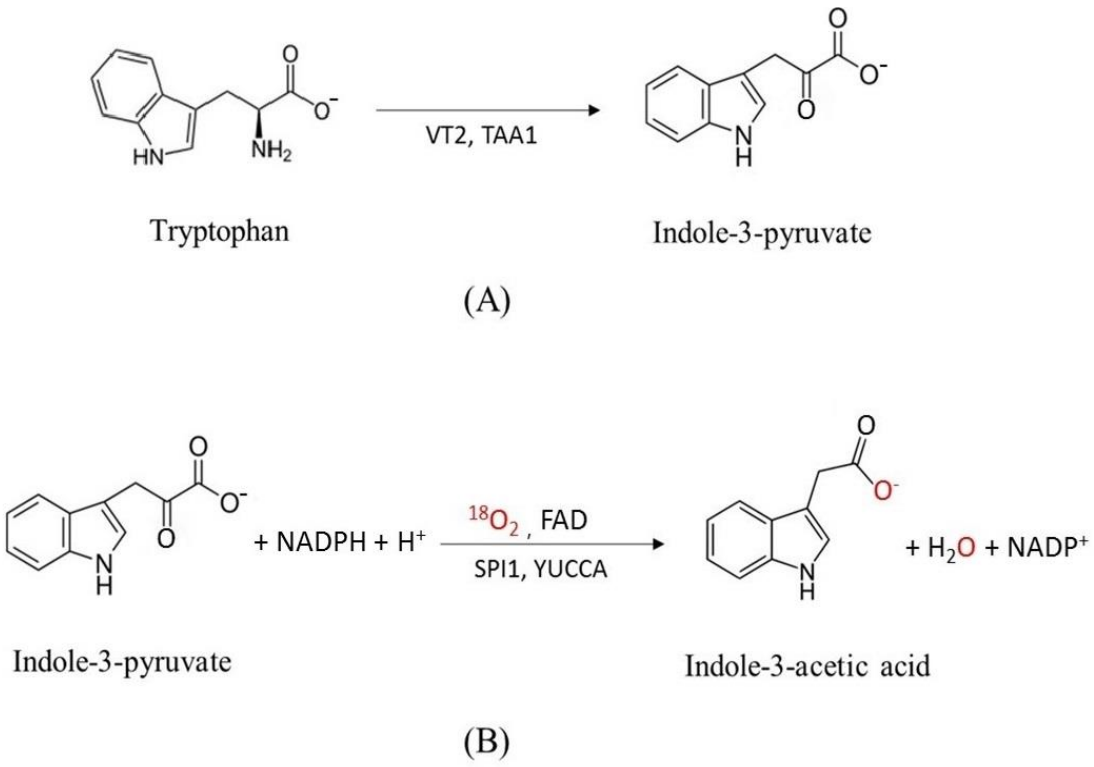

Figure 3-12. The two-step reaction of IAA biosynthesis via the VT2/SPI1 (or TAA1/YUCCA) pathway. The first step is tryptophan catalyzed to indole-3-pyruvate by a tryptophan transaminase (Panel A), and the second step is the intermediate indole-3-pyruvate converts to indole-3-acetic acid by the flavin-containing monooxygenase (Panel B). The red font color shows the isotopic labeled ^{18}O incorporated into the reaction product.

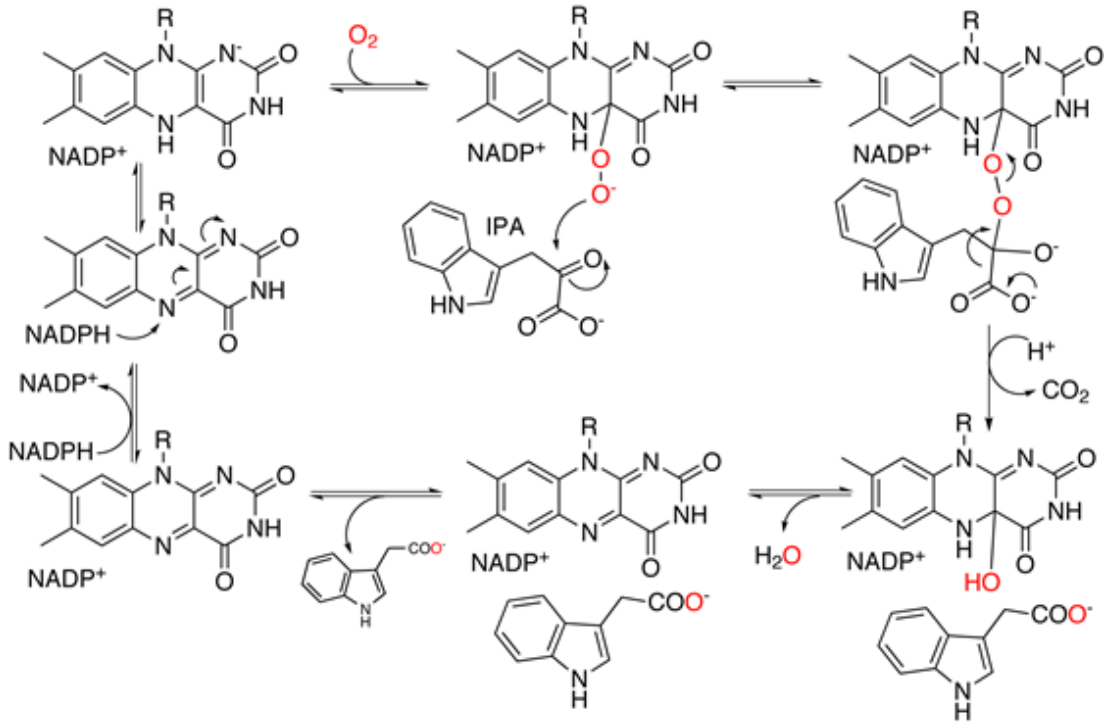

Figure 3-13. The YUCCA reaction mechanism. The red font color shows the isotopic labeled ^{18}O incorporated into the reaction.

3.7 Literature Cited

Bandurski RS and Schulze A (1974) Concentrations of indole-3-acetic acid and its esters in *Avena* and *Zea*. Plant Physiology **54**: 257-262

Bernardi J, Lanubile A, Li Q, Kumar D, Kladnik A, Cook SD, Ross JJ and Marocco A and Chourey PS (2012) Impaired auxin biosynthesis in the defective endosperm18 mutant is due to mutational loss of expression in the ZmYuc1 gene encoding endosperm-specific YUCCA1 protein in maize. Plant Physiology **160**: 1318-1328

Comai L and Kosuge T (1982) Cloning and characterization of iaaM, a virulence determinant of *Pseudomonas savastanoi* **149**: 40-46

Culler AH (2007) Tryptophan-dependent indole-3-acetic-acid biosynthesis pathway in *Zea mays.* Ph.D. dissertation, University of Minnesota, 84 pp.

Dai X, Mashiguchi K, Chen Q, Kasahara H, Kamiya Y, Ojha S, Dubois J, Ballou D and Zhao Y (2013) The biochemical mechanism of auxin biosynthesis by an *Arabidopsis* YUCCA flavin-containing monooxygenase. Journal of Biological Chemistry **288**: 1448-1457

Gallavotti A, Barazesh S, Malcomber S, Hall D, Jackson D, Schmidt RJ and McSteen P (2008) sparse inflorescence1 encodes a monocot-specific YUCCA-like gene required for vegetative and reproductive development in maize. Proceedings of the National Academy of Sciences of the United States of America **105**: 15196-15201

Kriechbaumer V, Park WJ, Piotrowski M, Meeley RB, Gierl A and Glawischnig E (2007) Maize nitrilases have a dual role in auxin homeostasis and β-cyanoalanine hydrolysis. Journal of Experimental Botany **58**: 4225-4233

LeClere S, Schmelz EA and Chourey PS (2010) Sugar levels regulate tryptophan-dependent auxin biosynthesis in developing maize kernels. Plant Physiology **153**: 306-318

Lehmann T, Hoffmann M, Hentrich M and Pollmann S (2010) Indole-3-acetamide-dependent auxin biosynthesis: a widely distributed way of indole-3-acetic acid production? European Journal of Cell Biology **89**: 895-905

Mashiguchi K, Tanaka K, Sakai T, Sugawara S, Kawaide H, Natsume M, Hanada A, Yaeno T, Shirasu K, Yao H, McSteen P, Zhao Y, Hayashi K, Kamiya Y and Kasahara H (2011) The main auxin biosynthesis pathway in

Arabidopsis. Proceedings of the National Academy of Sciences of the United States of America **108**: 18512-18517

Nemoto K, Hara M, Suzuki M, Seki H, Muranaka T and Mano Y (2009) The NtAMI1 gene functions in cell division of tobacco BY-2 cells in the presence of indole-3-acetamide. FEBS Letters **583**: 487-492

Nonhebel H, Yuan Y, Al-Amier H, Pieck M, Akor E, Ahamed A, Cohen JD, Celenza JL and Normanly J (2011) Redirection of tryptophan metabolism in tobacco by ectopic expression of an *Arabidopsis* indolic glucosinolate biosynthetic gene. Phytochemistry **72**: 37-48

Park WJ, Kriechbaumer V, Muller A, Piotrowski M, Meeley RB, Gierl A and Glawischnig E (2003) The nitrilase ZmNIT2 converts indole-3-acetonitrile to indole-3-acetic acid. Plant Physiology **133**: 794-802

Phillips KA, Skirpan AL, Liu X, Christensen A, Slewinski TL, Hudson C, Barazesh S, Cohen JD, Malcomber S and McSteen P (2011) *vanishing tassel2* encodes a grass-specific tryptophan aminotransferase required for vegetative and reproductive development in maize. Plant Cell **23**: 550-566

Pollmann S, Neu D and Weiler EW (2003) Molecular cloning and characterization of an amidase from *Arabidopsis thaliana* capable of converting indole-3-acetamide into the plant growth hormone, indole-3-acetic acid. Phytochemistry **62**: 293-300

Quittenden LJ, Davies NW, Smith JA, Molesworth PP, Tivendale ND and Ross JJ (2009) Auxin biosynthesis in pea: characterization of the tryptamine pathway. Plant Physiology **151**: 1130-1138

Seo M, Akaba S, Oritani T, Delarue M, Bellini C, Caboche M and Koshiba T (1998) Higher activity of an aldehyde oxidase in the auxin-overproducing *superroot1* mutant of *Arabidopsis thaliana*. Plant Physiology **116**: 687-693

Stepanova AN, Robertson-Hoyt J, Yun J, Benavente LM, Xie DY, Dolezal K, Schlereth A, Jurgens G and Alonso JM (2008) TAA1-mediated auxin biosynthesis essential for hormone crosstalk and plant development. Cell **133**: 177-191

Tao Y, Ferrer JL, Ljung K, Pojer F, Hong F, Long JA, Li L, Moreno JE, Bowman ME, Ivans LJ, Cheng Y and Lim J (2008) Rapid synthesis of auxin via a new tryptophan-dependent pathway is required for shade avoidance in plants. Cell **133**: 164-176

Tivendale ND, Davies NW, Molesworth PP, Davidson SE, Smith JA, Lowe EK, Reid JB and Ross JJ (2010) Reassessing the role of N-hydroxytryptamine in auxin biosynthesis. Plant Physiology **154**: 1957-1965

Ueno M, Shibata H, Kihara J, Honda Y and Arase S (2003) Increased tryptophan decarboxylase and monoamine oxidase activities induce Sekiguchi lesion formation in rice infected with *Magnaporthe grisea*. The Plant Journal **36**: 215–228

Yamada M, Greenham K, Prigge MJ, Jensen PJ and Estelle M (2009) The TRANSPORT INHIBITOR RESPONSE2 gene is required for auxin synthesis and diverse aspects of plant development. Plant Physiology **151**: 168-179

Yamamoto Y, Kamiya N, Morinaka Y, Matsuoka M and Sazuka T (2007) Auxin biosynthesis by the YUCCA genes in rice. Plant Physiology **143**: 1362-1371

Zhao Y, Christensen SK, Fankhauser C, Cashman JR, Cohen JD, Weigel D and Chory J (2001) A role for flavin monooxygenase-like enzymes in auxin biosynthesis. Science **291**: 306-309

Chapter 4

Inhibitor Assays on IAA Biosynthesis Pathways in the Maize Endosperm *in vitro* Enzyme System

Overview

Genetic approaches to the study of IAA biosynthesis mutants meet tremendous difficulties due to the genetic redundancy of the tryptophan-dependent IAA biosynthesis pathways. This study aims to find effective inhibitors that can potentially be used to block specific IAA biosynthesis routes, at different development stages, under various environmental stresses. This chapter describes the analysis of four groups of compounds, including indole derivative inhibitors, tryptophan transaminase inhibitors, kynurenine pathway related inhibitors, and yucasin. It is demonstrated that yucasin with a Ki value of 74.75 nM is a very potent inhibitor in the maize endosperm *in vitro* system, and is very likely inhibiting YUCCA. This study also demonstrated that AOPP, which is likely inhibiting TAA1, and MPP^+ iodide are also good inhibitors in tryptophan-dependent IAA biosynthesis.

4.1 Introduction

Despite the fact that IAA is one of the most important plant hormones controlling plant growth and development, and despite the many dramatic advances that have been made improving our understanding of IAA biosynthesis in recent years (reviewed by Tivendale et al., 2014), many aspects of IAA biosynthesis still remain unclear. Attempts to characterize IAA biosynthesis have been hindered by major obstacles including: biosynthetic complexity due to multiple routes that plants can take to produce IAA; and the genetic redundancy in IAA biosynthesis and its regulation. Genetic approaches studying IAA biosynthesis have proven to be difficult due to the very severe, lethal (Cheng et al., 2006) or sterile (Stepanova et al., 2008) phenotypes of the IAA biosynthetic mutants.

In this study, a biochemical approach using inhibitors has been adopted as a promising approach for studying IAA biosynthesis. This approach could make it possible to selectively target specific enzymes in IAA biosynthesis, temporarily blocking IAA biosynthesis in plant seedlings or specific tissue types, at different development stages. In this chapter, multiple known and potential inhibitors of IAA biosynthesis are evaluated for inhibition of IAA synthesis by the maize endosperm *in vitro* system to determine their efficacy against the maize YUCCA pathway.

4.1.1 Indole derivative inhibitors

Inhibition by indole analogues that target IAA biosynthesis was first reported in the maize endosperm *in vitro* system by Ilic et al. in 1999. By applying 60 μM inhibitors in the maize endosperm *in vitro* system, and measuring the production of [^{14}C]tryptophan and [^{14}C]IAA, they identified 11 out of 30 indole analogues that have some inhibitory effect on IAA biosynthesis. From the strongest inhibitor to the weakest they are: 2-mercaptobenzimidazole, 5-fluoroindole, 5-chloroindole, 6-fluoroindole, 4-hydroxyindole, triazolopyridine, 5-bromoindole, 7-benzyloxyindole, indazole, 6-cyanoindole and hypoxanthine. Among these 11 inhibitors, 2-mercaptobenzimidazole, 5-fluoroindole, 5-chloroindole and 6-fluoroindole had more inhibitory effects on the IAA biosynthesis over other compounds. 5-Fluoroindole and 5-chloroindole showed inhibition of both tryptophan biosynthesis and IAA biosynthesis, while 2-mercaptobenzimidazole totally blocked IAA biosynthesis without decreasing the tryptophan biosynthesis activity.

A follow-up study was conducted on the inhibitory effects of 2-mercaptobenzimidazole and 6-fluoroindole in Arabidopsis *in vivo* (Ludwig-Müller et al., 2010). It reported that Arabidopsis seedlings showed no significant change in phenotype

compared with control seedlings following application of 2-mercaptobenzimidazole. 6-fluoroindole, however, produced severe seedling development defect phenotypes when applied at the concentrations about 50-100 μM. While 4-hydroxyindole, which exhibited similar inhibitory effects as 6-fluoroindole (Ilic et al., 1999), showed no effects on plants (Ludwig-Müller et al., 2010). Further research is needed to confirm whether 6-fluoroindole was interfering with IAA biosynthesis or homeostasis.

4.1.2 Tryptophan transaminase inhibitors

4.1.2.1 AVG and AOPP

Among the tryptophan-dependent IAA biosynthetic pathways, the IPyA pathway is a two-step reaction and involves two enzyme classes. The first reaction step is the conversion of the substrate tryptophan to the intermediate IPyA, which is catalyzed by tryptophan amino-transferases that belong to the TAA1/TAR family (Mashiguchi et al., 2011 and Won et al., 2011). The second reaction step is the conversion of the intermediate IPyA to the product IAA, which is catalyzed by a group of flavin-containing monooxygenases called YUCCAs (Dai et al., 2013).

A class of inhibitors that target at tryptophan transferases in IPyA pathway was first reported by Soeno *et al.* in 2010. From this study using large-scale transcriptome data, their group discovered two TAA1/TARs inhibitors, L-α-(2-aminoethoxyvinyl)glycine (AVG) and L-α-aminooxy-phenylpropionic acid (AOPP). AVG was known and often used as an inhibitor in the study of ethylene biosynthesis (Yu et al., 1979; Mauch et al., 1984; Ligero et al., 1991; Ma et al., 1998; Bregoli et al., 2002 and Swarup et al., 2007). Soeno and coworker's study showed that both AVG and AOPP

do not inhibit the expression of ethylene marker genes in Arabidopsis whole seedling or root development. Instead, AVG and AOPP had a strong anti-auxin activity targeting TAA1/TARs, which was independent of ethylene activities. Their result also reported that the IC_{50} of AVG was 47 μM and the IC_{50} of AOPP was 0.77 μM in the reaction of tryptophan conversion to IPyA in Arabidopsis.

A recent paper published by Narukawa-Nara et al. in 2016 reported that AOPP and its derivatives are inhibitors that target at tryptophan aminotransferase in the IPyA pathway. By comparing the inhibited enzyme activities of TAA1 *in vitro* in presence of 14 AOPP derivatives with functional group substitutions, and the docking simulation analysis on these compounds, they determined that the TAA1 inhibition characteristic of AOPP and its derivatives was from the aminooxy and carboxy groups in the compounds. Moreover, the protection on the aminooxy and carboxy group of AOPP and its derivatives increased their inhibition activity *in vivo*. The *Ki* of AOPP was 350.4 nM in the inhibition of converting tryptophan to IPyA by the TAA1 recombinant enzyme *in vitro*. By the aid of quantitative real-time PCR (qRT-PCR), they also demonstrated that the auxin-responsive genes were down-regulated in 7-day-old Arabidopsis seedlings after 3-hour incubation in the medium containing 1 μM, 10 μM and 100 μM AOPP. This evidence inferred AOPP targeted at IAA biosynthesis pathways and caused the endogenous IAA deficiency, which in turn decreases the expression of auxin-responsive genes.

4.1.2.2 Kynurenine pathway related inhibitors

In order to adapt to many environmental changes, plant hormones crosstalk in many different tissues and developmental stages in response to different environmental

cues. Some ethylene-insensitive mutants showed auxin biosynthesis defect phenotypes, such as *wei2, wei7* (Stepanova et al., 2005) and *wei8* (Stepanova et al., 2008). In a library screen searching for suppressors of the constitutive ethylene response phenotypes in Arabidopsis, He et al. (He et al., 2011) discovered a small molecule L-kynurenine (Kyn). By studying the conversion of tryptophan to IPyA *in vitro* using *Escherichia coli*-purified TAA1, and by analyzing the computational docking and molecular modeling result, they then realized that Kyn was a competitive inhibitor of TAA1/TARs in the IAA biosynthesis IPyA pathway, with a *Ki* value of 11.52 μM, comparing to the *Km* of TAA1 was 61.61 μM. Moreover, they found that Kyn is an alternative substrate of TAA1 producing kynurenic acid *in vitro*, which was the same metabolic product of kynurenine catalyzed by kynurenine aminotransferases (KATs) in animals.

In the animal tryptophan catabolic pathway to make NAD, NADP, serotonin, melatonin, tryptamine, quinolinic acid and kynurenic acid from the essential amino acid tryptophan, the intermediate kynurenine is an important a branch point, and can be converted to kynurenic acid by KATs, to quinolinic acid by kynurenine 3-monooxygenases (KMOs), or to anthranillic acid by kynureninase. This pathway is also known as kynurenine pathway (Amaral et al., 2013 and Schwarcs et al., 2012). A study showed that Arabidopsis lacks key enzymes in the kynurenine pathway (Katoh et al., 2006), instead, Arabidopsis adopts only the aspartate pathway. Thus, it is suggested that kynurenine pathway may not participated in the tryptophan catabolism in dicot plants (Noctor et al., 2011). Interestingly, monocot plants have enzymes involves in both aspartate pathways and kynurenine pathways. As a matter of fact, all the enzymes involved in the five steps of synthesize quinolinic acid via the kynurenine pathway are

present in monocot plants (Katoh and Hashimoto, 2004). The existence of kynurenine pathway in monocots suggested that monocot may have different tryptophan metabolism than dicot plants, thus, the tryptophan-dependent IAA biosynthesis pathways in monocot plants may have great differences comparing to dicot plants. Furthermore, based on the reason that 1) kynurenine shares some structural similarity to tryptophan, and it competitively inhibits the binding of tryptophan; and 2) kynurenine can be catabolized as a substrate by TAA1 *in vitro* in a way that resembles the animal kynurenine pathway KATs route; and 3) JM6 is a KMOs inhibitor (Reinhart et al., 2011) and MPP^+ iodide is a KATs inhibitor (Heikkila et al., 1984 and Langston et al., 1984), both JM6 and MPP^+ iodide were tested in this Chapter as potential TAA1 inhibitors.

4.1.3 Yucasin

Nishimura et al. (2014) has discovered a potent IAA biosynthesis inhibitor, 5-(4-chlorophenyl)-4H-1,2,4-triazole-3-thiol, which they named *yucasin*. This compound was identified in a chemical library screen using a maize coleoptile tip *in vivo* system. In this system, IAA levels decreased to about one fifth of the initial level when 50 μM yucasin applied. They also demonstrated that yucasin inhibited the IPyA to IAA conversion *in vitro* by a His-tagged AtYUC1 recombinant protein with cofactors FAD and NADPH in a dose dependent manner, although IPyA non-enzymatic conversion was also observed in the experiment. Through an *in silico* molecular docking study of yucasin, it was determined that the binding affinity for yucasin to TAA1 was 10 times lower than either tryptophan or the TAA1 inhibitor kynurenine. Moreover, the additive inhibition from yucasin and kynurenine produced similar phenotype to yucasin inhibition. These results suggested that yucasin is likely an inhibitor that specifically targets YUCCA enzymes.

Further study in Arabidopsis showed yucasin suppressed the IAA over-expression phenotype of *35S::YUC1 in vivo*.

4.2 Materials and Methods

In this Chapter, 8 inhibitors were tested in the maize endosperm *in vitro* system. For each inhibitor, a wide range of inhibition concentrations were first tested by an initial inhibition assay. By analyzing the results from these initial inhibition assays, a narrower concentration range was selected flanking the K_I apparent for further investigation of each inhibitor discussed in this chapter. Each inhibitor experiment was repeated in three replications.

In the experiments from this chapter, the reaction volume of each inhibitor at each concentration is 2.5 mL. The components of each 2.5 mL reaction tube include maize endosperm enzyme sample, [$^{13}C_{11}$,$^{15}N_2$]tryptophan substrate solution, the testing inhibitor solution at certain concentration, 50 mM POPSO buffer pH 8.5, containing 4 mM EDTA, and freshly prepared 1 M ascorbate solution. The maize enzyme component of the reaction was prepared before the start of the inhibition experiment. The maize endosperm (stage 2 purification) aliquots were thawed on ice and used in this experiment. The enzyme purification of maize endosperm is discussed in Section 2.2.1. 5 mL 50 mM POPSO buffer pH 8.5, containing 4 mM EDTA was added into per mL of maize endosperm. The maize enzyme mixture was homogenized well by a glass homogenizer (only needed about 10 passes up and down because the maize endosperm stage 2 aliquots were homogenized well before they stored in -80 °C freezer). To achieve a reaction volume of 2.5 mL, 2.3 mL maize enzyme homogenate was transferred into a 15 mL Falcon tube, and 2.5 µL of 1 M ascorbic acid was added into the enzyme homogenate to

reach a final concentration of 1 mM in the reaction. Volumes of 50 µL of each inhibitor solution at various concentrations were added into the reaction tube. The concentration ranges used for each inhibitor are discussed in Section 4.2.1. The substrate concentration for all the inhibitor experiments used in this chapter was 5.78 µM. [$^{13}C_{11}$,$^{15}N_2$]tryptophan solution was usually freshly made, or sometimes prepared in very small batches (usually 2-5 aliquots of 1 mL solution) and stored in -80 °C freezer. For some inhibitor experiment, [$^{13}C_{11}$,$^{15}N_2$]tryptophan concentration and solution volume used in the reaction were varied among different inhibition experiments. Thus, about 50 µL POPSO buffer was added to the Falcon tubes to compensate for differences in order to maintain a consistent 2.5 mL reaction volume.

4.2.1 Indole derivative inhibitors

4.2.1.1 2-Mercaptobenzimidazole

Based on the result from the preliminary investigation on the inhibitor 2-mercaptobenzimidazole (2-MBI), five inhibitor concentrations of the maize endosperm reaction, 0.1 µM, 0.5 µM, 1 µM, 5 µM and 10 µM, were tested. The molecular weight of 2-MBI (EC # 205-736-8, Sigma Aldrich, St Louis, MO) is 150.2 g/mol. A 10 mM 2-MBI stock solution was made by dissolving 1.5 mg of 2-MBI in 1 mL 50% isopropanol. A series of 2-MBI solutions with the concentrations of 5 µM, 25 µM, 50 µM, 250 µM and 500 µM were made by serial dilutions using the 10 mM stock solution in 50% isopropanol. In each reaction tube designated to test the maize enzyme activity under the effect of the inhibitor at certain concentration, 50 µL of corresponding inhibitor solution was used. In the reaction control tube, 50 µL of 50% isopropanol with no inhibitor

addition was used. The concentration of [$^{13}C_{11}$,$^{15}N_2$]tryptophan solution prepared for this experiment was 160 μM. In order to achieve the substrate concentration of 5.78 mM in the 2.5 mL reaction system, 90.3 μL [$^{13}C_{11}$,$^{15}N_2$]tryptophan solution was used.

Before the start of the experiment, the components of the reaction, except the inhibitor solution and the substrate solution, were added into a 15 mL Falcon tube and mixed well. The 15 mL Falcon tube containing the maize enzyme sample was placed in a 25 °C water bath a few minutes before starting the reaction. The 50 μL inhibitor solution was mixed with the 90.3 μL [$^{13}C_{11}$,$^{15}N_2$]tryptophan solution in a 1.5 mL Eppendorf tube. Start the reaction by transferring the inhibitor and substrate solution mixture into the 15mL Falcon tube containing the maize endosperm sample. The start time was recorded. The Falcon tube was kept in a 25°C water bath. During the course of the reaction, the Falcon tube was gently rocked every minute.

Duplicate 0.25 mL samples were taken out of the reaction tube and quenched at each the time points: 1 minute, 2 minutes and 4 minutes. For quantification purpose, 15 ng [$^{13}C_6$]indole-3-acetic-acid was used as the internal standard in each 0.25 mL reaction aliquot. To quench the reaction simultaneously, both duplicates of aliquots were boiled in water at the same time for 5 minutes. One of the duplicate samples was then centrifuged at 10,000 × g for 5 minutes. Then the supernatant was transferred (obtaining 0.2 mL from 0.25 mL reaction aliquot) to a new tube pre-loaded with 0.2 mL of 50:50 1 M phosphoric acid to sodium phosphate buffer pH 2.5 to a final volume of 0.4 mL. The first duplicate sample was then used for further IAA extraction, IAA methylation and data collection; the other sample was immediately stored in the -80 °C freezer. The backup duplicate was only used if data were lost during experiments, especially in the sample boiling and IAA

methylation processes. Otherwise it was discarded after the data collection was finished.

To measure the maize endosperm enzyme activity under the influences of 2-MBI of varied concentrations, IAA was extracted and methylated from each reaction aliquots. The initial velocities of [$^{13}C_{10}$,$^{15}N_1$]IAA synthesis were determined by calculating the ratio of [$^{13}C_{10}$,$^{15}N_1$]IAA ions at *m/z* 140, to the internal standard [$^{13}C_6$] IAA ions at *m/z* 136. The IAA extraction and methylation protocol is described in Section 2.2.2.2, and the protocol for quantifying IAA using isotope dilution GC-MS is described in Section 2.2.2.3.

The *Ki* value was then determined by analyzing the reaction initial velocities within the 4-minutes reaction window under different inhibitor concentrations and fitting linear regression in the program Sigma Plot 12.5.

4.2.1.2 6-Fluoroindole

Based on the results from the preliminary investigation on the inhibitor 6-fluoroindole (6-FI), seven inhibitor concentrations, 0.1 μM, 0.5 μM, 1 μM, 5 μM, 10 μM, 50 μM and 100 μM, were selected to be tested in the maize endosperm reaction system. The molecular weight of 6-FI (CAS # 399-51-9, Sigma Aldrich, St Louis, MO) is 135.14 g/mol. A 10 mM 6-FI stock solution was made by dissolving 1.35 mg 6-FI in 1 mL 50% isopropanol. A series of 6-FI solutions with the concentrations of 5 μM, 25 μM, 50 μM, 250 μM, 500 μM, 2.5 mM and 5 mM were made by serial dilutions using the 10 mM stock 6-FI solution.

The IAA biosynthesis activity of maize endosperm in seven 15 mL Falcon tubes containing 0.1 μM, 0.5 μM, 1 μM, 5 μM, 10 μM, 50 μM and 100 μM 6-FI respectively were measured. The reaction components, the experimental protocol and the data analysis

procedure were the same as the 2-MBI inhibition experiment described in Section 4.2.1.1, except that the inhibitor and its concentration series are as noted above.

4.2.2 AOPP and AVG

4.2.2.1 L-Aminooxyphenylpropionic acid

Based on the result from the preliminary investigation on the inhibitor L-Aminooxyphenylpropoionic acid (AOPP), five AOPP inhibitor concentrations, 0.1 μM, 0.5 μM, 1 μM, 5 μM and 10 μM, were selected to be tested in the maize endosperm reaction system. The molecular weight of AOPP (Item # 010-18931, Wako Pure Chemical Industries, Ltd., Tokyo, Japan) is 181.19 g/mol. 10mM AOPP stock solution was made by dissolving 1.81 mg AOPP in 1 mL 50% isopropanol. A series of AOPP solutions with the concentrations of 5 μM, 25 μM, 50 μM, 250 μM and 500 μM were made by serial dilutions using the 10 mM AOPP stock solution.

The reaction components, the experimental protocol and the data analysis procedure were the same as the 2-MBI inhibition experiment described in Section 4.2.1.1, except that the substrate solution concentrations, the inhibitor and its concentration series are as noted above.

The reaction was started by adding the mixture of 50 μL inhibitor solution at the specified concentrations and 124 μL [$^{13}C_{11}$,$^{15}N_2$]tryptophan solution (the concentration of [$^{13}C_{11}$,$^{15}N_2$]tryptophan substrate solution was 116.5 μM) into the maize endosperm enzyme sample in a 15 mL Falcon tube. As in the 2-MBI inhibition experiment, duplicate reaction aliquots were quenched at the time point of 1 minute, 2 minutes, and 4 minutes. One duplicate copy of the reaction aliquots was used for IAA extraction, IAA

methylation and data analysis, whereas the other copy was serving as a backup set of samples.

The IAA biosynthetic activity of maize endosperm was measured in five 15 mL Falcon tube containing 0.1 μM, 0.5 μM, 1 μM, 5 μM and 10 μM AOPP respectively. In each of the reactions, the initial velocities of each reaction was determined by fitting a linear regression for [$^{13}C_{10}$,$^{15}N_1$]IAA synthesized in the first 4 minutes of the reaction and the *Ki* value was determined as described above.

4.2.2.2 L-α-(2-Aminoethoxyvinyl) glycine

Based on the result from the preliminary investigation on the inhibitor L-α-(2-Aminoethoxyvinyl)glycine (AVG), five AVG inhibitor concentrations, 1 μM, 5 μM, 10 μM, 50 μM, 100 μM, were selected to be tested in the maize endosperm reaction system. The molecular weight of AVG (Item # 20-4468, Hoffmann-La Roche Inc., Basel, Switzerland) is 160 g/mol. 10 mM AVG stock solution was made by dissolving 1.6 mg AOPP in 1 mL 50% isopropanol. A series of AVG solutions with the concentrations of 50 μM, 250 μM, 500 μM, 2.5 mM and 5 mM were made by serial dilutions using the 10 mM AVG stock solution.

The reaction was started by adding the mixture of 50 μL inhibitor solution at the specified concentrations and 92.2 μL [$^{13}C_{11}$,$^{15}N_2$]tryptophan solution (the concentration of [$^{13}C_{11}$,$^{15}N_2$]tryptophan substrate solution was 156.8 μM) into the pre-prepared maize endosperm enzyme sample in a 15 mL Falcon tube.

The enzyme reaction components, the experimental protocol, the data collection and analysis procedure were the same as the 2-MBI inhibition experiment described in section 4.2.1.1, except that the substrate solution concentrations, the inhibitor and its

concentration series are as listed above.

4.2.3 Kynurenine pathway related inhibitors

4.2.3.1 Kynurenine

Based on the results from the preliminary investigation on the kynurenine (Kyn), seven Kyn inhibitor concentrations, 0.1 μM, 0.5 μM, 1 μM, 5 μM, 10 μM, 50 μM, and 100 μM, were selected to be tested in the maize endosperm reaction system. The molecular weight of L-kynurenine (CAS # 2922-83-0, Sigma Aldrich, St Louis, MO) is 208.21 g/mol. 10mM Kyn stock solution was made by dissolving 2.08 mg Kyn in 1 mL 50% isopropanol. A series of Kyn solutions with the concentrations of 5 μM, 25 μM, 50 μM, 250 μM, 500 μM, 2.5 mM, and 5 mM were made by serial dilutions using the 10 mM Kyn stock solution.

The reaction was started by adding the mixture of 50 μL inhibitor solution at the specified concentrations and 92.2 μL [$^{13}C_{11}$,$^{15}N_2$]tryptophan solution (the concentration of [$^{13}C_{11}$,$^{15}N_2$]tryptophan substrate solution was 156.8 μM) into the pre-prepared maize endosperm enzyme sample in a 15 mL Falcon tube.

The enzyme reaction components, the experimental protocol, the data collection and analysis procedure were the same as the 2-MBI inhibition experiment described in Section 4.2.1.1, except that the substrate solution concentrations, the inhibitor and its concentration series are as listed above.

4.2.3.2 KMO inhibitor: JM6

Based on the results from the preliminary investigation on the inhibitor JM6, five JM6 inhibitor concentrations, 0.1 μM, 0.5 μM, 1 μM, 5 μM, 10 μM, were selected to be

tested in the maize endosperm reaction system. JM6 is also known as 2-(3,4-Dimethoxybenzenesulfonylamino)-4-(3-nitrophenyl)-5-(piperidin-1-yl)methylthiazole (CAS # 1008119-83-2, Sigma Aldrich, St Louis, MO). The molecular weight of JM6 is 518.61 g/mol. A 10mM JM6 stock solution was made by dissolving 5.19 mg JM6 in 1mL 50% isopropanol. A series of JM6 solutions with the concentrations of 5 μM, 25 μM, 50 μM, 250 μM and 500 μM were made by serial dilutions using the 10 mM JM6 stock solution.

The reaction was started by adding the mixture of 50 μL inhibitor solution at the specified concentrations and 92.2 μL [$^{13}C_{11}$,$^{15}N_2$]tryptophan solution (the concentration of [$^{13}C_{11}$,$^{15}N_2$]tryptophan substrate solution was 156.8 μM) into the pre-prepared maize endosperm enzyme sample in a 15 mL Falcon tube.

The enzyme reaction components, the experimental protocol, the data collection and analysis procedure were the same as the 2-MBI inhibition experiment described in Section 4.2.1.1, except that the substrate solution concentrations, the inhibitor and its concentration series are as detailed above.

4.2.3.3 KAT inhibitor: MPP^+ iodide

Based on the results from the preliminary investigation on the inhibitor MPP^+ iodide, four MPP^+ iodide inhibitor concentrations, 0.1 μM, 0.5 μM, 1 μM and 5 μM, were selected to be tested in the maize endosperm reaction system. The molecular weight of MPP^+ iodide is 297.13 g/mol. 10 mM MPP^+ iodide stock solution was made by dissolving 2.97 mg MPP^+ iodide in 1 mL 50% isopropanol. A series of MPP^+ iodide solutions with the concentrations of 5 μM, 25 μM, 50 μM and 250 μM were made by serial dilutions using the 10 mM MPP^+ iodide stock solution.

The reaction was started by adding the mixture of 50 μL inhibitor solution at the specified concentrations and 92.2 μL [$^{13}C_{11}$,$^{15}N_2$]tryptophan solution (the concentration of [$^{13}C_{11}$,$^{15}N_2$]tryptophan substrate solution was 156.8 μM) into the pre-prepared maize endosperm enzyme sample in a 15 mL Falcon tube.

The enzyme reaction components, the experimental protocol, the data collection and analysis procedure were the same as the 2-MBI inhibition experiment described in Section 4.2.1.1, except that the substrate solution concentrations, the inhibitor and its concentration series are as given above.

4.2.4 Yucasin

Based on the results from the preliminary investigation on the inhibitor MPP^+ iodide, five yucasin inhibitor concentrations, 0.01 nM, 0.1 nM, 1 nM, 10 nM and 100 nM, were selected to be tested in the maize endosperm reaction system. The molecular weight of yucasin is 211.67 g/mol. A 10 mM yucasin stock solution was made by dissolving 2.12 mg yucasin in 1 mL 50% isopropanol. A series of yucasin solutions with the concentrations of 1 nM, 10 nM, 100 nM, 1 μM and 10 μM were made by serial dilutions using the 10 mM yucasin stock solution.

The reaction was started by adding the mixture of 50 μL inhibitor solution at the specified concentrations and 92.2 μL [$^{13}C_{11}$,$^{15}N_2$]tryptophan solution (the concentration of [$^{13}C_{11}$,$^{15}N_2$]tryptophan substrate solution was 156.8 μM) into the pre-prepared maize endosperm enzyme sample in a 15 mL Falcon tube.

The enzyme reaction components, the experimental protocol, the data collection and analysis procedure were the same as the 2-MBI inhibition experiment described in Section 4.2.1.1, except that the substrate solution concentrations, the inhibitor and its

concentration series are as listed above.

4.3 Results and Discussions.

The inhibition constant (*Ki*) for each inhibitor is listed in **Table 4.1** by inhibitor class.

4.3.1 Indole derivative inhibitors

4.3.1.1 2-Mercaptobenzimidazole

In this experiment, the initial velocity of maize endosperm IAA biosynthesis with no inhibitor addition is 57.62 ng [$^{13}C_{11}$,$^{15}N_2$]tryptophan converted to [$^{13}C_{10}$,$^{15}N_1$]IAA per mL reaction per minute (S.D. +/- 1.88 ng min^{-1} mL^{-1}) (data not plotted in figure). The reaction initial velocity decreased to 45.91 ng min^{-1} mL^{-1} (S.D. +/- 3.65 ng min^{-1} mL^{-1}) with the addition of 0.1 μM of 2-MBI; 36.29 ng min^{-1} mL^{-1} (S.D. +/- 3.47 ng min^{-1} mL^{-1}) with the addition of 0.5 μM of 2-MBI; 25.25 ng min^{-1} mL^{-1} (S.D. +/- 2.65 ng min^{-1} mL^{-1}) with the addition of 1 μM 2-MBI; 16.61 ng min^{-1} mL^{-1} (S.D. +/- 2.20 ng min^{-1} mL^{-1}) with the addition of 5 μM of 2-MBI; and 9.05 ng min^{-1} mL^{-1} (S.D. +/- 1.08 ng min^{-1} mL^{-1}) with the addition of 10 μM of 2-MBI. The *Ki* of 2-MBI in the maize endosperm IAA biosynthesis system is 2.84 μM. The result is shown in **Figure 4-2**. The indole analogue, 2-MBI, is not an inhibitor targeting tryptophan biosynthesis (Ilić et al., 1999). However, with a *Ki* value of 2.84 μM, this study concluded that 2-MBI is a very potent inhibitor in IAA biosynthesis. Follow up experimentation for characterizing the mode of action for 2-MBI can be done through additive inhibition test. In the additive inhibition test, the inhibition effect resulted from the combination of 2-MBI and yucasin beyond that observed for yucasin alone would support the conclusion that 2-MBI are TAA1/TARs

inhibitors. This simple test would help elucidate its molecular target.

4.3.1.2 6-Fluoroindole

In this experiment, the initial velocity of maize endosperm IAA biosynthesis was 55.79 ng min^{-1} mL^{-1} (S.D. +/- 1.71 ng min^{-1} mL^{-1}) with the addition of 0.1 μM of 6-FI; 51.25 ng min^{-1} mL^{-1} (S.D. +/- 4.04 ng min^{-1} mL^{-1}) with the addition of 0.5 μM of 6-FI; 42.43 ng min^{-1} mL^{-1} (S.D. +/- 4.80 ng min^{-1} mL^{-1}) with the addition of 1 μM 6FI; 36.71 ng min^{-1} mL^{-1} (S.D. +/- 3.33 ng min^{-1} mL^{-1}) with the addition of 5 μM of 6-FI; 32.1 ng min^{-1} mL^{-1} (S.D. +/- 5.38 ng min^{-1} mL^{-1}) with the addition of 10 μM of 6-FI; 38.54 ng min^{-1} mL^{-1} (S.D. +/- 2.21 ng min^{-1} mL^{-1}) with the addition of 50 μM of 6-FI; and 31.8 ng min^{-1} mL^{-1} (S.D. +/- 4.57 ng min^{-1} mL^{-1}) with the addition of 100 μM of 6-FI. The *Ki* of 6-FI in the maize endosperm IAA biosynthesis system is 300.83 μM. The result is shown in **Figure 4-3**. This result demonstrated that 6-fluoroindole with a *Ki* of 300.83 μM is not an inhibitor of IAA biosynthesis in the maize endosperm *in vitro* system. This data suggests that the application of high concentrations of 6-FI, which gave rise to severe development defects in Arabidopsis *in vivo* (Ludwig-Müller J et al., 2010), may not be acting through the inhibition of IAA biosynthesis. When also considering the results from the 4-hydroxyindole studies, which shared an inhibitory pattern similar 6-FI, but which showed no obvious phenotype defects in the same Arabidopsis *in vivo* experiment, one may hypothesize that the phenotype defects resulting from 6-FI application may come from auxin homeostasis, instead of inhibition of IAA biosynthesis.

4.3.2 AOPP and AVG

4.3.2.1 L-Aminooxyphenylpropionic acid

In this experiment, the initial velocity was 48.27 ng min^{-1} mL^{-1} (S.D. +/- 4.63 ng min^{-1} mL^{-1}) with the addition of 0.1 μM of AOPP; 43.1 ng min^{-1} mL^{-1} (S.D. +/- 4.62 ng min^{-1} mL^{-1}) with the addition of 0.5 μM of AOPP; 44.07 ng min^{-1} mL^{-1} (S.D. +/- 3.56 ng min^{-1} mL^{-1}) with the addition of 1 μM AOPP; 27.94 ng min^{-1} mL^{-1} (S.D. +/- 2.19 ng min^{-1} mL^{-1}) with the addition of 5 μM of AOPP; and 18.53 ng min^{-1} mL^{-1} (S.D. +/- 1.33 ng min^{-1} mL^{-1}) with the addition of 10 μM of AOPP. The *Ki* of AOPP in the maize endosperm IAA biosynthesis system is 6.18 μM. The result is shown in **Figure 4-4**. The result suggested that AOPP with a *Ki* of 6.18 μM in tryptophan conversion to IAA is a good inhibitor in the maize endosperm *in vitro* system, possibly targeting at TAA1/TARs.

4.3.2.2 L-α-(2-Aminoethoxyvinyl)glycine

In this experiment, the initial velocity was 38.48 ng min^{-1} mL^{-1} (S.D. +/- 2.09 ng min^{-1} mL^{-1}) with the addition of 1 μM of AVG; 42.18ng min^{-1} mL^{-1} (S.D. +/- 3.93 ng min^{-1} mL^{-1}) with the addition of 5 μM of AVG; 36.24 ng min^{-1} mL^{-1} (S.D. +/- 1.91 ng min^{-1} mL^{-1}) with the addition of 10 μM AVG; 34.48 ng min^{-1} mL^{-1} (S.D. +/- 2.60 ng min^{-1} mL^{-1}) with the addition of 50 μM of AVG; and 29.43 ng min^{-1} mL^{-1} (S.D. +/- 2.14 ng min^{-1} mL^{-1}) with the addition of 100 μM of AVG. The *Ki* of AVG in the maize endosperm IAA biosynthesis system is 293.30 μM. The result is shown in **Figure 4-5**. The data suggested that AVG with a *Ki* of 293.30 μM is not an effective inhibitor in the conversion of tryptophan to IAA in the maize endosperm *in vitro* system.

4.3.3 Kynurenine pathway related inhibitors

4.3.3.1 Kynurenine

In this experiment, the initial velocity was 24.03 ng min^{-1} mL^{-1} (S.D. +/- 3.12 ng min^{-1} mL^{-1}) with the addition of 0.1 μM of Kyn; 24.12ng min^{-1} mL^{-1} (S.D. +/- 2.1 ng min^{-1} mL^{-1}) with the addition of 0.5 μM of Kyn; 20.96 ng min^{-1} mL^{-1} (S.D. +/- 1.87 ng min^{-1} mL^{-1}) with the addition of 1 μM Kyn; 19.26 ng min^{-1} mL^{-1} (S.D. +/- 1.82 ng min^{-1} mL^{-1}) with the addition of 5 μM of Kyn;16.96 ng min^{-1} mL^{-1} (S.D. +/- 1.54 ng min^{-1} mL^{-1}) with the addition of 10 μM of Kyn; 8.80 ng min^{-1} mL^{-1} (S.D. +/- 2.87 ng min^{-1} mL^{-1}) with the addition of 50 μM of Kyn; and 5.29 ng min^{-1} mL^{-1} (S.D. +/- 0.56 ng min^{-1} mL^{-1}) with the addition of 100 μM of Kyn. The *Ki* of Kyn in the maize endosperm IAA biosynthesis system is 29.33 μM. The result is shown in **Figure 4-6**.

4.3.3.2 KMO inhibitor: JM6

In this experiment, the initial velocity was 22.22 ng min^{-1} mL^{-1} (S.D. +/- 1.51 ng min^{-1} mL^{-1}) with the addition of 0.1 μM of JM6; 21.19 ng min^{-1} mL^{-1} (S.D. +/- 0.94 ng min^{-1} mL^{-1}) with the addition of 0.5 μM of JM6; 19.74 ng min^{-1} mL^{-1} (S.D. +/- 1.85 ng min^{-1} mL^{-1}) with the addition of 1 μM JM6; 17.73 ng min^{-1} mL^{-1} (S.D. +/- 0.83 ng min^{-1} mL^{-1}) with the addition of 5 μM of JM6; and 13.92 ng min^{-1} mL^{-1} (S.D. +/- 2.05 ng min^{-1} mL^{-1}) with the addition of 10 μM of JM6. The *Ki* of JM6 in the maize endosperm IAA biosynthesis system is 17.65 μM. The result is shown in **Figure 4-7**.

4.3.3.3 KAT inhibitor: MPP^+ iodide

In this experiment, the initial velocity was 19.17 ng min^{-1} mL^{-1} (S.D. +/- 0.17 ng min^{-1} mL^{-1}) with the addition of 0.1 μM of MPP^+ iodide; 17.47ng min^{-1} mL^{-1} (S.D. +/-

1.04 ng min^{-1} mL^{-1}) with the addition of 0.5 μM of MPP^+ iodide; 14.58 ng min^{-1} mL^{-1} (S.D. +/- 1.14 ng min^{-1} mL^{-1}) with the addition of 1 μM MPP^+ iodide; and 10.71 ng min^{-1} mL^{-1} (S.D. +/- 1.90 ng min^{-1} mL^{-1}) with the addition of 5 μM of MPP^+ iodide. The *Ki* of MPP^+ iodide in the maize endosperm IAA biosynthesis system is 6.60 μM. The result is shown in **Figure 4-8**.

The data of the kynurenine pathway related inhibitors showed that Kyn with a *Ki* of 29.33 μM is also not a very effective TAA1/TARs inhibitor in this system, whereas JM6 with a *Ki* of 17.65 μM and MPP^+ iodide with a *Ki* of 6.60 μM could potentially be effective inhibitors. In order to test the hypothesis that JM6 and MPP^+ iodide are inhibitors that target TAA1/TARs, the future experimentation could test the additive inhibition pattern of JM6 (or MPP^+ iodide) with yucasin. Additional inhibition beyond that observed for yucasin alone would support the conclusion that JM6 and MPP^+ are TAA1/TARs inhibitors.

4.3.4 Yucasin

In this experiment, the initial velocity was 37.17 ng min^{-1} mL^{-1} (S.D. +/- 2.63 ng min^{-1} mL^{-1}) with the addition of 0.01 nM of yucasin; 31.70 ng min^{-1} mL^{-1} (S.D. +/- 4.26 ng min^{-1} mL^{-1}) with the addition of 0.1 nM of yucasin; 33.79 ng min^{-1} mL^{-1} (S.D. +/- 2.35 ng min^{-1} mL^{-1}) with the addition of 1 nM yucasin; 28.02 ng min^{-1} mL^{-1} (S.D. +/- 2.54 ng min^{-1} mL^{-1}) with the addition of 10 nM yucasin; and 13.95 ng min^{-1} mL^{-1} (S.D. +/- 2.25 ng min^{-1} mL^{-1}) with the addition of 100 nM of yucasin. The *Ki* of yucasin in the maize endosperm IAA biosynthesis system is 74.75 nM. The result is shown in **Figure 4-9**. It was determined that in the maize endosperm *in vitro* system, yucasin with a *Ki* value of 74.75 nM is a very potent inhibitor that targets at YUCCAs and blocks the IPyA

pathway. Since the IPyA pathway contributes 80% or more of the IAA that synthesized from tryptophan-dependent pathways (result from Chapter 2), the application of yucasin can be used as a good inhibitor to target at YUCCAs and dramatically decrease IAA synthesis via this pathway in plants.

One of the future research directions of this inhibitor project is to combine the research in Chapter 3 and Chapter 4 and study the IAA biosynthesis pathways *in vitro* and *in vivo*. By applying the same apparatus and similar experimental setup of ^{18}O-labeling experiment discussed in Chapter 3, we can answer the question that whether these inhibitors are specific to IPyA pathways. By supplying specific IAA biosynthesis inhibitors to whole seedlings or specific tissues, we will be able to obtain viable null mutants of IAA biosynthesis (especially the IPyA route), along with the aid of ^{18}O labeling technique, we may investigate further on the role of IPyA route of IAA biosynthesis in many auxin-mediated responses.

4.5 Tables

Inhibitor Class	Inhibitors	*Ki* Value
Indole derivatives	2-MBI	2.84 μM
	6-FI	300.83 μM
TAA1inhibitors	AOPP	6.18 μM
	AVG	293.30 μM
Kyn-related TAA1 inhibitors	Kyn	29.33 μM
	JM6	17.65 μM
	MPP^+	6.60 μM
Yucasin	Yucasin	74.75 nM

Table 4-1. The inhibition constant (Ki) for each inhibitor listed by 4 inhibitor classes: indole derivatives including 2-MBI and 6-FI, TAA1 inhibitors including AOPP and AVG, TAA1 inhibitors related to kynurenine pathway including Kyn, JM6 and MPP^+ iodide, and a YUCCA inhibitor, yucasin.

4.6 Figures

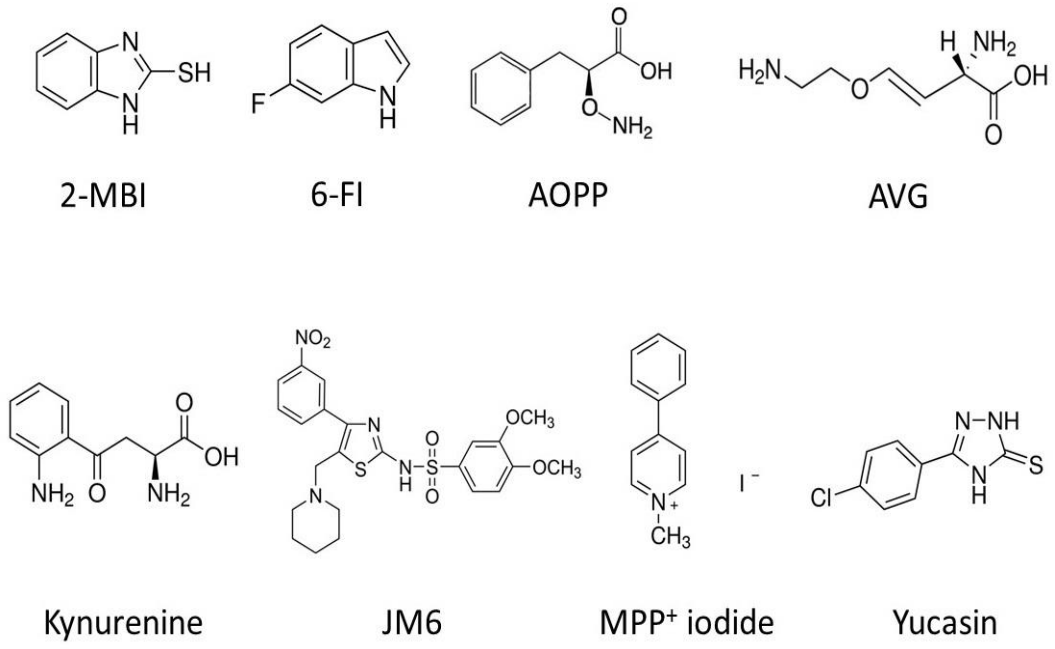

Figure 4-1. Chemical structures of inhibitors tested in Chapter 4. They are 2-MBI, 6-FI, AOPP, AVG, Kyn, JM6, MPP$^+$ iodide, and yucasin.

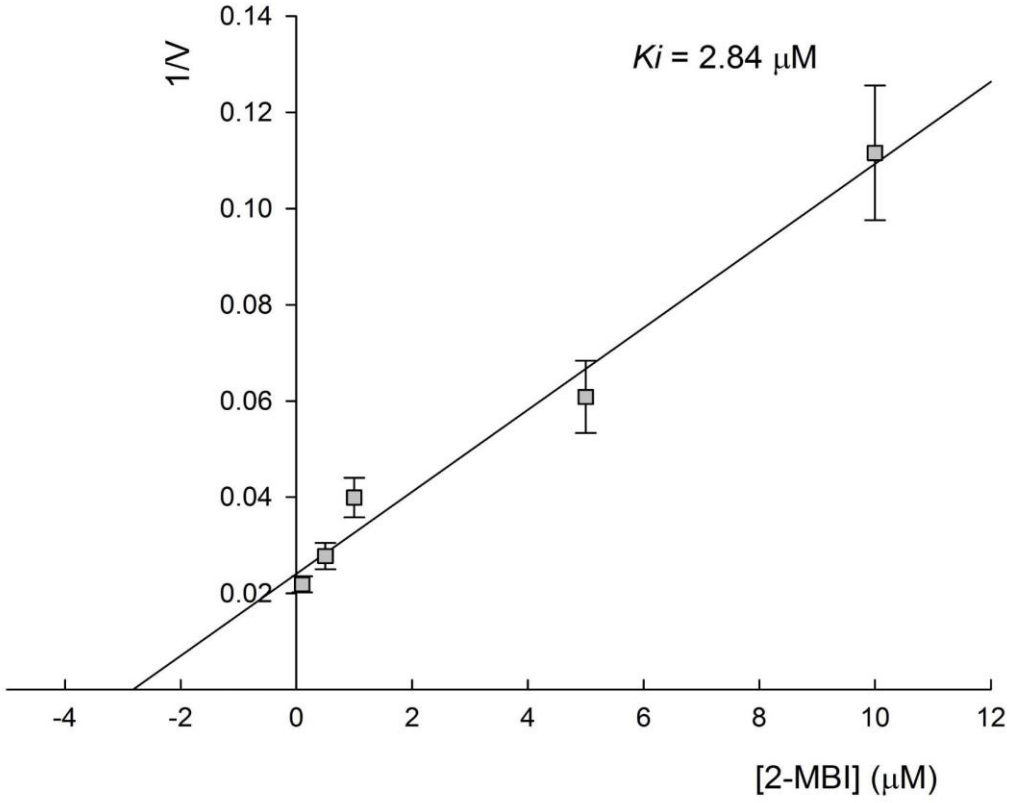

Figure 4-2. Dixon plot of 2-MBI inhibition. The substrate concentration used in the reaction was 5.78 μM, which is the Km value of tryptophan in the maize endosperm enzyme sample. The inhibitor concentrations used in the experiments were 0.1 μM, 0.5 μM, 1 μM, 5 μM and 10 μM. Based on the analysis of the Dixon plot, the Ki value of 2-MBI was determined to be 2.84 μM.

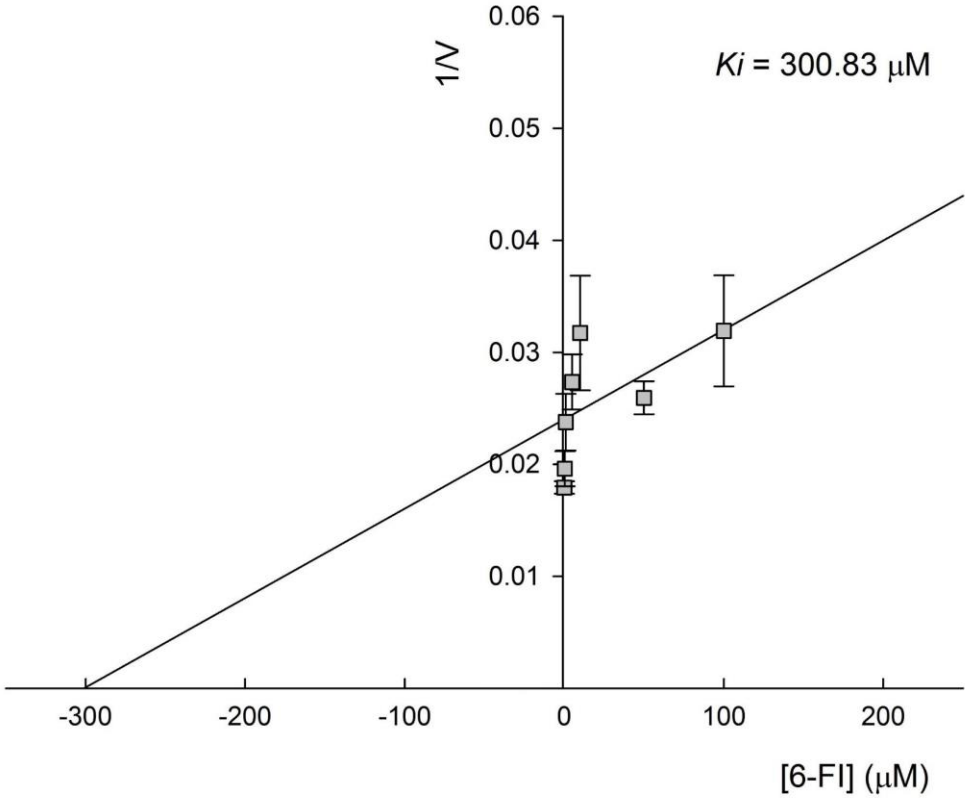

Figure 4-3. Dixon plot of 6-FI inhibition. The substrate concentration used in the reaction was 5.78 μM, which is the Km value of tryptophan in the maize endosperm enzyme sample. The inhibitor concentrations used in the experiments were 0.1 μM, 0.5 μM, 1 μM, 5 μM, 10 μM, 50 μM and 100 μM. Based on the analysis of the Dixon plot, the Ki value of 6-FI was determined to be 300.83 μM.

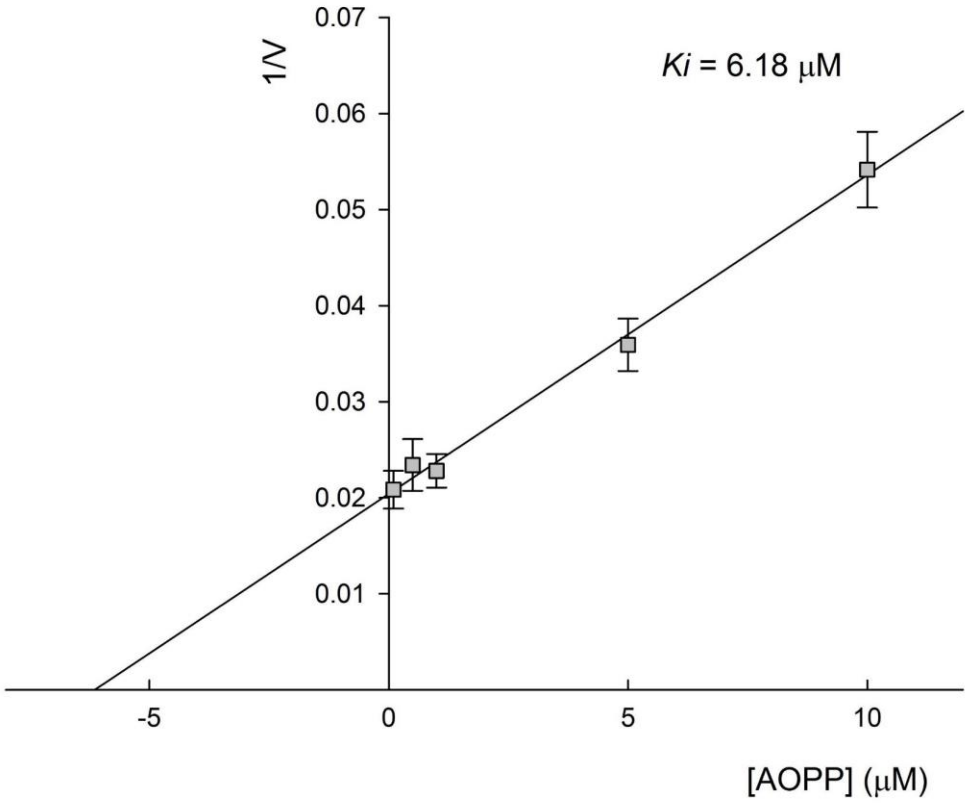

Figure 4-4. Dixon plot of AOPP inhibition. The substrate concentration used in the reaction was 5.78 μM, which is the Km value of tryptophan in the maize endosperm enzyme sample. The inhibitor concentrations used in the experiments were 0.1 μM, 0.5 μM, 1 μM, 5 μM and 10 μM. Based on the analysis of the Dixon plot, the Ki value of AOPP was determined to be 6.18 μM.

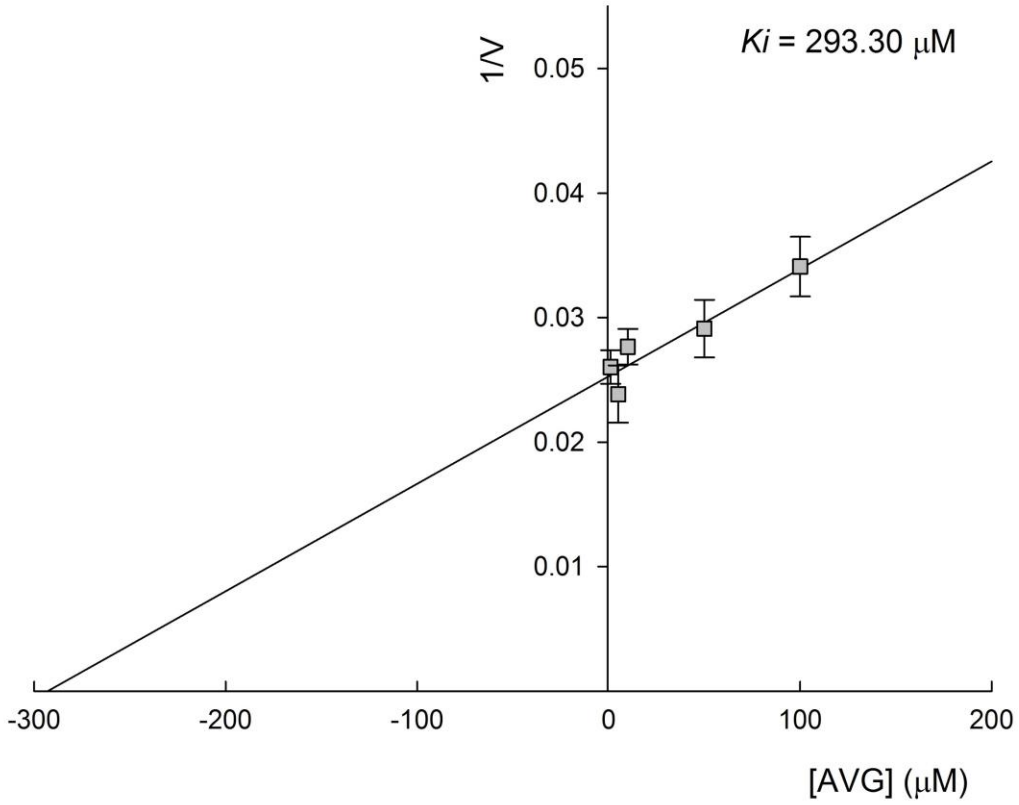

Figure 4-5. Dixon plot of AVG inhibition. The substrate concentration used in the reaction was 5.78 μM, which is the Km value of tryptophan in the maize endosperm enzyme sample. The inhibitor concentrations used in the experiments were 1 μM, 5 μM, 10 μM, 50 μM and 100 μM. Based on the analysis of the Dixon plot, the Ki value of AVG was determined to be 293.3 μM.

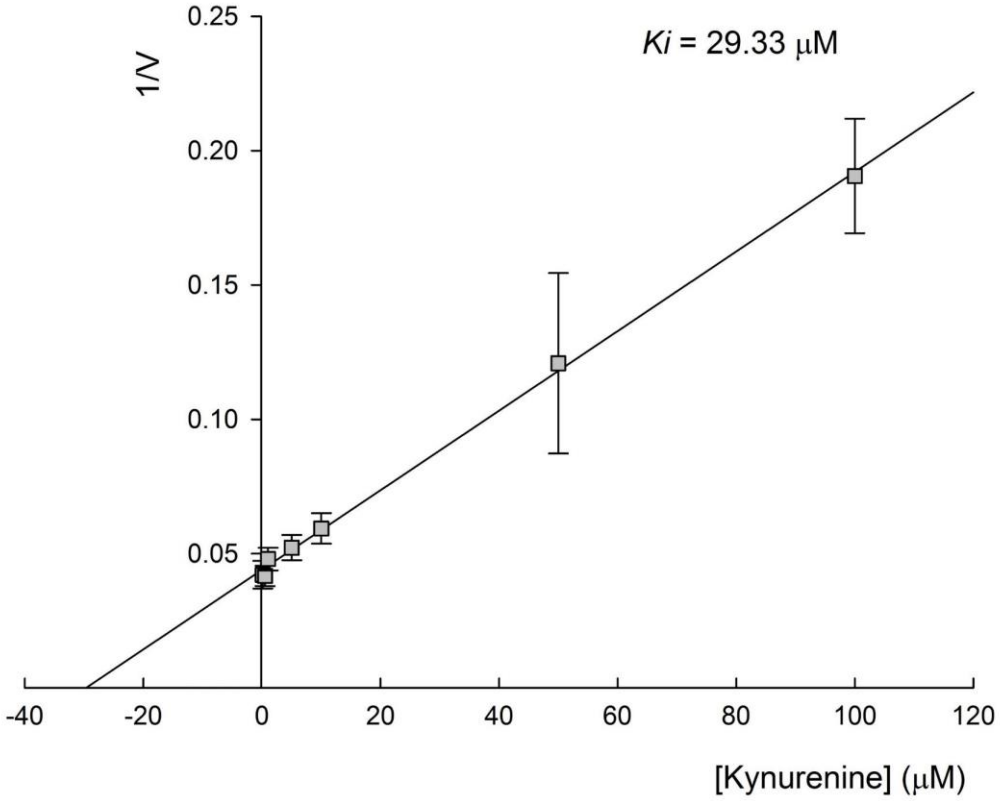

Figure 4-6. Dixon plot of kynurenine inhibition. The substrate concentration used in the reaction was 5.78 μM, which is the Km value of tryptophan in the maize endosperm enzyme sample. The inhibitor concentrations used in the experiments were 0.1 μM, 0.5 μM, 1 μM, 5 μM, 10 μM, 50 μM and 100 μM. Based on the analysis of the Dixon plot, the Ki value of Kyn was determined to be 29.33 μM.

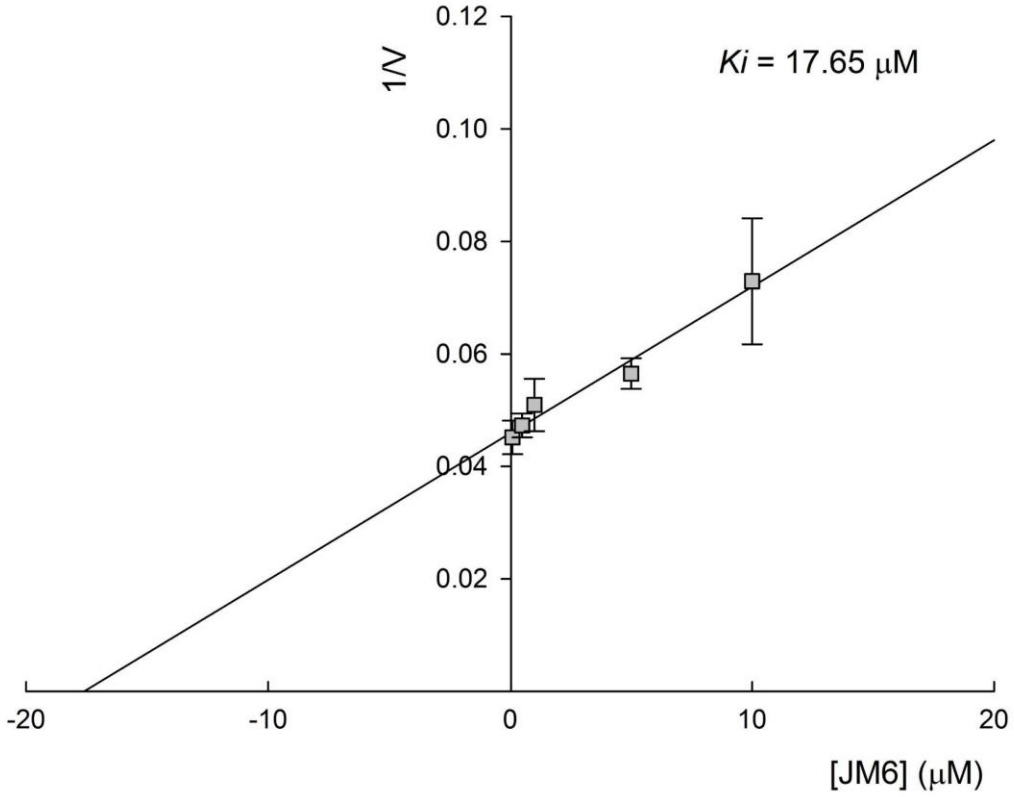

Figure 4-7. Dixon plot of JM6 inhibition. The substrate concentration used in the reaction was 5.78 μM, which is the Km value of tryptophan in the maize endosperm enzyme sample. The inhibitor concentrations used in the experiments were 0.1 μM, 0.5 μM, 1 μM, 5 μM and 10 μM. Based on the analysis of the Dixon plot, the Ki value of JM6 was determined to be 17.65 μM.

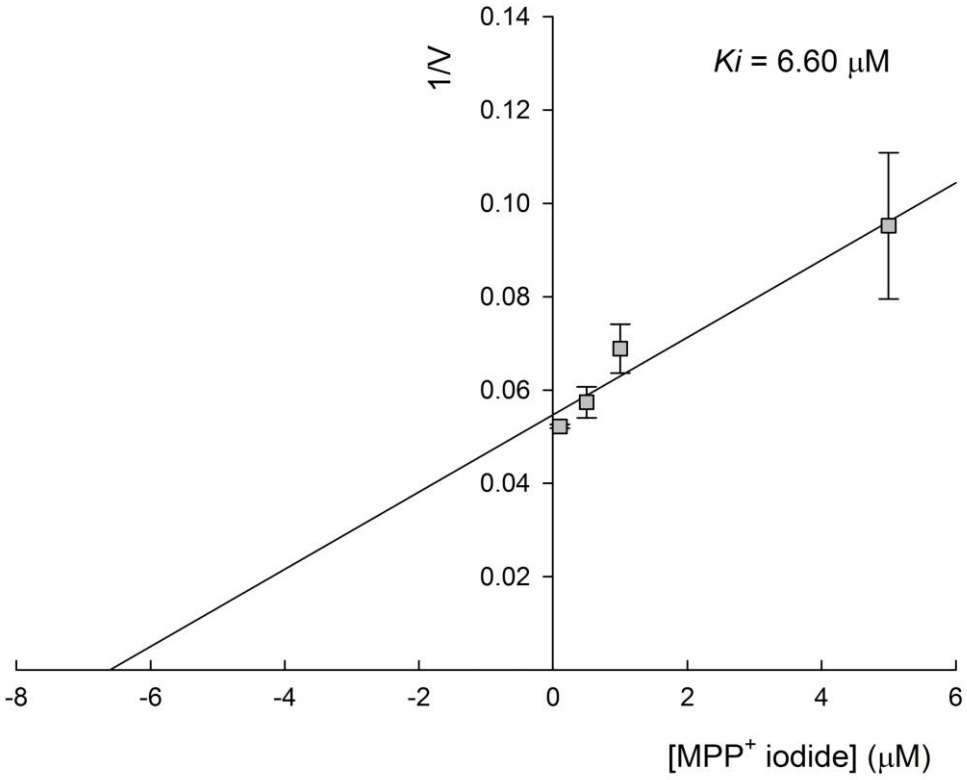

Figure 4-8. Dixon plot of MPP^+ iodide inhibition. The substrate concentration used in the reaction was 5.78 μM, which is the Km value of tryptophan in the maize endosperm enzyme sample. The inhibitor concentrations used in the experiments were 0.1 μM, 0.5 μM, 1 μM, and 5 μM. Based on the analysis of the Dixon plot, the Ki value of MPP^+ iodide was determined to be 6.6 μM.

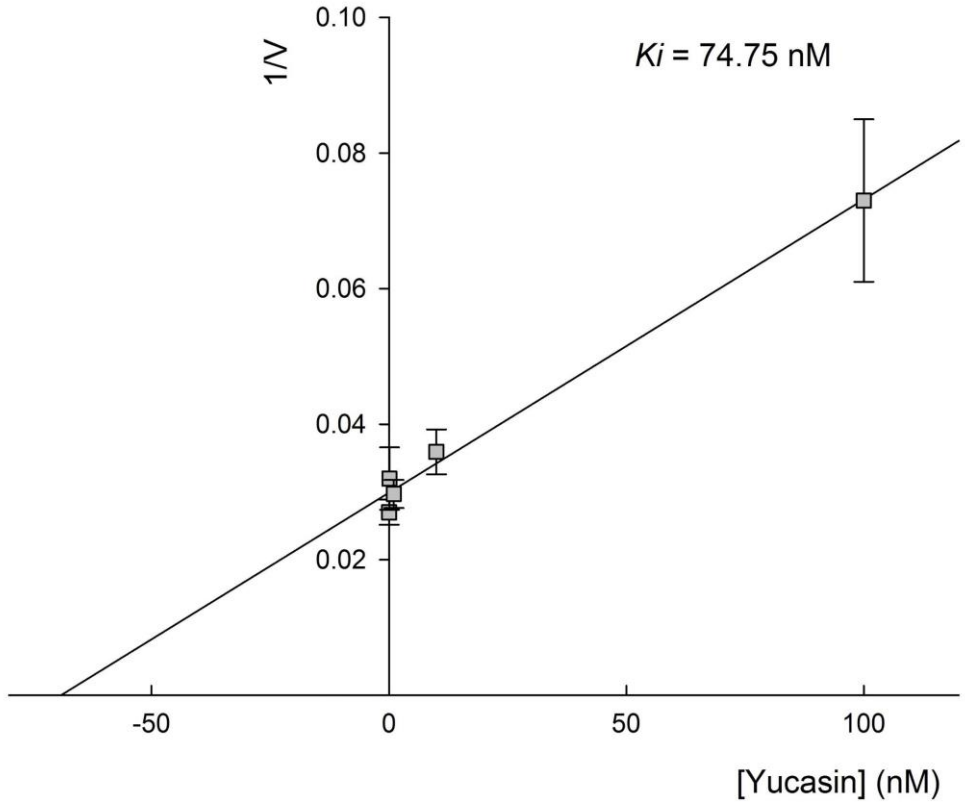

Figure 4-9. Dixon plot of yucasin inhibition. The substrate concentration used in the reaction was 5.78 μM, which is the Km value of tryptophan in the maize endosperm enzyme sample. The inhibitor concentrations used in the experiments were 0.01nM, 0.1 nM, 1 nM, 10 nM, and 100 nM. Based on the analysis of the Dixon plot, the Ki value of yucasin was determined to be 74.75 nM.

4.7 Literature Cited

Amaral M, Levy C, Heyes DJ, Lafite P, Outeiro TF, Giorgini F, Leys D and Scrutton NS (2013) Stuctural basis of kynurenine 3-monooxygenase inhibition. Nature **496**: 382-385

Bregoli AM, Scaramagli S, Costa G, Sabatini E, Ziosi V, Biondi S and Torrigiani P (2002) Peach (Prunus persica) fruit ripening: aminoethoxyvinylglycine (AVG) and exogenous polyamines affect ethylene emission and flesh firmness. Physiologia Plantarum **114**: 472-481

Cheng Y, Dai X and Zhao Y (2006) Auxin biosynthesis by the YUCCA flavin monooxygenases controls the formation of floral organs and vascular tissues in Arabidopsis Genes & Development **20**: 1790-1799

Dai X, Mashiguchi K, Chen Q, Kasahara H, Kamiya Y, Ojha S, DuBois J, Ballou D and Zhao Y (2013) The biochemical mechanism of auxin biosynthesis by an Arabidopsis YUCCA favin-containing monooxygenase. The Journal of Biological Chemistry **288**: 1448-1457

He W, Brumos J, Li H, Ji Y, Ke M, Gong X, Zeng Q, Li W, Zhang X, An F, Wen X, Li P, Chu J, Sun X, Yan C, Yan N, Xie DY, Raikhel N, Yang Z, Stepanova AN, Alonso JM and Guo H (2011) A small-molecule screen identifies L-Kynurenine as a competitive inhibitor of TAA1/TAR activity in ethylene-directed auxin biosynthesis and

root growth in Arabidopsis. The Plant Cell **23**: 3944-3960

Heikkila RE, Manzino L, Cabbat FS and Duvoisin RC (1984) Protection against the dopaminergic neurotoxicity of 1-methyl-4-phenyl-1,2,5,6-tetrahydropyridine by monoamine oxidase inhibitors. Nature **311**: 467-469

Ilić N, Östin A and Cohen JD (1999) Differential inhibition of indole-3-acetic acid and tryptophan biosynthesis by indole analogues. I. Tryptophan dependent IAA biosynthesis. Journal of Plant Growth Regulation **27**: 57-62

Langston JW, Irwin I, Langston EB and Forno LS (1984) 1-Methyl-4-phenylpyridinium ion (MPP^+): Identification of a metabolite of MPTP, a toxin selective to the substantia nigra. Neuroscience Letters **48**: 87-92

Ligero F, Caba JM, Lluch C and Olivares J (1991) Nitrate inhibition of nodulation can be overcome by the ethylene inhibitor aminoethoxyvinylglycine. Plant Physiology **97**: 1221-1225

Ludwig-Müller J, Denk K, Cohen JD and Quint M (2010) An inhibitor of tryptophan-dependent biosynthesis of indole-3-acetic acid alters seedling development in *Arabidopsis*. Journal of Plant Growth Regulation **29**: 242-248

Katoh A, Hashimoto T (2004) Molecular biology of pyridine nucleotide and nicotine

biosynthesis. Frontiers in Bioscience **9**: 1577-1586

Katoh A, Uenohara K, Akita M, Hashimoto T (2006) Early steps in the biosynthesis of NAD in the Arabidopsis start with aspartate and occur in the plastid. Plant Physiology **141**: 851-857

Ma JH, Yao JL, Cohen D and Morris B (1998) Ethylene inhibitors enhance in vitro root formation from apple shoot cultures. Plant Cell Reports **17**: 211-214

Mashiguchi K, Tanaka K, Sakai T, Sugawara S, Kawaide H, Natsume M, Hanada A, Yaeno T, Shirasu K, Yao H, McSteen P, Zhao Y, Hayashi K, Kamiya Y and Kasahara H (2011) The main auxin biosynthesis pathway in *Arabidopsis*. Proceedings of the National Academy of Sciences of the United States of America **108**: 18512-18517

Mauch F, Hadwiger LA and Boller T (1984) Ethylene: Symptom, Not Signal for the Induction of Chitinase and β-1,3-Glucanase in Pea Pods by Pathogens and Elicitors. Plant physiology **76**: 607-611

Narukawa-Nara M, Nakamura A, Kikuzato K, Kakei Y, Sato A, Mitani Y, Yamasaki-Kokudo Y, Ishii T, Hayashi K, Asami T, Ogura T, Yoshida S, Fujioka S, Kamakura T, Kawatsu T, Tachikawa M, Soeno K and Shimada Y (2016) Aminooxy-napthylpropionic acid and its derivatives are inhibitors of auxin biosynthesis targeting L-tryptophan aminotransferase: structure-activity relationships. The Plant Journal **87**: 245-

257

Nishimura T, Hayashi K, Suzuki H, Gyohda A, Takaoka C, Sakaguchi Y, Matsumoto S, Kasahara H, Sakai T, Kato J, Kamiya Y and Koshiba T (2014) Yucasin is a potent inhibitor of YUCCA, a key enzyme in auxin biosynthesis. The Plant Journal **77**: 352-366

Noctor G, Hager J and Li S (2011) Biosynthesis of NAD and its manipulation in plants. Advances in Botanical Research **58**:153-201

Reinhart PH and Kelly JW (2011) Treating the periphery to ameliorate neurodegenerative diseases. Cell **145**: 813-814

Schwarcz R, Bruno JP, Muchowaski PJ and Wu HQ (2012) Kynurenines in the mammalian brain: when physiology meets pathology. Nature Reviews Neuroscience **13**: 465-477

Soeno K, Goda H, Ishii T, Ogura T, Tachikawa T, Sasaki E, Yoshida S, Fujioka S, Asami T and Shimada Y (2010) Auxin biosynthesis inhibitors, indentified by a genomics-based approach, provide insights into auxin biosynthesis. Plant & Cell Physiology **51**: 524-536

Stepanova AN, Hoyt JM, Hamilton AA and Alonso JM (2005) A link between

ethylene and auxin uncovered by the characterization of two root-specific ethylene-insensative mutants in Arabidopsis. The Plant Cell **17**: 2230-2242

Stepanova AN, Robertson-Hoyt J, Yun J, Benavente LM, Xie DY, Dolezal K, Schlereth A, Jürgens G, and Alonso JM (2008) TAA1-mediated auxin biosynthesis is essential for hormone crosstalk and plant development. Cell **133**: 177-191

Swarup R, Perry P, Hagenbeek D, Van Der Straeten D, Beemster G TS, Sandberg G, Bhalerao R, Ljung K and Bennett MJ (2007) Ethylene upregulates auxin biosynthesis in Arabidopsis seedlings to enhance inhibition of root cell elongation. The Plant Cell **19**: 2186-2196

Tivendale ND, Ross JJ and Cohen JD (2014) The shifting paradigms of auxin biosynthesis. Trends in Plant Science **19**: 44-51

Won C, Shen X, Mashiguchi K, Zheng Z, Dai X, Cheng Y, Kasahara H, Kamiya Y, Chory J and Zhao Y (2011) Conversion of tryptophan to indole-3-acetic acid by tryptophan aminotransferases of Arabidopsis and YUCCAs in *Arabidopsis*. Proceedings of the National Academy of Sciences of the United States of America **108**: 18518-18523

Yu YB and Yang SF (1979) Auxin-induced ethylene production and its inhibition by aminoethyoxyvinylglycine and cobalt ion. Plant Physiology **64**: 1074-1077

Bibliography

Abeles FB and Rubinstein B (1964) Regulation of ethylene evolution and leaf abscission by auxin. Plant Physiology 39: 963-969

Amaral M, Levy C, Heyes DJ, Lafite P, Outeiro TF, Giorgini F, Leys D and Scrutton NS (2013) Stuctural basis of kynurenine 3-monooxygenase inhibition. Nature 496: 382-385

Bainbridge K, Guyomarc S, Bayer E, Swarup R, Bennett M, Mandel T and Kuhlemeier (2008) Auxin influx carriers stabilize phyllotactic patterning. Genes & Development 22: 810-823

Bak S and Feyereisen R (2001) The involvement of two P450 enzymes, CYP83B1 and CYP83A1, in auxin homeostasis and glucosinolate biosynthesis. Plant Physiology 127: 108-118

Bandurski R, Cohen J, Slovin J, and Reinecke D (1995) Auxin biosynthesis and metabolism, in Plant Hormones: Physiology, Biochemistry and Molecular Biology, P Davies, Editor, Kluwer Academic Publishers: Dordrecht, Boston, London. ISBN 0-7923-2984-8. p. 39-65

Bandurski RS and Schulze A (1974) Concentrations of indole-3-acetic acid and its esters in *Avena* and *Zea*. Plant Physiology 54: 257-262

Barbez E, Kubeš M, Rolčík J, Béziat C, Pěnčík A, Wang B, Rosquete MR, Zhu J, Dobrev P, Lee Y, Zažímalovà E, Petrášek J, Geisler M, Friml J and Kleine-Vehn J (2012) A novel putative auxin carrier family regulates intracellular auxin homeostasis in plants. Nature 485: 119-122

Barlier I, Kowalczyk M, Marchant A, Ljung K, Bhalerao R, Bennett M, Sandberg G and Bellini C (2000) The SUR2 gene of Arabidopsis thaliana encodes the cytochrome P450 CYP83B1, a modulator of auxin homeostasis. Proceedings of the National Academy of Sciences of the United States of America 97: 14819-14824

Bartel B and Fink GR (1994) Differential regulation of an auxin-producing nitrilase gene family in Arabidopsis thaliana. Plant Biology 91: 6649-6653

Bernardi J, Lanubile A, Li Q, Kumar D, Kladnik A, Cook SD, Ross JJ and Marocco A and Chourey PS (2012) Impaired auxin biosynthesis in the defective endosperm18 mutant is due to mutational loss of expression in the ZmYuc1 gene encoding endosperm-specific YUCCA1 protein in maize. Plant Physiology 160: 1318-1328

Blakesley D, Weston GD and Hall JF (1991) The role of endogenous auxin in root initiation. Plant Growth Regulation 10: 341-353

Bialek K and Cohen JD (1986) Isolation and partial characterization of the major amide-linked conjugate of indole-3-acetic acid from *Phaseolus vulgaris L*. Plant Physiology 80: 99-104

Bregoli AM, Scaramagli S, Costa G, Sabatini E, Ziosi V, Biondi S and Torrigiani P (2002) Peach (Prunus persica) fruit ripening: aminoethoxyvinylglycine (AVG) and exogenous polyamines affect ethylene emission and flesh firmness. Physiologia Plantarum 114: 472-481

Chamarro J, Östin A and Sandberg G (2001) Metabolism of indole-3-acetic acid by orange (*Citrus sinensis*) flavedo tissue during fruit development. Phytochemistry 57, 179–187.

Chen Q, Dai X, De-Paoli H, Cheng Y, Takebayashi Y, Kasahara H, Kamiya Y and Zhao Y (2014) Auxin overproduction in shoots cannot rescue auxin deficiencies in Arabidopsis roots. Plant Cell Biology 55: 1072-1079

Cheng Y, Dai X and Zhao Y (2006) Auxin biosynthesis by the YUCCA flavin monooxygenase controls the formation of floral organs and vascular tissues in Arabidopsis. Genes & Development 20: 1790-1799

Cohen JD (1984) Convenient apparatus for the generation of small amounts of diazomethane. Journal of Chromatography A 303: 193-196

Cohen JD, Baldi BG and Slovin JP (1986) 13C6-[Benzene Ring]-indole-3-acetic acid a new internal standard for quantitative mass spectral analysis of indole-3-acetic acid in plants. Plant Physiology 80: 14-19

Cohen JD and Bandurski RS (1982) Chemistry and physiology of the bound auxins. Annual Review of Plant Physiology 33: 403-430

Cohen JD, Slovin JP and Hendrickson AM (2003) Two genetically discrete pathways convert tryptophan to auxin: more redundancy in auxin biosynthesis. Trends in plant sciences 8:197-199

Comai L and Kosuge T (1982) Cloning and characterization of iaaM, a virulence determinant of *Pseudomonas savastanoi* 149: 40-46

Culler AH (2007) Tryptophan-dependent indole-3-acetic-acid biosynthesis pathway in *Zea mays.* Ph.D. dissertation, University of Minnesota, 84 pp.

Culler AH (2007) Tryptophan-dependent indole-3-acetic-acid biosynthesis pathway in *Zea mays.* Ph.D. dissertation, University of Minnesota, 105 pp.

Dai X, Mashiguchi K, Chen Q, Kasahara H, Kamiya Y, Ojha S, Dubois J, Ballou D and Zhao Y (2013) The biochemical mechanism of auxin biosynthesis by an Arabidopsis

YUCCA flavin-containing monooxygenase. Journal of Biological Chemistry 288: 1448-1457

Ellis CM, Nagpal P, Young JC, Hagen G, Guilfoyle TJ and Reed JW (2005) *AUXIN RESPONSE FACTOR1* and *AUXIN RESPONSE FACTOR2* regulate senescence and floral organ abscission in Arabidopsis thaliana. Development 132: 4563-4574

Enders TA and Strader LC (2015) Auxin activity: Past, present, and future. American Journal of Botany 102: 180-196

Epstein E and Ludwig-Müller J (1993) Indole-3-butyric acid in plants: occurrence, synthesis, metabolism and transport. Physiologia Plantarum 88: 382-389

Ernstsen A, Sandberg G and Lundström K (1987) Identification of oxindole-3-acetic acid, and metabolic conversion of indole-3-acetic acid to oxindole-3-acetic acid in Pinus sylvestris seeds. Planta 172: 47–52

Friml J and Ding Z (2010) Auxin regulates distal stem cell differentiation in Arabidopsis roots. Proceedings of the National Academy of Science 107: 12046-12051

Fukuda H (2004) Signals that control plant vascular cell differentiation. Nature Reviews Molecular Cell Biology 5: 379-391

Gallavotti A, Barazesh S, Malcomber S, Hall D, Jackson D, Schmidt RJ and McSteen P (2008) sparse inflorescence1 encodes a monocot-specific YUCCA-like gene required for vegetative and reproductive development in maize. Proceedings of the National Academy of Sciences of the United States of America 105: 15196-15201

He W, Brumos J, Li H, Ji Y, Ke M, Gong X, Zeng Q, Li W, Zhang X, An F, Wen X, Li P, Chu J, Sun X, Yan C, Yan N, Xie DY, Raikhel N, Yang Z, Stepanova AN, Alonso JM and Guo H (2011) A small-molecule screen identifies L-Kynurenine as a competitive inhibitor of TAA1/TAR activity in ethylene-directed auxin biosynthesis and root growth in Arabidopsis. The Plant Cell 23: 3944-3960

Heikkila RE, Manzino L, Cabbat FS and Duvoisin RC (1984) Protection against the dopaminergic neurotoxicity of 1-methyl-4-phenyl-1,2,5,6-tetrahydropyridine by monoamine oxidase inhibitors. Nature 311: 467-469

Hull AK, Vij R and Celenza JL (2000) *Arabidopsis* cytochrome P450s that catalyze the first step of tryptophan-dependent indole-3-acetic acid biosynthesis. Proceedings of the National Academy of Sciences of the United States of America 97: 2379-2384

Ilić N, Östin A and Cohen JD (1999) Differential inhibition of indole-3-acetic acid and tryptophan biosynthesis by indole analogues. I. Tryptophan dependent IAA biosynthesis. Journal of Plant Growth Regulation 27: 57-62

Ikeda Y, Men S, Fischer U, Stepanova AN, Alonso JM, Ljung K and Grebe M (2009) Local auxin biosynthesis modulates gradient directed planar polarity in Arabidopsis. Nature Cell Biology 11: 731-738

Jacobs WP (1993) A search for some angiosperm hormones and their metabolites in *Caulerpa paspaloides* (Chlorophyta). Journal of Phycology 29: 595–600

Jensen PJ and Bandurski RS (1994) Metabolism and synthesis of indole-3-acetic acid (IAA) in *Zea mays*. Plant Physiology 106: 343-351

Jones AR, Kramer EM, Knox K, Swarup R, Bennett MJ, Lazarus CM, Leyser HMO and Grierson CS (2008) Auxin transport through non-hair cell sustains root-hair development. Nature Cell Biology 11: 78-84

Kai K, Horita J, Wakasa K and Miyagawa H (2007) Three oxidative metabolites of indole-3-acetic acid from *Arabidopsis thaliana*. Phytochemistry 68: 1651-1663

Kaminoto Y, Terasaka K, Hamamoto M, Takanashi K, Fukuda S, Shitan N, Sugiyama A, Suzuki H, Shibata D, Wang B, Pollmann S, Geisler M and Yazaki K (2012) Arabidopsis ABCB21 is a facultative auxin importer/exporter regulated by cytoplasmic auxin concentration. Plant Cell Physiology 53: 2090-2100.

Katoh A, Hashimoto T (2004) Molecular biology of pyridine nucleotide and nicotine

biosynthesis. Frontiers in Bioscience 9: 1577-1586

Katoh A, Uenohara K, Akita M, Hashimoto T (2006) Early steps in the biosynthesis of NAD in the Arabidopsis start with aspartate and occur in the plastid. Plant Physiology 141: 851-857

Korasick DA, Enders TA and Strader LC (2013) Auxin biosynthesis and storage forms. Journal of Experimental Botany 64: 2541-2555

Kriechbaumer V, Park WJ, Piotrowski M, Meeley RB, Gierl A and Glawischnig E (2007) Maize nitrilases have a dual role in auxin homeostasis and β-cyanoalanine hydrolysis. Journal of Experimental Botany 58: 4225-4233

Lam HK, McAdam SAM, McAdam EL and Ross JJ (2015) Evidence that chlorinated auxin is restricted to the *Fabaceae* but not to the *Fabeae*. Plant Physiology 168: 798-803

Langston JW, Irwin I, Langston EB and Forno LS (1984) 1-Methyl-4-phenylpyridinium ion (MPP^+): Identification of a metabolite of MPTP, a toxin selective to the substantia nigra. Neuroscience Letters 48: 87-92

Larson ER (2016) A fresh look at the role of auxin in PIN trafficking. Plant Physiology 172: 821-822

Last RL, Bissinger PH, Mahoney DJ, Radwanski ER and Fink GR (1991) Tryptophan mutants in Arabidopsis: the consequences of duplicated tryptophan synthase beta genes. The Plant Cell 3: 345-358

LeClere S, Schmelz EA and Chourey PS (2010) Sugar levels regulate tryptophan-dependent auxin biosynthesis in developing maize kernels. Plant Physiology 153: 306-318

Lehmann T, Hoffmann M, Hentrich M and Pollmann S (2010) Indole-3-acetamide-dependent auxin biosynthesis: A widely distributed way of indole-3-acetic acid production? European Journal of Cell Biology 89: 895-905

Lewer P and Bandurski RS (1987) Occurrence and metabolism of 7-hydroxy-2-indolinone-3-acetic acid in Zea mays. Phytochemistry 26:1247-1250

Ligero F, Caba JM, Lluch C and Olivares J (1991) Nitrate inhibition of nodulation can be overcome by the ethylene inhibitor aminoethoxyvinylglycine. Plant Physiology 97: 1221-1225

Liu CM, Xu ZH and Chua NH (1993) Auxin polar transport is essential for the establishment of bilateral symmetry during early plant embryogenesis. Plant Cell 5: 621-630

Liu X (2012) Roles of multiple mechanisms in regulating auxin levels during plant growth and development. Ph.D. dissertation, University of Minnesota, 35-37 pp.

Ljung K (2013) Auxin metabolism and homeostasis during plant development. Development 140: 943-950

Ljung K, Hull AK, Celenza J, Yamada M, Estelle M, Normanly J and Sandberg G (2005) Sites and regulation of auxin biosynthesis in Arabidopsis roots. The Plant Cell 17: 1090-1104

Ljung K, Hull AK, Kowalczyk M, Marchant A, Celenza J, Cohen JD and Sandberg G (2002) Biosynthesis, conjugation, catabolism and homeostasis of indole-3-acetic acid in Arabidopsis thaliana. Plant Molecular Biology 50: 309-332

Ludwig-Müller (2011) Auxin conjugates: their role for plant development and in the evoluation of land plants. Journal of Experimental Botany 62: 1757-1773

Ludwig-Müller J, Denk K, Cohen JD and Quint M (2010) An inhibitor of tryptophan-dependent biosynthesis of indole-3-acetic acid alters seedling development in *Arabidopsis*. Journal of Plant Growth Regulation 29: 242-248

Ma JH, Yao JL, Cohen D and Morris B (1998) Ethylene inhibitors enhance in vitro root formation from apple shoot cultures. Plant Cell Reports 17: 211-214

Mano Y and Nemoto K (2012) The pathway of auxin biosynthesis in plants. Journal of Experimental Botany 63: 2853-2872

Mashiguchi K, Tanaka K, Sakai T, Sugawara S, Kawaide H, Natsume M, Hanada A, Yaeno T, Shirasu K, Yao H, McSteen P, Zhao Y, Hayashi K, Kamiya Y and Kasahara H (2011) The main auxin biosynthesis pathway in *Arabidopsis.* Proceedings of the National Academy of Sciences of the United States of America 108: 18512-18517

Mauch F, Hadwiger LA and Boller T (1984) Ethylene: Symptom, Not Signal for the Induction of Chitinase and β-1,3-Glucanase in Pea Pods by Pathogens and Elicitors. Plant physiology 76: 607-611

Mellor N, Band LR, Pěnčík A, Novák O, Rashed A, Holman T, Wilson MH, Voß U, Bishopp A, King JR, Ljung K, Bennett MJ and Owen MR (2016) Dynamic regulation of auxin oxidase and conjugating enzymes AtDAO1 and GH3 modulates auxin homeostasis. Proceedings of the National Academy of Sciences of the United States of America 113:11022-11027

Michalczuk L, Cooke TJ and Cohen JD (1992) Auxin levels at different stages of carrot somatic embryogenesis. Phytochemistry 31:1097-1103

Mikkelsen MD, Naur P and Halkier BA (2004) *Arabidopsis* mutants in the C-S lyase of glucosinolate biosynthesis establish a critical role for indole-3-acetaldoxime in auxin homeostasis. The Plant Journal 37: 770-777

Narukawa-Nara M, Nakamura A, Kikuzato K, Kakei Y, Sato A, Mitani Y, Yamasaki-Kokudo Y, Ishii T, Hayashi K, Asami T, Ogura T, Yoshida S, Fujioka S, Kamakura T, Kawatsu T, Tachikawa M, Soeno K and Shimada Y (2016) Aminooxy-napthylpropionic acid and its derivatives are inhibitors of auxin biosynthesis targeting L-tryptophan aminotransferase: structure-activity relationships. The Plant Journal 87: 245-257

Nemoto K, Hara M, Suzuki M, Seki H, Muranaka T and Mano Y (2009) The NtAMI1 gene functions in cell division of tobacco BY-2 cells in the presence of indole-3-acetamide. FEBS Letters 583: 487-492

Nishimura T, Hayashi K, Suzuki H, Gyohda A, Takaoka C, Sakaguchi Y, Matsumoto S, Kasahara H, Sakai T, Kato J, Kamiya Y and Koshiba T (2014) Yucasin is a potent inhibitor of YUCCA, a key enzyme in auxin biosynthesis. The Plant Journal 77: 352-366

Noctor G, Hager J and Li S (2011) Biosynthesis of NAD and its manipulation in plants. Advances in Botanical Research 58:153-201

Nonhebel HM, Kruse LI and Bandurski RS (1985) Indole-3-acetic acid catabolism in *Zea mays* seedlings. Metabolic conversion of oxindole-3-acetic acid to 7-hydroxy-2-oxindole-3-acetic acid 7'-O-beta-D-glucopyranoside. J Biol Chem. 260:12685-12689

Nonhebel H, Yuan Y, Al-Amier H, Pierck M, Akor E, Ahamed A, Cohen JD, Celenza JL and Normanly J (2010) Redirection of tryptophan metabolism in tobacco by ectopic expression of an Arabidopsis indolic glucosinolate biosynthetic gene. Phytochemistry 72: 37-48

Normanly J (2010) Approaching cellular and molecular resolution of auxin biosynthesis and metabolism. Cold Spring Harbor Perspecives in Biology 2: a001594

Normanly J, Cohen JD and Fink GR (1993) Arabidopsis thaliana auxotrophs reveals a tryptophan-independent biosynthesis pathway for indole-3-acetic acid. Proceedings of the National Academy of Science 90: 10355-10359

Normanly J, Grisafi P, Fink GR and Bartel B (1997) Arabidopsis mutants resistant to the auxin effects of indole-3-acetonitrile are defective in the nitrilase encoded by the NIT1 gene. The Plant Cell 9: 1781-1790

Normanly J, Slovin JP and Cohen JD (2010) Auxin biosynthesis and metabolism. In: Plant Hormones: Biosynthess, Signal Transduction, Action! (3rd edition). P.J. Davies, ed. Springer Netherlands. Pages 36-62

Ohashi-Ito K, Oguchi M, Kojima M, Sakakibara H and Fukuda H (2013) Auxin-associated initiation of vascular cell differentiation by LONESOME HIGHWAY. Development 140: 765-769

Östin A, Kowalyczk M, Bhalerao RP and Sandberg G (1998) Metabolism of indole-3-acetic acid in Arabidopsis. Plant Physiology 118: 285-296

Ouyang J, Shao X and Li J (2000) Indole-3-glycerol phosphate, a branchpoint of indole-3-acetic acid biosynthesis from the tryptophan biosynthetic pathway in *Arabidopsis thaliana*. The Plant Journal 24: 327-333

Overvoorde P, Fukaki H and Beeckman T (2010) Auxin control of root development. Cold Spring Harbor Perspectives in Biology 2: a001537

Ozga JA, Kaur H, Savada RP and Reinecke (2017) DM Hormonal regulation of reproductive growth under normal and heat-stress conditions in legume and other model crop species. J Exp Bot [doi: 10.1093/jxb/erw464]

Park WJ, Kriechbaumer VK, Müller A, Piotrowski M, Meeley RB, Gierl A and Glawischnig E (2003) The nitrilase ZmNIT2 converts indole-3-acetonitrile to indole-3-acetic acid. Plant Physiology 133: 794-802

Patten CL and Glick BR (1996) Bacterial biosynthesis of indole-3-acetic acid. Canadian Journal of Microbiology 42: 207-220

Péret B, Swarup K, Ferguson A, Seth M, Yang Y, Dhondt S, James N, Casimiro I, Perry P, Syed A, Yang H, Reemmer J, Venison E, Howells C, Perez-Amador MA, Yun J, Alonso J, Beemster GTS, Laplaze L, Murphy A, Bennett MJ, Nielsen E and Swarup R (2012) AUX/LAX genes encoded a family of auxin influx transporters that perform distinct functions during Arabidopsis development. The Plant Cell 24: 2874-2885

Peterson SV, Johansson AI, Kowalczyk M, Makoveychuk A, Wang JY, Moritz T, Grebe M, Benfey PN, Sandberg G and Ljung K (2009) An auxin gradient and maximum in the Arabidopsis root apex shown by high-resolution cell-specific analysis of IAA distribution and synthesis. The Plant Cell 21: 1659-1668

Phillips KA, Skirpan AL, Liu X, Christensen A, Slewinski TL, Hudson C, Barazesh S, Cohen JD, Malcomber S and McSteen P (2011) *vanishing tassel2* encodes a grass-specific tryptophan aminotransferase required for vegetative and reproductive development in maize. Plant Cell 23: 550-566

Pieck M, Yuan Y, Godfrey J, Fisher C, Zolj S, Vaughan D, Thomas N, Wu C, Ramos J, Lee N, Normanly J and Celenza JL (2015) Auxin and tryptophan homeostasis are facilitated by the ISS1/VAS1 aromatic aminotransferase in *Arabidopsis*. Genetics 201:185-199

Pollmann S, Müller A, Piotrowski M and Weiler EW (2002) Occurrence and formation of indole-3-acetamide in *Arabidopsis thaliana*. Planta 216, 155-161

Pollmann S, Neu D, Lehmann T, Berkowitz O, Schäfer T and Weiler EW (2006) Subcellular localization and tissue specific expression of amidase 1 from Arabidopsis thaliana. Planta 224: 1241-1253

Pollmann S, Neu D and Weiler EW (2003) Molecular cloning and characterization of an amidase from Arabidopsis thaliana capable of converting indole-3-acetamide into the plant growth hormone, indole-3-acetic acid. Phytochemistry 62: 293-300

Porco S, Pencik A, Rashed A, Voß U, Casanova-Sáez R, Bishopp A, Golebiowska A, Bhosale R, Swarup R, Swarup K, Peňáková P, Novák O, Staswick P, Hedden P, Phillips AL, Vissenberg K, Bennett MJ and Ljung K (2016) Dioxygenase-encoding AtDAO1 gene controls IAA oxidation and homeostasis in Arabidopsis. Proceedings of the National Academy of Sciences of the United States of America 113:11016-1102

Qin G, Gu H, Zhao Y, Ma Z, Shi G, Yang Y, Pichersky E, Chen H, Liu M, Chen Z and Qu LJ (2005) An indole-3-acetic acid carboxylmethyltransferase regulates Arabidopsis leaf development. The Plant Cell 17: 2693-2704

Quittenden LJ, Davies NW, Smith JA, Molesworth PP, Tivendale ND and Ross JJ (2009) Auxin biosynthesis in pea: Characterization of the tryptamine pathway. Plant Physiology 151: 1130-1138

Radwanski ER, Barczak AJ and Last RL (1996) Characterization of tryptophan synthase alpha subunit mutants of Arabidopsis thaliana. Molecular and General Genetics 253: 353-361

Rajagopal R, Tsurusaki K, Kannangara G, Kuraishi S and Sakurai N (1994) Natural Occurrence of indoleacetamide and amidohydrolase activity in etiolated aseptically-grown squash seedlings. Plant & Cell Physiology 35: 329-339

Rampey RA, LeClere S, Kowalczyk M, Ljung K, Sandberg G and Bartel B (2004) A family of auxin-conjugated hydrolases that contributes to free indole-3-acetic acid levels during Arabidopsis germination. Plant Physiology 135: 978-988

Rekoslavskaya NI (1995) Pathways of indoleacetic acid and tryptophan synthesis in developing maize endosperm: studies *in vitro*. Russian Journal of Plant Physiology 42:143–151.

Reinhart PH and Kelly JW (2011) Treating the periphery to ameliorate neurodegenerative diseases. Cell 145: 813-814

Riov J and Bangerth F (1992) Metabolism of auxin in tomato fruit tissue: Formation of high molecular weight conjugates of oxindole-3-acetic acid via the oxidation of indole-3-acetylaspartic acid. Plant Physiology 100, 1396-1402

Schmidt RC, Muller A, Hain R, Bartling D and Weiler EW (1996) Transgenic tobacco plants expressing the Arabidopsis thaliana nitrilase II enzyme. The Plant Journal 9: 683-691

Schwarcz R, Bruno JP, Muchowaski PJ and Wu HQ (2012) Kynurenines in the mammalian brain: when physiology meets pathology. Nature Reviews Neuroscience 13: 465-477

Seo M, Akaba S, Oritani T, Delarue M, Bellini C, Caboche M and Koshiba T (1998) Higher activity of an aldehyde oxidase in the auxin-overproducing *superroot1* mutant of *Arabidopsis thaliana*. Plant Physiology 116: 687-693

Shani E, Salehin M, Zhang Y, Sanchez SE, Doherty C, Wang R, Mangado CC, Song L, Tal I, Pisanty O, Ecker JR, Kay SA, Pruneda-Paz J and Estelle M (2017) Plant Stress tolerance requires auxin-sensitive Aux/IAA transcriptional repressors. Current Biology 27: 437-444

Simon S and Petrášek J (2011) Why plants need more than one type of auxin. Plant Sci. 180:454–460.

Soeno K, Goda H, Ishii T, Ogura T, Tachikawa T, Sasaki E, Yoshida S, Fujioka S, Asami T and Shimada Y (2010) Auxin biosynthesis inhibitors, indentified by a genomics-based approach, provide insights into auxin biosynthesis. Plant & Cell Physiology 51: 524-536

Staswick PE, Serban B, Rowe M, Tiryaki I, Maldonado MT, Maldonado MC and Suza W (2005) Characterization of an Arabidopsis enzyme family that conjugates amino acids to indole-3-acetic acid. The Plant Cell 17: 616-627

Stepanova AN and Alonso JM (2016) Auxin catabolism unplugged: Role of IAA oxidation in auxin homeostasis. Proceedings of the National Academy of Sciences of the United States of America 113:10742-10744

Stepanova AN, Hoyt JM, Hamilton AA and Alonso JM (2005) A link between ethylene and auxin uncovered by the characterization of two root-specific ethylene-insensative mutants in Arabidopsis. The Plant Cell 17: 2230-2242

Stepanova AN, Robertson-Hoyt J, Yun J, Benavente LM, Xie DY, Doležal K, Schlereth A, Jürgens G and Alonso JM (2008) TAA1-mediated auxin biosynthesis essential for hormone crosstalk and plant development. Cell 133: 177-191

Sugawara S, Hishiyama S, Jikumaru Y, Hanada A, Nishimura T, Koshiba T, Zhao Y, Kamiya Y and Kasahara H (2009) Biochemical analyses of indole-3-acetaldoxime-

dependent auxin biosynthesis in *Arabidopsis*. Proceedings of the National Academy of Sciences of the United States of America 106: 5430-5435

Swarup R, Perry P, Hagenbeek D, Van Der Straeten D, Beemster G TS, Sandberg G, Bhalerao R, Ljung K and Bennett MJ (2007) Ethylene upregulates auxin biosynthesis in Arabidopsis seedlings to enhance inhibition of root cell elongation. The Plant Cell 19: 2186-2196

Taiz L and Zeiger E (2010) Plant Physiology. Sinauer Associates Inc., Publishers, Sunderland, Massachusetts U.S.A

Tam YY, Epstein E and Normanly J (2000) Characterization of auxin conjugates in *Arabidopsis*. Low steady-state levels of indole-3-acetyl-aspartate, indole-3-acetyl-glutamate, and indole-3-acetyl-glucose. Plant Physiology 123: 589-596

Tao Y, Ferrer JL, Ljung K, Pojer F, Hong F, Long JA, Li L, Moreno JE, Bowman ME, Ivans LJ, Cheng Y and Lim J (2008) Rapid synthesis of auxin via a new tryptophan-dependent pathway is required for shade avoidance in plants. Cell 133: 164-176

Thimann KV and Schneider CL (1939) The relative activity of different auxins. American Journal of Botany 26: 328-333

Tivendale ND, Davidson SE, Davies NW, Smith JA, Dalmais M, Bendahmane AI, Quittenden LJ, Sutton L, Bala RK, Signor CL, Thompson R, Horne J, Reid JB and Ross JJ (2012) Biosynthesis of the halogenated auxin, 4-chloroindole-3-acetic acid. Plant Physiology 159: 1055-1063

Tivendale ND, Davies NW, Molesworth PP, Davidson SE, Smith JA, Lowe EK, Reid JB and Ross JJ (2010) Reassessing the role of N-Hydroxytryptamine in auxin biosynthesis. Plant Physiology 154: 1957-1965

Tivendale ND, Ross JJ and Cohen JD (2014) The shifting paradigms of auxin biosynthesis. Trend in Plant Science 19: 44-51

Ueno M, Shibata H, Kihara J, Honda Y and Arase S (2003) Increased tryptophan decarboxylase and monoamine oxidase activities include Sekiguchi lesion formation in rice infected with *Magnaporthe grisea*. The Plant Journal 36: 215-228

Vandenbussche F, Petrášek J, Žádníková P, Hoyerová K, Pešek B, Raz V, Swarup R, Bennett M, Zažímalová E, Benková E and Van Der Straeten D (2010) The auxin influx carriers AUX1 and LAX3 are involved in auxin-ethylene interactions during apical hook development in Arabidopsis thaliana seedlings. Development 137: 597-606

Walz A, Park S, Slovin JP, Ludwig-Müller J, Momonoki YS and Cohen JD (2002) A gene encoding a protein modified by the phytohormone in indoleacetic acid. Proceedings of the National Academy of Sciences of the United States of America 99: 1718-1723

Wang B, Chu J, Yu T, Xu Q, Sun X, Yuan J, Xiong G, Wang G, Wang Y and Li J (2015) Tryptophan-independent auxin biosynthesis contributes to early embryogenesis in *Arabidopsis*. Proceedings of the National Academy of Sciences of the United States of America 112: 4821–4826

Went FW and Thimann KV (1937) Phytohormones. Macmillan, New York, New York, USA

Won C, Shen X, Mashiguchi K, Zheng Z, Dai X, Cheng Y, Kasahara H, Kamiya Y, Chory J and Zhao Y (2011) Conversion of tryptophan to indole-3-acetic acid by tryptophan aminotransferases of Arabidopsis and YUCCAs in *Arabidopsis*. Proceedings of the National Academy of Sciences of the United States of America 108: 18518-18523

Woodward AW and Bartel B (2005) Auxin: Regulation, action and interaction. Annals of Botany 95: 707-735

Yamada M, Greenham K, Prigge MJ, Jensen PJ and Estelle M (2009) The TRANSPORT INHIBITOR RESPONSE2 gene is required for auxin synthesis and diverse aspects of plant development. Plant Physiology 151: 168-179

Yamamoto Y, Kamiya N, Morinaka Y, Matsuoka M and Sazuka T (2007) Auxin biosynthesis by the YUCCA genes in rice. Plant Physiology 143: 1362-1371

Yu YB and Yang SF (1979) Auxin-induced ethylene production and its inhibition by aminoethyoxyvinylglycine and cobalt ion. Plant Physiology 64: 1074-1077

Záveská Drábková L, Dobrev PI and Motyka V (2015) Phytohormone profiling across the bryophytes. PLoS One 10, e0125411

Zhang J, Lin JE, Harris C, Pereira FCM, Wu F, Blakeslee JJ and Peer WA (2016) DAO1 catalyzes temporal and tissue-specific oxidative inactivation of auxin in *Arabidopsis thaliana*. Proceedings of the National Academy of Sciences of the United States of America 113:11010–11015

Zhao Y (2010) Auxin biosynthesis and its role in plant development. Annual Review of Plant Biology 61: 49-64.

Zhao Y (2014) Auxin biosynthesis. The Arabidopsis Book. doi: 10.1199/tab.0173

Zhao Y, Christensen SK, Fankhauser C, Cashman JR, Cohen JD, Weigel D and Chory J (2001) A role for flavin monooxygenase-like enzymes in auxin biosynthesis. Science 291: 306-309

Zhao Y, Hull AK, Gupta NR, Goss KA, Alonso J, Ecker JR, Normanly J, Chory J and Celenza JL (2002) Trp-dependent auxin biosynthesis in Arabidopsis: involvement of cytochrome P450s CYP79B2 and CYP79B3. Genes & Development 16: 3100-3112

Zhao Z, Zhang Y, Liu X, Zhang X, Liu S, Yu X, Ren Y, Zheng X, Zhou K, Jiang L, Guo X, Gai Y, Wu C, Zhai H, Wang H and Wan J (2013) A role for a dioxygenase in auxin metabolism and reproductive development in rice. Developmental Cell 27:113–112

Zhang J, Lin JE, Harris C, Pereira FCM, Wu F, Blakeslee JJ and Peer WA (2016) DAO1 catalyzes temporal and tissue-specific oxidative inactivation of auxin in Arabidopsis thaliana. Proceedings of the National Academy of Science of the United States of America 113: 11010-11015.

Zheng Z, Guo Y, Novak O, Dai X, Zhao Y, Ljung K, Noel JP and Chory J (2013) Coordination of auxin and ethylene biosynthesis by the aminotransferase VAS1. Nat. Chem. Biol. 9: 244–246.

Zažímalová E, Murphy AS, Yang H, Hoyerová K, and Hošek P (2010) Auxin transporters - Why so many? Cold Spring Harbor Perspectives in Biology 2: a001552

Appendix A

Molecular Cloning, Protein Purification and Enzyme Activity of Exogenously Expressed YUCCA1 and YUCCA2 Proteins in *Escherichia coli*

Overview

In this study, high background noise of IAA yield from IPyA non-enzymatic conversion has been observed in the enzyme activity test using the exogeneous expressed YUCCA proteins, which is in an agreement of papers reported by other research groups. To address this issue, catalase has been used to successfully remove hydrogen peroxide that contributes to the automatic conversion of IPyA to IAA. By removing the interference of IAA yield from the IPyA non-enzymatic conversion, the oxygen depletion experiment indicated that the exogeneous expressed YUCCA enzyme has very low activity in the reaction of converting IPyA to IAA.

5.1 Molecular Cloning of *YUCCA1, YUCCA2* and *TEV238* genes

5.1.1 Construction of the plasmids pET4a-*YUCCA1* and pET4a-*TEV238*

In order to optimize the protein expression levels in *Escherichia coli*, the *YUCCA1* gene (At4g32540.1) has been synthesized with rare codons of wild type *YUCCA1* replaced. The *YUCCA1* gene was inserted into the pET-42a-c(+) expression vector through the BamHI and HindIII restriction enzyme sites by the company GenScript (Piscataway, NJ, USA).

The fusion protein expressed by the recombinant plasmid *pET4a-YUCCA1* is YUCCA1 with a GST tag and a His tag on the N-terminus. The affinity tags on the YUCCA1 fusion protein can be optionally removed by TEV protease. There are two tabacco etch virus (TEV) protease cleavage site designed on the upstream of the N-terminus and downstream of the C-terminus of the *YUCCA1* coding sequence. The

recombinant plasmid map of *pET42a-YUCCA1* is shown in **Figure 5-1 Panel A**, and the YUCCA1 fusion protein expressed by this plasmid is shown in **Figure 5-1 Panel B**.

The plasmid *pET4a-TEV238* was designed in a similar way. With rare codons replaced, the *TEV238* gene was inserted into the *pET4a* vector through the BamHI and HindIII restriction enzyme sites. The fusion protein expressed by this vector is a TEV protease with a GST tag and a His tag. The TEV protease fusion protein can cleave the affinity tag off the YUCCA1 fusion proteins in the purification columns.

5.1.2 pGEX-YUCCA2 plasmid

The plasmid *pGEX-YUCCA2* was given by Dr. Hiroyuki Kasahara from the Plant Science Center, RIKEN, Japan.

5.2 *E. coli* transformation and protein expression

All three plasmids (*pET4a-YUCCA1*, *pET4a-TEV238* and *pGEX-YUCCA2)* have been transformed into *E. coli* BL21 Star (DE3) and BL21 Star (DE3) pLysS (Catalog number C602003, Thermo Fisher Scientific, Waltham, MA, USA) strains respectively. The BL21 Star (DE3) *E. coli* strain can enhance the protein yield with increased mRNA stability by incorporating a mutation on the *rne-1* gene, which encodes RNaseE and is one of the major sources for mRNA degradation. The BL21 Star (DE3) pLysS strain expresses a T7 RNA polymerase inhibitor and prevents the leaky expressions. The *pGEX-YUCCA2* plasmid was also transformed into the *E. coli* Rosetta 2 (DE3) strain (Catalog number 71397-3, Novagen, Madison, USA) which can increase the expression level of eukaryotic proteins in *E. coli* by providing tRNAs for rare codons. Multiple colonies from each transformation have been tested for selecting optimal expression

strain. The SDS-PAGE result of exogenously expressed proteins is shown in **Figure 5-2**. The in-gel digestion experiment on YUCCA1 fusion protein was performed, and the protein sequence of YUCCA1 fusion protein was confirmed by MALDI-TOF and LC-MS/MS. The result of LC-MS/MS is shown in **Figure 5-3**.

5.3 Protein purification of YUCCA fusion proteins

YUCCA fusion proteins have been tested for achieving its optimal expression level with high enzyme activity. It was determined that the best expression and purification protocol among all tested conditions are as follow: Grow *E. coli* BL21 Star (DE3) strain carrying the recombinant plasmid in Terrific Broth (TB) media, and induce the protein expression by adding 1mM IPTG when the O.D. of the culture reached to 1.2. The protein expression was induced for 48 hours on a shaker at 120 rpm under 18 °C. The *E. coli* cells were collected and resuspended in the lysis buffer. The components of lysis buffer are 1.4M NaCl, 100mM Na_2HPO_4, 18mM KH_2PO_4, 27mM KCl and 0.1mM PMSF at pH 7.3. This lysis buffer was also used as the binding and washing buffer in GST tag purification. The resuspended *E. coli* solution was French pressed and the lysate was centrifuged at 13000 rpm for 40 minutes at 4 °C.

5.3.1 Soluble fraction purification

The experiment result indicated that YUCCA1 and YUCCA2 protein can express in both soluble and insoluble (inclusion bodies) forms within bacterial cells. The soluble fraction of YUCCA1 and YUCCA2 was purified using GST column. The elution buffer used was the washing buffer with the addition of 10mM glutathione and 0.1% Triton X-100 at pH 8.0. The enzyme concentration was then determined by the Bradford test. The

concentration of YUCCA1 fusion protein was 0.98 mg/ml, the concentration of YUCCA2 was 0.77 mg/ml, and the concentration of elution fraction of negative control BL21 Star (DE3) strain has no eluted protein.

5.3.2 Inclusion body purification

Enzyme activity was also attempted to retain in the fraction of inclusion bodies. The inclusion bodies were solubilized in the lysis/binding/washing buffer containing 8M urea, and then fast renatured by dilution or slowly renatured by dialysis with gradual removal of urea in the present of FAD cofactor. The result indicated enzymes purified from inclusion bodies have no observable activity (See **Figure 5-4**).

5.4 YUCCA enzyme activity test

The enzyme activity has analyzed by three different analytical methods, including UV spectrometer, HPLC, and GC-MS. Among these methods, GC-MS was determined as the most sensitive, accurate and effective method for detecting the IAA production. A repeatable experimental and analytical procedure has been established as described in previous chapters.

5.4.1 IPyA to IAA conversion by YUCCA fusion proteins

In this experiment, the enzyme reactions were conducted in 1400 μl PBS buffer with 40 μM FAD, 1mM NADPH, 100 μM IPyA and 200 μg of purified YUCCA fusion proteins. The YUCCA fusion proteins used in the enzyme reactions were obtained from the soluble fraction of the exogenously expressed YUCCA proteins through GST affinity tag purification. The reaction was started by adding the substrate IPyA. During the

progression of the reaction, 100 μl aliquots were taken out of the reaction at certain time intervals and immediately quenched by adding 5 μl acid mixture of 0.75M HCl and 0.125M H_3PO_4. [$^{13}C_6$]IAA was used as the internal standard for quantification purposes. The procedures for IAA methylation and data analysis were the same as described in previous chapters. The result indicated that the exogenously expressed YUCCA1 and YUCCA2 may be able to convert IPyA to IAA, although the initial velocities of the reactions were very low and a significant portion of the IAA production was from the IPyA non-enzymatic conversion (See **Figure 5-5**).

5.4.2 Oxygen-depleted experiment on YUCCA2 fusion protein

In order to remove the non-enzymatic conversion of IPyA to IAA in the presence of hydrogen peroxide, 6,875 unit of catalase was added to the 2.5 mL reaction system. The experimental apparatus setup of this experiment was similar to the oxygen-depleted experiment described in Chapter 3. The reaction system of 2500 μl PBS buffer with 40 μM FAD, 1mM NADPH, and 400 μg of purified YUCCA fusion proteins was sealed in the glass reaction vial, and then argon flushed to remove oxygen in the vial. The reaction was started by injecting 100 μM IPyA substrate. 100 μl aliquots were taken out of the glass vial by syringes at certain time intervals and immediately quenched by adding 5 μl acid mixture of 0.75M HCl and 0.125M H_3PO_4. In this experiment, the first 40 minutes were the oxygen-depleted stage. The reaction was exposed to the air after 40 minutes. [$^{13}C_6$]IAA was used as the internal standard for quantification purposes. The procedures for IAA methylation and data analysis were the same as described in previous chapters.

The oxygen-depleted experiment confirmed that YUCCA is an oxygen-dependent enzyme that can catalyze the conversion of IPyA to IAA enzymatically, although the enzyme activity is very low. (See **Figure 5-6, panel A and panel B**).

Compare to the experiment with the addition of catalase, it is suggested that without the addition of catalase, a significant portion of IPyA was converted to IAA non-enzymatically in this reaction system (see **Figure 5-7**).

5.5 Figures

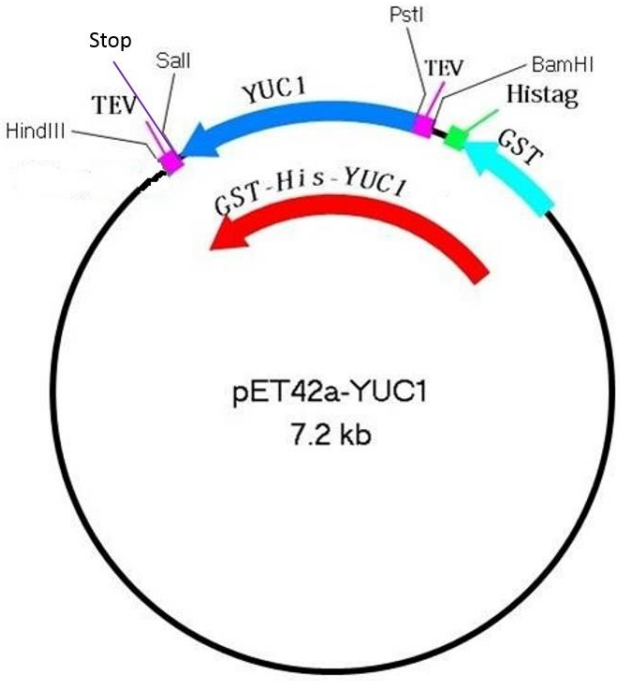

(A)

N-GST/6xHis/Thrombin/S-tag/FactorXa/TEV/YUC1(stop,stop)-C
(B)

Figure 5-1. The map of pET42a-YUCCA1 recombinant plasmid (Panel A); and the YUCCA1 fusion protein expressed by this plasmid (Panel B)

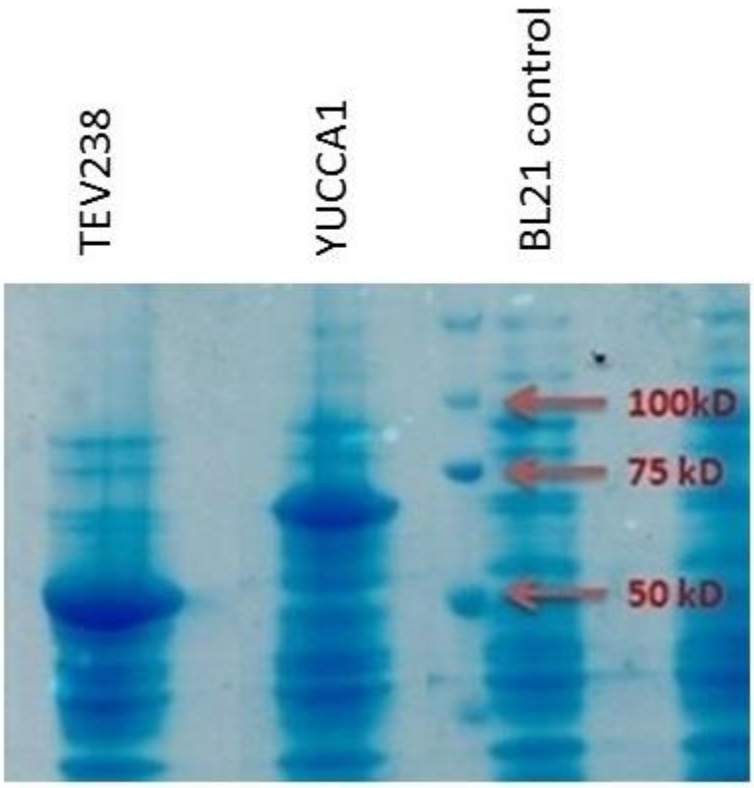

Figure 5-2. Expression of GST-tagged His-tagged YUCCA1 protein and GST-tagged His-tagged TEV238 protein. The molecular weight of YUC1 fusion protein is 79kD, and the molecular weight of TEV238 fusion protein is 59kD.

Figure 5-3. The LC-MS/MS result confirming the expressed protein is a fusion protein of GST-Histag-YUCCA1 protein.

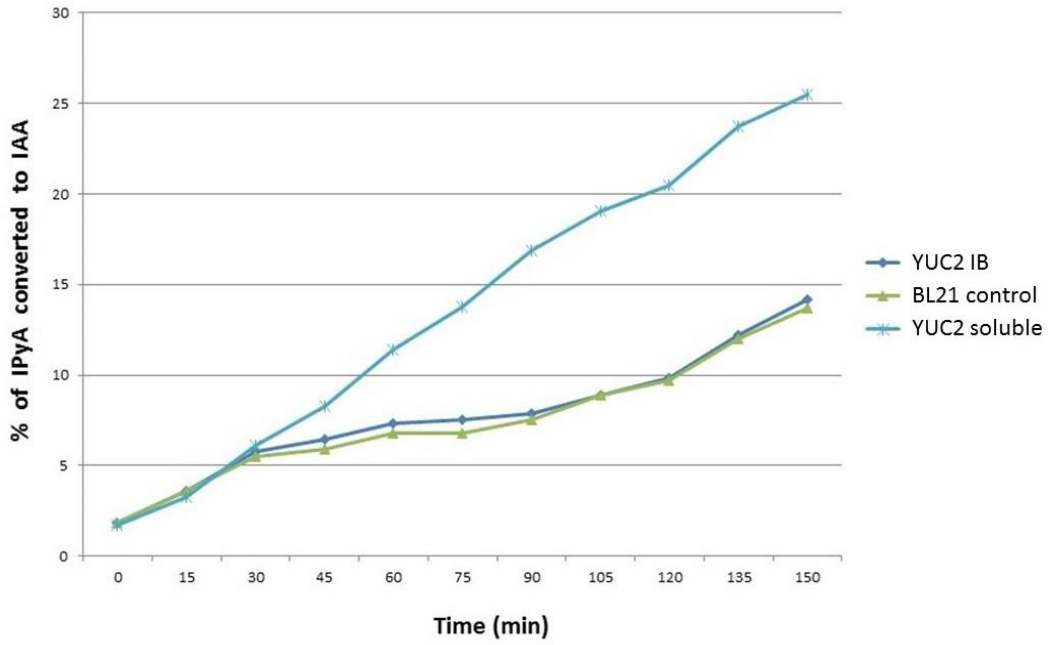

Figure 5-4. Enzyme activity of the soluble fraction purification and the inclusion body fraction purification of YUCCA2. BL21 is the negative control.

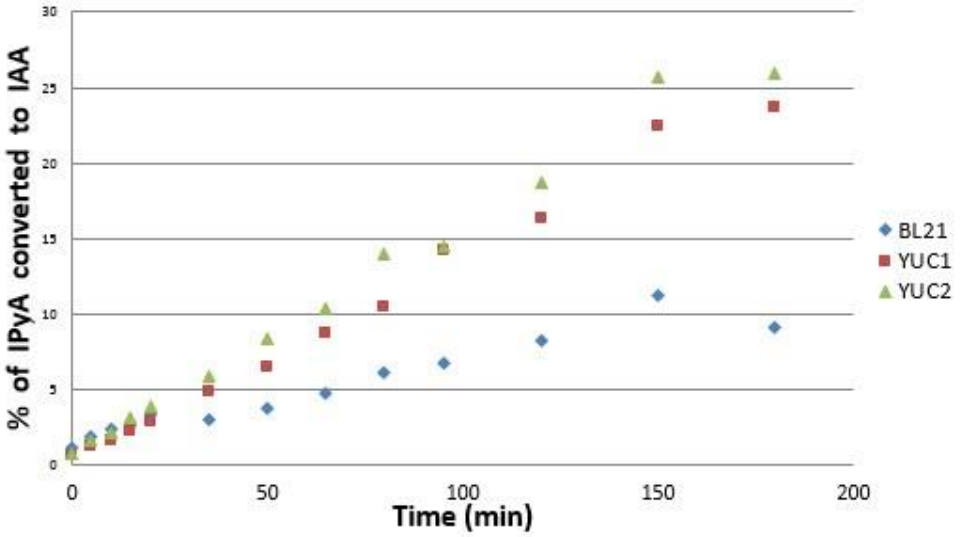

Figure 5-5. Enzyme activity of YUCCA1 and YUCCA2 (soluble fraction using GST column purification). BL21 is the negative control.

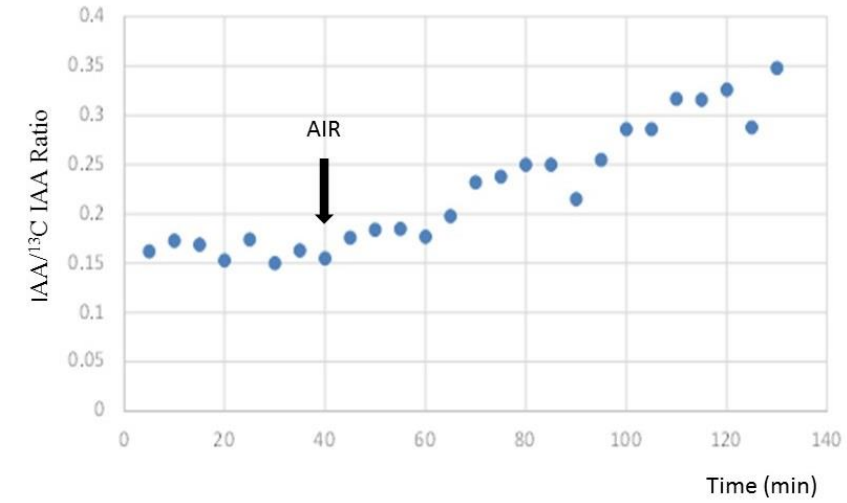

(A)

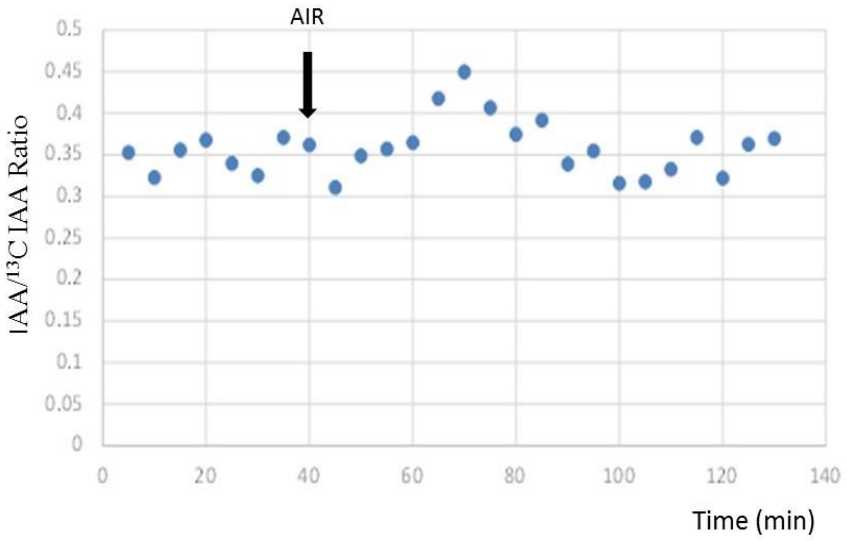

(B)

Figure 5-6. Enzyme activity of YUCCA2 in oxygen depletion experiment with catalase addition. Panel A was the reaction with YUCCA2 enzyme. Panel B was the reaction of negative control with boiled YUCCA2 enzyme.

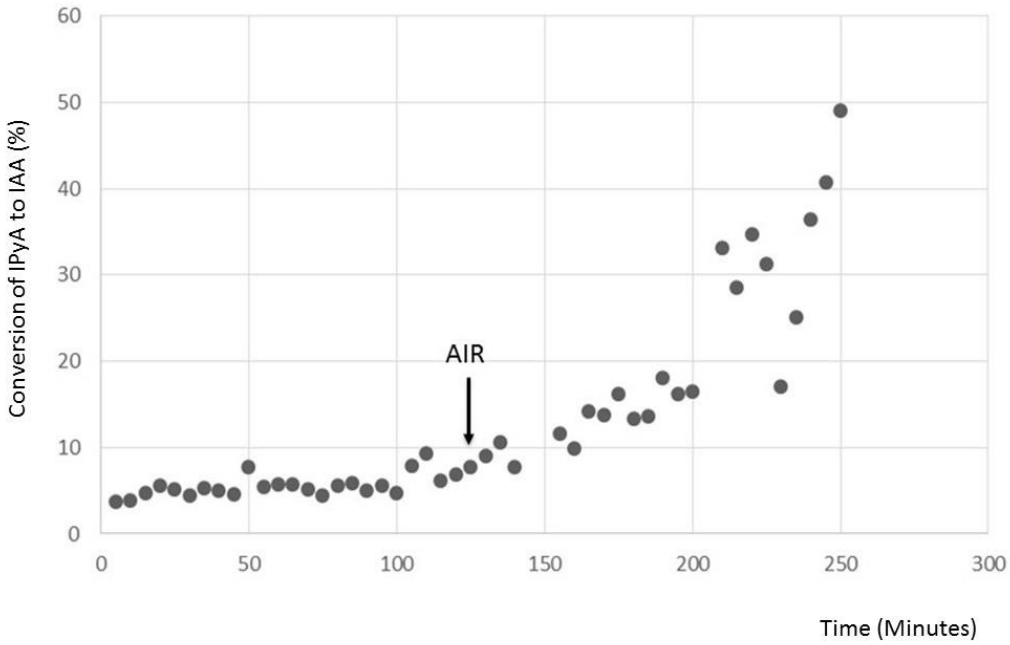

Figure 5-7. Conversion of IPyA to IAA by YUCCA2 enzyme with no catalase addition.

Appendix B

Molecular Cloning, Protein Expression and Purification, and Protein Structure Modeling of *Plasmodium falciparum* CDPK1

Overview

For understanding molecular mechanisms of CDPKs, it is important to further our current knowledge in CDPKs dynamic structure. This study has completed the PfCDPK1 molecular cloning, protein expression and purification, and proposed the possible PfCDPK1 structure using the swiss modeling tool. This model may be used for determining PfCDPK1 dynamic structures, especially for revealing the currently unknown autoinhibitory junction domain structure. The junction domain is a unique structure in CDPKs which is not present in humans, thus information from this project could be applicable for designing drugs against malaria. Furthermore, the structure dynamics of PfCDPK1 may implicate CDPKs functions in plants.

6.1 Introduction

Calcium-dependent protein kinases (CDPKs) are a family of protein kinases that exist only in plants and some protists. Coupling with Ca^{2+} signal transductions and hormone networks, CDPKs are involved in many fundamental pathways in plants, however the molecular mechanisms of CDPK functions in plants are not yet known (reviewed by Harper and Harmon, 2005). Study of CDPK function has proven difficult because there are 34 CDPK isoforms and many CDPK-related protein kinases in the *Arabidopsis thaliana* CDPK-SnRK superfamily (reviewed by Hrabak *et al*., 2003). And also, there are only a few obvious phenotypes observed for CDPK knockouts in plants, such as, AtCPK4 and AtCPK11 double mutants show a pleiotropic ABA-insensitive and a resulting salt-insensitive phenotype (Zhu *et al*., 2007), CPK17 and CPK34 double knockout in *Arabidopsis* shows a near male sterility (Myers *et al.*, 2009). This proposed study will analyze CDPK functions in *Plasmodium falciparum*, a protist which has only 5

CDPK isoforms. Moreover, a targeted gene disruption study has shown that *P. falciparum* calcium-dependent protein kinase 1 (PfCDPK1) seems to be essential for the survival of *P. falciparum* (Kato *et al.,* 2008).

6.1.1 CDPKs in plants

Previous studies have identified and examed the evolutionary origins of all the *Arabidopsis* kinases belonging to the CDPK-SnRK superfamily based on the *Arabidopsis* genome sequences. This calcium-regulated kinase superfamily is composed of CDPKs, CDPK-related kinases (CRKs), phosphoenolpyruvate carboxylase kinases (PPCKs), PEP carboxylase kinase-related kinases (PEPRKs), calmodulin-dependent protein kinases (CaMKs), calcium and calmodulin-dependent protein kinases (CCaMKs) and SNF1-related kinases (SnRKs) families (reviewed by Hrabak *et al*., 2003). Plant CDPKs are most similar to mammalian origin calmodulin-dependent protein kinases (CaMKs) (Hanks and Hunter, 1995) and they may have evolved from the fusion of an ancestral CaMK and a calmodulin (CaM) (Hardie, 1999). In *Arabidopsis* CDPK-SnRK superfamily, CDPKs which has 34 isoforms falling into 12 subfamilies is the largest family (reviewed by Harper, Breton and Harmon, 2004). Although the role of CDPKs functioning in plants is not clear, there are growing evidences indicating that CDPKs are involved in almost every aspect of the plant's growth and development coupling with the Ca^{2+} signaling and plant hormone networks (Harper and Harmon, 2005). The plant physiological mechanisms mediated by CDPKs include, pollen tube growth (Taylor and Hepler, 1997; Schiott *et al*., 2004; Myers *et al*., 2009), oil body biogenesis in groundnut, sesame, cotton, sunflower, soybean and safflower(Anil et al., 2003), seed germination and early plant development (Abo-el-Saad and Wu, 1995; Anil and Sankara Rao, 2000;

Anil and Sankara Rao, 2001), plant defense against pathogen attacks (Lee and Rudd, 2002), plant response to environmental stresses, such as salinity, drought and cold (Ma and Wu, 2007; Zhu *et al*., 2007).

6.1.2 CDPKs in protists

CDPKs widely exist in some protists. One of the most popular protists used in CDPKs research is *P. falciparum*, because it is the major malaria-causing parasite. There are only five CDPK isoforms that are found in *P. falciparum*. It has been reported that PfCDPK1 is involved in the regulation of parasite motility during egress and invasion and seems to be essential for the survivial of *P. falciparum* (Kato *et al.,* 2008). PfCDPK4 may be connected with induction of exflagellation in male gametocytes of *P. falciparum* (Billker *et al.*, 2004).

6.1.3 Domain Structure of CDPKs

The primary structure of most CDPKs contains 4 functional domains, as shown in **Figure 6-1**, an N-terminal variable domain (V), a protein kinase domain (PK), an autoinhibitory junction domain (J), and a calcium-dependent/calmodulin-like domain (CLD) with four EF hand motifs. Some exceptions have a CLD with one or two EF hand motifs, such as AtCPK25 (reviewed by Hrabak *et al*., 2003). Many CDPKs have a predicted myristoylation site and a nearby palmitoylation site in the N-terminal domain, and these sites seem to be important for the membrane binding property of CDPKs (Lu and Hrabak, 2000). The X-ray crystal structure of the junction domain and calcium-dependent/calmodulin-like domain was revealed (Chandran *et al*., 2006). However, the homology modeling of the protein kinase domain that is proposed by a study on

autophosphorylation patterns with enzyme kinetics remains undetermined (Hegeman *et al*., 2006). In all, structure of CDPK functioning as a whole is not clear. Specifically, the way that the junction domain connects the protein kinase domain to the calcium-dependent domain structurally, and the dynamic scaffold functions need to be determined.

6.1.4 Current model for CDPK activation

Current model for CDPK activation is shown in **Figure 6-2**. With no calcium present, autoinhibitory junction domain binds to the active site of protein kinase domain as a pseudosubstrate, thus CDPK is inactive; with sufficient level of calcium present, the binding of calcium to EF hands will result in protein conformational change and release the junction domain from blocking the active site, thus CDPK is activated (reviewed by Harper *et al*., 2005; Hegeman *et al*., 2006). The actual protein structural dynamics has not been revealed; experiments proposed in this project will test this model and may demonstrate the mechanism of CDPK activation.

6.2 Molecular cloning, protein expression and purification of PfCDPK1

PfCDPK1 plasmid was donated by Dr. Jeffery Harper at University of Nevada (the original clone was obtained by RT-PCR from plasmodium total RNA template from Dr. Elizabeth Winzler at the Scripps Research Institute). The plasmid has been successfully cloned into *Escherichia coli* DH5α and BL21 (DE3) strains respectively. The plasmid map is shown in **Figure 6-3**.

6.2.1 Construction the pET4a-*pfCDPK1* plasmid

In order to optimize the protein expression levels in *Escherichia coli*, *pfCDPK1* has been synthesized with rare codons of wild type *pfCDPK1* replaced. The *pfCDPK1* gene was inserted into the pET-42a-c(+) expression vector through the BamHI and HindIII restriction enzyme sites by the company GenScript (Piscataway, NJ, USA).

The fusion protein expressed by the recombinant plasmid *pET4a-pfCDPK1* is pfCDPK1 with a GST tag and a His tag on the N-terminus. The affinity tags on the fusion protein can be optionally removed by TEV protease. There are two tabacco etch virus (TEV) protease cleavage site designed on the upstream of the N-terminus and downstream of the C-terminus of the *CDPK1* coding sequence. The recombinant plasmid map of *pET42a-pfCDPK1* is shown in **Figure 6-4.**

6.2.2 Protein expression and purification

His-tagged PfCDPK1 has been expressed in *E. coli* BL21 Star (DE3) strain, under the induction of isopropyl 1-thio-β-galactopyranoside (IPTG). Multiple colonies from each transformation have been tested for selecting optimal expression strain. To achieve the optimal expression level, the culture was first inoculated in LB medium overnight, and then the saturated culture was diluted into the fresh LB medium in the ratio of 1:20. The diluted culture was placed at 37C shaker. When the O.D. reached to 1.0, the culture was cooled on ice for 30 minutes, and 1mM IPTG was added. The protein expression was induced for 4 hours on a shaker at 250 rpm under 37 °C. The *E. coli* cells were collected and resuspended in the lysis buffer. The components of lysis buffer are 150mM NaCl, 50mM Tris, 5mM EDTA and 0.15mM PMSF at pH 8. This lysis buffer was also used as the binding buffer in GST tag purification. The resuspended *E. coli* solution was French

pressed and the lysate was centrifuged at 13000 rpm for 40 minutes at 4 °C. The cell lysate, supernatant and pellet fraction were collected for further SDS-PAGE analysis. The supernatant was subjected to pass through a 0.45 filter, and then loaded to the GST column for 2 times. The GST column was washed 3 times with the wash buffer (the ingredient of the wash buffer is the same as lysis buffer minus 5mM EDTA). The fusion protein was eluted with the elution buffer. The elution buffer was made by adding 10mM reduced glutathione into the wash buffer. Each fraction from the purification steps was collected for the SDS-PAGE analysis, and the gel result of the exogenously expressed pfCDPK1 fusion protein is shown in **Figure 6-5**.

6.3 Alignment of CDPK isoforms

In this study, amino acid sequences of 34 *Arabidopsis* CPK isoforms and 8 protist CDPK isoforms were used for alignment: AtCPK1-34, PfCDPK1-4, TgCDPK1-3 (*Toxoplasma gondii*), and CpCDPK1 (*Cryptosporidium parvum*). These 42 isoforms were aligned by ClustalW. The result shows that PfCDPK1 protein shares 52% identity and 69% similarity to TgCDPK1 protein (PDB # 3HX4); 49% identity and 67% similarity to CpCDPK1(PDB # 3IGO); 61% identity and 77% similarity to TgCDPK3 (PDB #3HZT).

6.4 Protein structure modeling for PfCDPK1

6.4.1 Protein structure modeling for PfCDPK1 with calcium present

TgCDPK1 (PDB # 3HX4, **Figure 6-6**) and CpCDPK1 (PDB # 3IGO, **Figure 6-7**) were used as structure templates for query of pfCDPK1 structure in SwissModel

(http://swissmodel.expasy.org/) under the alignment mode. The predicted PfCDPK1 structures with calcium are consentaneous (**Figure 6-8** and **Figure 6-9**). The structure modeling is based on amino acid sequence homology, thus further experimental data from this proposed project are needed for confirming the structure of PfCDPK1 with calcium present.

6.4.2 Protein structure modeling for PfCDPK1 without calcium present

Currently there is only one CDPK protein structure without calcium present, TgCDPK3 (PDB #3HZT, **Figure 6-10**), published in the protein database. However, in this structure, a Mg^{2+} ion binds to one of the EF hand positions and the protein structure changes dramatically compared to the structures with calcium present (the calcium binding domain is coming from the back of the protein and blocking the ATP-binding pocket). No paper is published for this structure and the effect of Mg^{2+} on this structure is unknown. Thus, whether PfCDPK1 without calcium present will have similar structure is hard to predict based on this information.

6.5 Figures

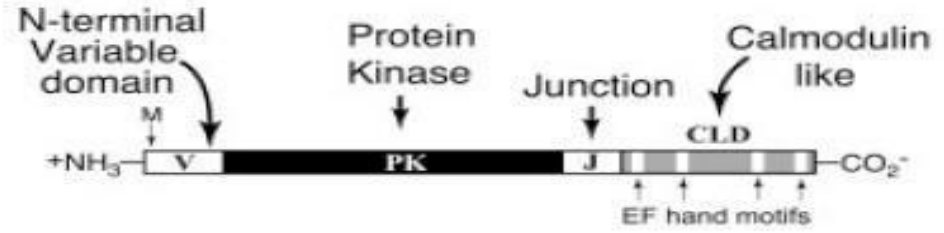

Figure 6-1. Diagram of domain structure of CDPKs (copied from Hegeman et al., 2006)

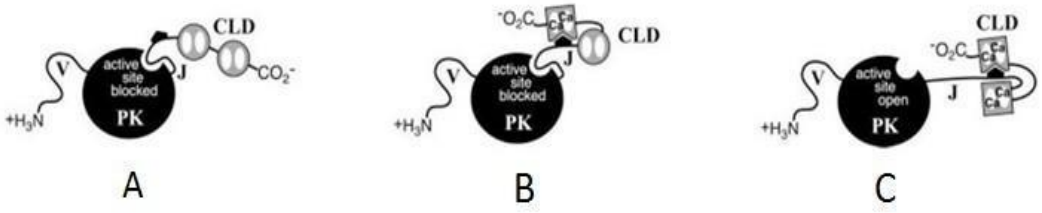

Figure 6-2. Diagram of CDPKs activation. A shows the autoinhibitory junction domain acts as a pseudosubstrate and blocks the kinase active site when no Ca^{2+} is present; B shows CDPK is still inactive with basal level of $[Ca^{2+}]$ (~100nM) present; C shows when $[Ca^{2+}] > 0.5$ -1μM, the active site is open. (copied from Hegeman et al., 2006)

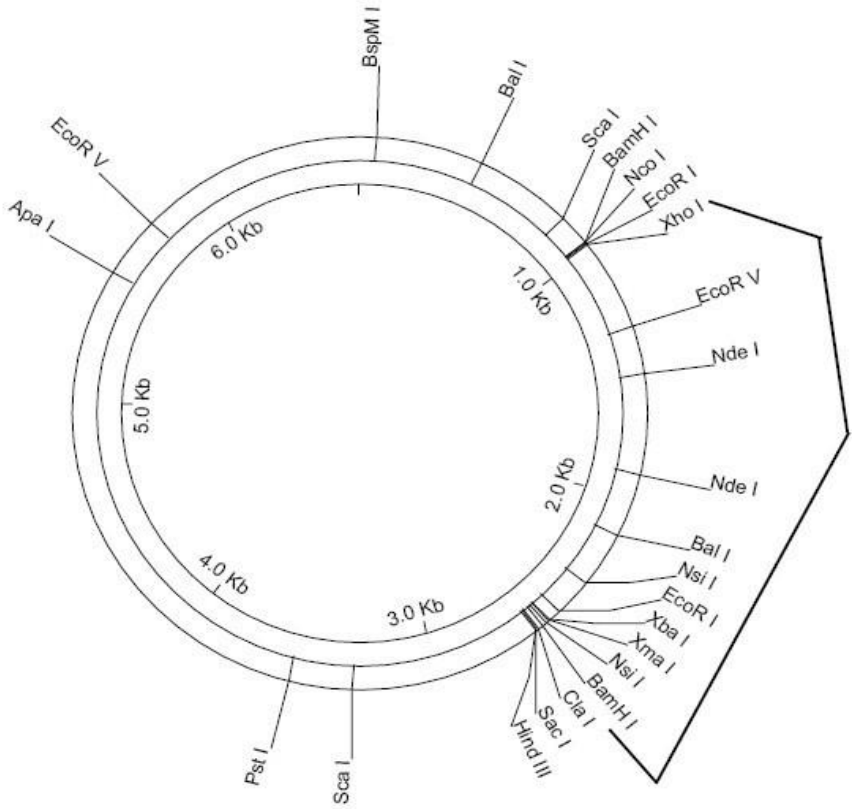

Figure 6-3. PfCDPK1 plasmid map (from Jeffery Harper's lab)

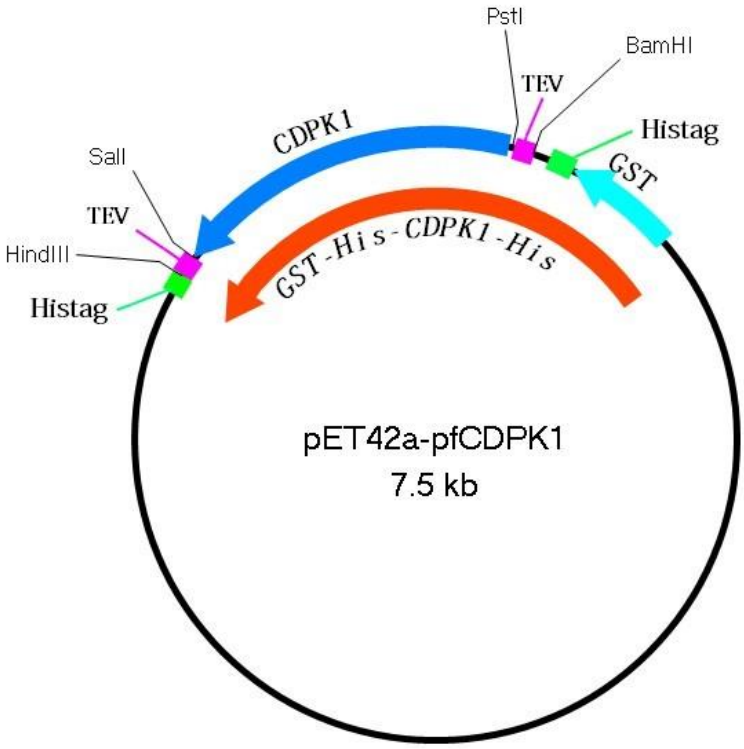

Figure 6-4. The map of pET42a-PfCDPK1 recombinant plasmid

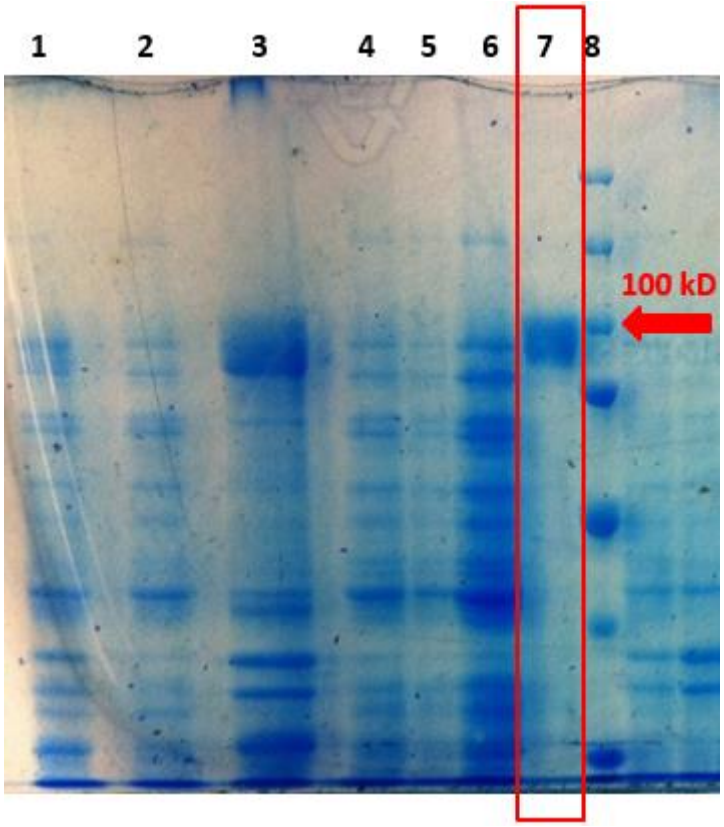

Figure 6-5. Expression of GST-tagged His-tagged CDPK1 protein. The molecular weight of CDPK fusion protein is 97kD. Lane 1: Cell pellet before lysis; Lane 2: Supernatant after French press and centrifuge; Lane 3: Pellet after French press and centrifuge; Lane 4: Supernatant after 0.45um filtration; Lane 5: Protein flow-through after GST column; Lane 6: Wash buffer fraction; Lane 7: Elution fraction of CDPK1 fusion protein; Lane 8: Protein marker.

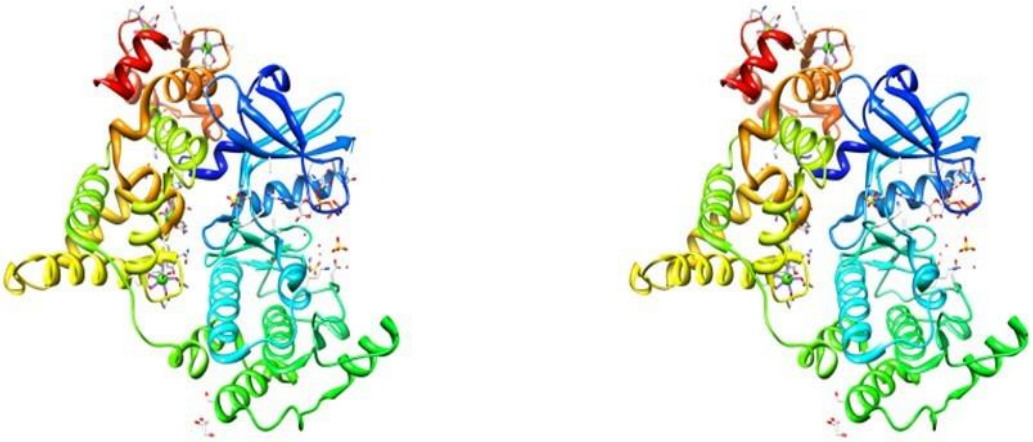

Figure 6-6. Stereo view (cross-eye) of TpCDPK1 structure (with calcium, PDB #3HX4)

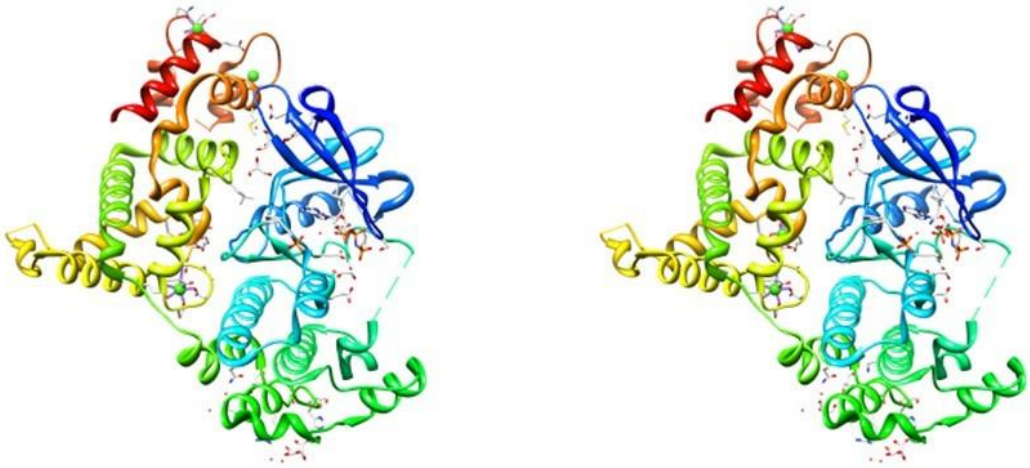

Figure 6-7. Stereo view (cross-eye) of CpCDPK1 structure (with calcium, PDB #3IGO)

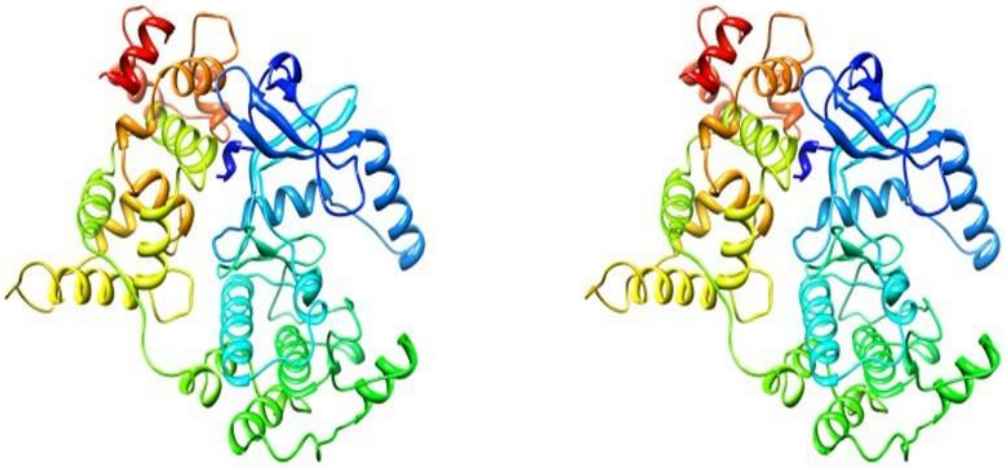

Figure 6-8. Stereo view (cross-eye) of PfCDPK1 (with calcium) protein structure model using TpCDPK1 (with calcium, PDB #3HX4) as template

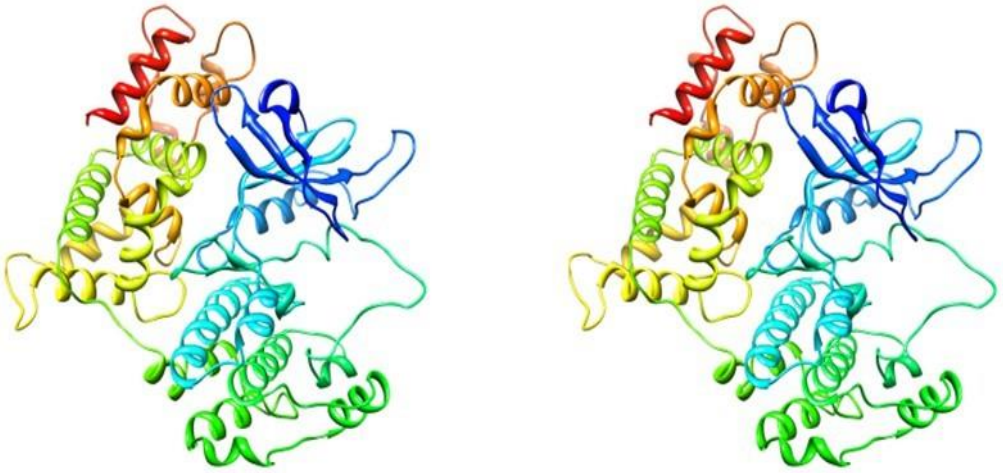

Figure 6-9. Stereo view (cross-eye) of PfCDPK1 (with calcium) protein structure model using CpCDPK1 (with calcium, PDB#3IGO) as template

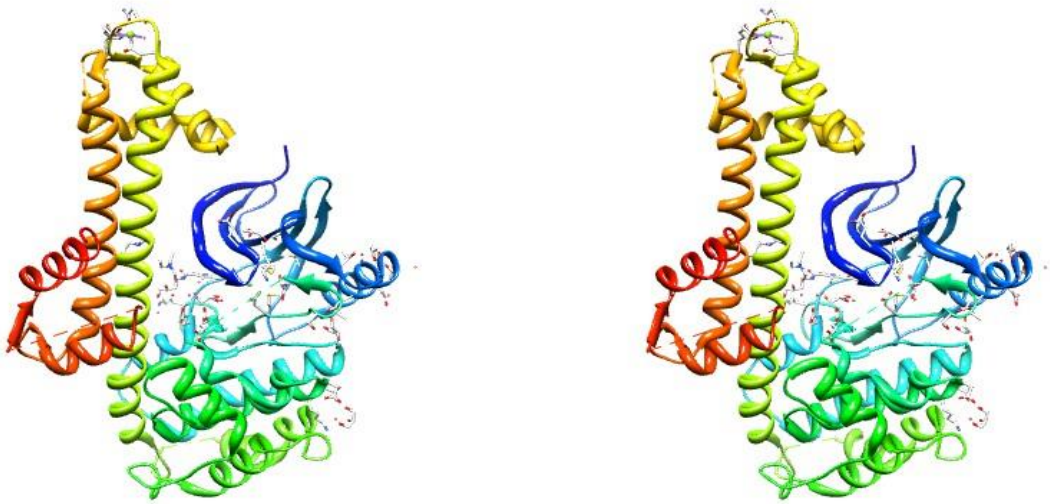

Figure 6-10. Stereo view (cross-eye) of CpCDPK1 structure (without calcium, with magnesium, PDB #3HZT)

6.6 Literature Cited

Abo-el-Saad M and Wu R (1995) A rice membrane calcium-dependent protein kinase is induced by gibberellins. Plant Physiology **108**: 787-793

Anil VS, Harmon, A.C and Rao KS (2003) Temporal association of Ca^{2+}-dependent protein kinase with oil bodies during seed development in Santalum album L.: Its biochemical characterization and significance. Plant Cell physiology **44**: 367-376

Anil VS and Rao KS (2000) Calcium-mediated signaling during sandalwood somatic embryogenesis. Role for exogenous calcium as second messenger. Plant Physiology **123**: 1301-1311

Anil VS and Rao KS (2001) Calcium-mediated signal transduction in plants: A perspective on the role of Ca2+ and CDPKs during early plant development. J. Plant Physiol. 158: 1237-1256.

Billker O, Dechamps S, Tewari R, Wenig G, Franke-Fayard B and Brinkmann V (2004) Calcium and a calcium-dependent protein kinase regulate gamete formation and mosquito transmission in a malaria parasite. Cell **117**: 503-514

Chandran V, Stollar EJ, Lindorff-Larsen K, Harper JF, Chazin WJ, Dobson CM, Luisi BF and Christodoulou J (2006) Structure of the regulatory apparatus of a

calcium-dependent protein kinase (CDPK): A novel mode of calmodulin-target recognition. Journal of Molecular Biology **357**: 400-410

Hanks SK, Hunter T (1995) The eukaryotic protein kinase superfamily: kinase (catalytic) domain structure and classification. FASEB J. **9**:576-596

Hardie DG (1999) Plant protein serine/threonine kinases: classification and functions. Annual Review of Plant Physiology and Plant Molecular Biology **50**: 97-131

Harper JF and Harmon A (2005) Plants, symbiosis and parasites: A calcium signaling connection. Nature **6**: 555-566

Harper JF, Breton G and Harmon A (2004) Decoding Ca^{2+} signals through plant protein kinases. Annual Review of Plant Physiology **55**: 263-288

Hegeman AD, Rodriguez M, Han BW, Uno Y, Phillips GN Jr, Hrabak EM, Cushman JC, Harper JF, Harmon AC and Sussman MR (2006) A phyloproteomic characterization of in vitro autophosphorylation in calcium-dependent protein kinases. Proteomics **6**: 3649-3664

Hrabak EM, Chan CW, Gribskov M, Harper JF, Choi JH, Halford N, Kudla J, Luan S, Nimmo HG, Sussman MR, Thomas M, Walker-Simmons K, Zhu JK and

Harmon AC (2003) The Arabidopsis CDPK-SnRK superfamily of protein kinase. Plant Physiology **132**: 666-680

Kato N, Sakata T, Breton G, Le Roch KG, Nagle A, Anderson C, Bursulaya B, Henson K, Johnson J, Kumar KA, Marr F, Mason D, McNamara C, Plouffe D, Ramachandran V, Spooner M, Tuntland T, Zhou Y, Peters EC, Chatterjee A, Schultz PG, Ward GE, Gray N, Harper J, Winzeler EA (2008) Gene expression signatures and smaill molecule compounds link a protein kinase to plasmodium falciparum motility. Nature **4**: 347-356

Lee J and Rudd JJ (2002) Calcium-dependent protein kinases: versatile plant signaling components necessary for pathogen defence. Trends in plant science **7**: 97-98

Lu SX and Hrabak EM (2002) An Arabidopsis calcium-dependent protein kinase is associated with the endoplasmic recticulum. Plant Physiology **128**: 1008-1021

Ma SY and Wu WH (2007) AtCPK23 functions in Arabidopsis responses to drought and salt stresses. Plant Molecular Biology **65**: 511-518

Myers C, Romanowsky SM, Barron YD, Garg S, Azuse CL, Curran A, Davis RM, Hatton J, Harman AC and Harper JF (2009) Calcium-dependent protein kinases regulate polarized tip growth in pollen tubes. The Plant Journal **59**: 528-539

Schiott M, Romanowsky SM, Baekgaard L, Jakobsen MK, Palmgren MG and Harper JF (2004) A plant plasma membrane Ca2+ pump is required for normal pollen tube growth and fertilization. Proceedings of the National Academy of Sciences of the United States of America **101**: 9502-9507

Taylor LP and Hepler PK (1997) Pollen germination and tube growth. Annual Review of Plant Physiology and Plant Molecular Biology **48**: 461-491

Zhu SY, Yu XC, Wang XJ, Zhao R, Li Y, Fan RC, Shang Y, Du SY, Wang XF, Wu FQ, Xu YH, Zhang XY and Zhang DP (2007) Two calcium-dependent protein kinases, CPK4 and CPK11, regulate abscisic acid signal transduction in Arabidopsis. Plant Cell **19**: 3019-3036